Electron Transfer and Hydride Transfer Reactions of Copper Hydrides

Michael Scott Eberhart

Submitted in partial fulfillment of the
requirements for the degree of
Doctor of Philosophy
in the Graduate School of Arts and Sciences

COLUMBIA UNIVERSITY

2016

Abstract

Electron Transfer and Hydride Transfer Reactions of Copper Hydrides

Michael Scott Eberhart

Copper hydrides such as $[Ph_3PCuH]_6$ (Stryker's Reagent) are textbook reagents in organic chemistry for the selective hydrogenation of α,β-unsaturated carbonyl compounds. Despite their widespread use both stoichiometrically and catalytically, there are many important questions about polynuclear copper hydrides that have not been answered.

I have investigated the electron transfer chemistry of $[Ph_3PCuH]_6$ and related copper hydrides. Copper hydrides ($E_{1/2}$ = –1.0 to –1.2 V vs FcH/FcH^+) are good one-electron reducing agents. Stopped-flow techniques have allowed the detection of electron transfer intermediates in copper hydride reactions.

The fate of the copper containing products after electron transfer or hydride transfer reactions has been investigated. An unusual cationic copper hydride, $[(Ph_3P)_7Cu_7H_6]^+$ was found to be the major product of these reactions. Methods of converting this species back to $[Ph_3PCuH]_6$ have been investigated. The chemistry of this cationic species plays an important role in catalytic use of copper hydrides.

Table of Contents

List of Schemes, Figures and Tables

Acknowledgements

I would like to thank my Ph.D. advisor Jack Norton for his mentoring during my time in graduate school. Jack is a brilliant chemist who relentlessly attacks the most difficult questions in chemistry. I have great admiration for Jack's dedication to producing only the highest quality scientific results and making the extra effort to write clear and succinct manuscripts. I thank him for his support and the intellectual freedom he has given me during graduate school. I also thank him for the annual group ski trip to Killington, VT.

I am grateful to Ged Parkin and George Flynn for serving on my graduate committee. They have provided valuable feedback and outside perspective on my research during my time in graduate school. Tianning Diao, Xavier Roy, Ged Parkin, and Tony Shaw served on my defense committee. I am grateful to them for the time they have spent on my defense and carefully examining my dissertation.

The past and present members of the Norton group have shared their vast knowledge and experience with me along with their friendship. In particular James Camara, Tony Shaw, and Deven Estes have been extremely helpful in helping with electrochemistry and techniques in the Norton lab. Shuo Liu has been a great collaborator over the past few months on the copper hydride project. I wish her the best of luck on continuing copper hydride chemistry and look forward to continued collaboration. I mentored Sophie Rubashkin on her undergraduate research project to investigate the reactivity of $[(dppbz)CuH]_3$ as a catalyst for hydrogenation of enone substrates and greatly appreciate her sense of humor and enthusiasm for the chemistry. I also

thank Travis Valadez, Jonathan Kuo, Jason Polisar, John Hartung, Jim Yang, Yue Hu, and Gang Li for being good colleagues and making the lab a pleasant place to work.

The Parkin group, especially Michelle Neary, Serge Ruccolo, Wes Sattler, and Ashley Zuzek have determined the X-ray structures of the compounds in this dissertation and provided many chemical insights and enthusiasm for this research. Josh Palmer has also been a good friend and I thank him for many useful discussions.

I would like to thank my wife Yan for all of her love and support. Yan is a brilliant chemist and I am truly grateful to her for all her support over these years while she was also doing her Ph.D. in chemistry at Brown.

Chapter 1- Structure of Copper Hydrides[1]

1.1 Introduction

Copper hydride was the first discovered transition metal hydride and has been known since 1844 when an insoluble form of copper hydride was first reported by Wurtz[2]. Material similar to that producted by Wurtz has been extensively studied over many years and displays several remarkable properties compared to other metal hydrides. Copper hydride is only slowly oxidized by water and can be produced by treating copper(II) salts with aqueous hypophosphorous acid.[2-3] Copper hydride formed by the Wurtz method is nearly stoichiometric with the formula CuH, but impurities of metallic copper and water are always present in its structure and copper hydride produced in this manner is insoluble. An anhydrous, "soluble" form of copper hydride can be formed in ether or pyridine solvent.[3-5] This "soluble" copper hydride can be dissolved using pyridines, phosphines, phosphites, or alkyl sulfides, presumably forming molecular copper hydrides.[3, 6] In the late 1960s and early 1970s, Lutsenko et al reported the first possibly stoichiometric and soluble copper hydrides,[7-9] but characterization of these compounds was limited to elemental analysis and the disappearance of the Sn-H IR stretching band of triethyltin hydride used to generate the reported hydrides. Shriver and Dilts raised doubts as to the reliability of these early reports;[6] however, in light of more recent procedures for preparing copper hydrides involving silanes,[10-11] the procedures of Lutsenko et al. could reasonably be expected to have resulted in copper hydrides. In particular, Lutsenko et al. used triphenylphosphine[7] and hexamethylphosphoramide[9] as ligands to generate copper hydrides. A hexanuclear copper hydride cluster with hexamethylphosphoramide ligands was later

crystallographically characterized by Caulton.[12] Whitesides et al. remarked that a 1:1 complex of CuH and tri-n-butylphosphine could be formed, although high solubility prevented its isolation.[5] Most importantly, in 1972, Osborn and Churchill reported the first crystallographically characterized copper hydride, $[Ph_3PCuH]_6$.[13] This species is now a textbook reagent in organic chemistry, commonly known as "Stryker's Reagent," and its chemistry is the subject of a much of my thesis.

1.2 Synthesis of Copper Hydrides

The early procedure of Churchill et al involved using sodium trimethoxyborohydride and $[Ph_3PCuCl]_4$.[13] Since that time, many borohydride reagents have been popular choices for synthesis of copper hydrides. [14-15] Another method suggested in 1979 for the preparation of $[Ph_3PCuH]_6$ involves reacting $LiAlH_4$ with $(Ph_3P)_3CuCl$ in ethereal solvent. It is relatively convenient so long as the stoichiometry is carefully controlled; an excess of $LiAlH_4$ will result in an unstable product. However, the most practical methods of synthesizing copper hydrides are hydrogenolysis of CuO^tBu species or the use of a silane as a stoichiometric reagent. Modern procedures for synthesis of copper hydrides typically involve the hydrogenolysis of CuO^tBu species in the presence of a ligand such as triphenylphosphine. The phosphine is typically used in significant excess because excess phosphine is important for the stabilization of some intermediates in the formation of copper hydride clusters.[16] Caulton was the first to demonstrate the formation of copper hydrides using hydrogen. In that procedure, $[CuO^tBu]_4$ was sublimed before use; copper t-butoxide is highly sensitive to oxygen and moisture which can cause complications. Stryker later demonstrated a simplified method that involves generating CuO^tBu *in situ*; it is simpler since all of the starting materials for the Stryker preparation are

commercially available. In our experience, commercial KO^{t}Bu is sufficiently pure when stored in a glovebox that the use of freshly prepared KO^{t}Bu or sublimed KO^{t}Bu is unnecessary. An advantage of the Caulton/Stryker method using hydrogen gas is that the corresponding copper deuterides can be synthesized economically and in extremely good isotopic purity. $[Ph_3PCuD]_6$ does not readily exchange with acidic protons in glass or in adventitious water so the isotopic purity is limited only to the isotopic purity of the deuterium gas used. Finally, another important method for synthesis of $[Ph_3PCuH]_6$ uses an organosilane in place of molecular hydrogen.[17] For the laboratory scale, this eliminates the need to handle hydrogen gas (although only one atmosphere of hydrogen is typically sufficient). Another advantage of using organosilanes is that copper(II) starting materials can be used.[11] Organosilanes can also be exploited when dealing with fluoride or oxygen containing species such as copper fluoride starting materials or carbon dioxide substrates; the strong Si-F and Si-O bonds can be used to drive these reactions when they are not otherwise thermodynamically feasible. However, there are some major drawbacks to using organosilanes. Many organosilanes are highly toxic, they are expensive, and the use of organosilanes results in poor atom economy. Lipshutz has used polymethylhydrosiloxane to reduce the drawbacks of toxicity and cost;[18] however, the tradeoff involves an impure polymeric material.

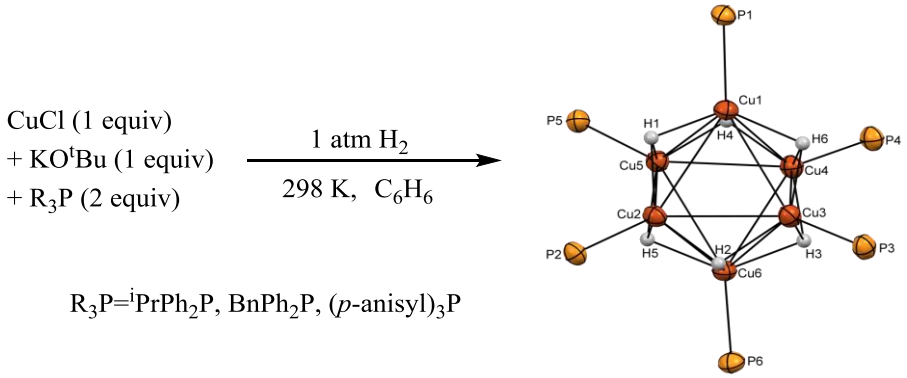

Scheme 1.1. Synthesis of hexameric copper hydrides can be accomplished with inexpensive reagents and 1 atm H_2.

1.3 Solid State Structures of Copper Hydrides Ligated by Monodentate Phosphines

In the solid state, monodentate phosphine copper hydride species tend to adopt a hexameric structure with six facially bridging hydride ligands. Many different copper sources can be used to synthesize $[Ph_3PCuH]_6$ including CuCl, $Cu(OAc)_2$, and $(Ph_3P)_3CuCl$.[11, 16-17, 19] None of these copper containing reagents have six copper atoms in a geometry similar to that found in the core of $[Ph_3PCuH]_6$. It is clear that hexameric copper hydrides are formed by a spontaneous self-assembly process. Kinetic or thermodynamic factors also appear to favor hexamers at ambient temperature conditions; there are a number of x-ray and neutron structures of hexameric copper hydrides with monodententate phosphine ligands[12-14, 20-21] and a single example of a pentanuclear triphenylphosphine copper hydride, $[Ph_3PCuH]_5$, which has been characterized crystallographically.[14] Recently Shuo Liu, a postdoctoral researcher in our lab has been able to reproduce that compound. This pentanuclear copper hydride is the only crystallographically characterized example of a nonhexameric neutral copper hydride with monodentate phosphines. In our lab, this compound was synthesized by keeping the reaction

well below room temperature, and White et al. also used below room temperature conditions to crystallize $[Ph_3PCuH]_5$. In White's case, hexanuclear copper hydride was actually the major product, only about 50 mg $[Ph_3PCuH]_5$ was produced on a ~0.5 g reaction scale. Crystallographic data on hexameric $[Ph_3PCuH]_6$ has been reported several times; from NMR data, it is also apparent that hexanuclear copper hydride is formed essentially every time; the ^1H chemical shift of the hydride ligands in $[Ph_3PCuH]_5$ has proven to be $\delta = 4.15$ in C_6D_6 (the hydride ligand resonance of $[Ph_3PCuH]_6$ is $\delta = 3.50$ in C_6D_6). Thermodynamic or kinetic issues should explain the observation that $[Ph_3PCuH]_5$ is less often formed than $[Ph_3PCuH]_6$. Pentameric $[Ph_3PCuH]_5$ may convert to $[Ph_3PCuH]_6$ under the right conditions; however, preliminary experiments in our lab suggest that a solution of $[Ph_3PCuH]_5$ does not convert to $[Ph_3PCuH]_6$ spontaneously at room temperature and has a tendency to decompose at ambient temperature. This suggests that kinetics determine whether pentameric or hexameric copper hydrides are formed; there may not be a kinetically favorable mechanism for pentameric copper hydrides to convert to hexameric copper hydrides even if thermodynamics would allow it.

The mechanisms by which copper hydrides self-assemble to form aggregates of certain nuclearity have not been studied, but it is interesting to consider how this occurs and if a hexameric copper hydride is formed from a pentanuclear species or some other route. Common copper reagents for the synthesis of $[Ph_3PCuH]_6$ such as $(Ph_3P)_3CuCl$ are monomeric (this species may also be formed in situ from Ph_3P and CuCl) leading to the conclusion that formation of a dinuclear species is a logical first step. Stryker has remarked that the presence of excess phosphine ligand is important;[16] this suggests that lower nuclearity (<6 Cu atoms) copper hydrides likely require stabilization by more than one phosphine ligand per copper and may still obey the 18 electron rule. A trimeric copper hydride with six total PR_3 ligands would be

structurally analogous to the $[dppbzCuH]_3$ copper hydride discussed later in this chapter. Finally, dimerization of two trimers seems like a reasonable route that would not involve a copper hydride pentamer; we have also investigated a trinuclear copper hydride (discussed later in this chapter) which resembles half of the $[Ph_3PCuH]_6$ structure with a different phosphine ligand. A sequence of possible reactions that could lead to $[Ph_3PCuH]_6$ is shown in scheme 1.2.

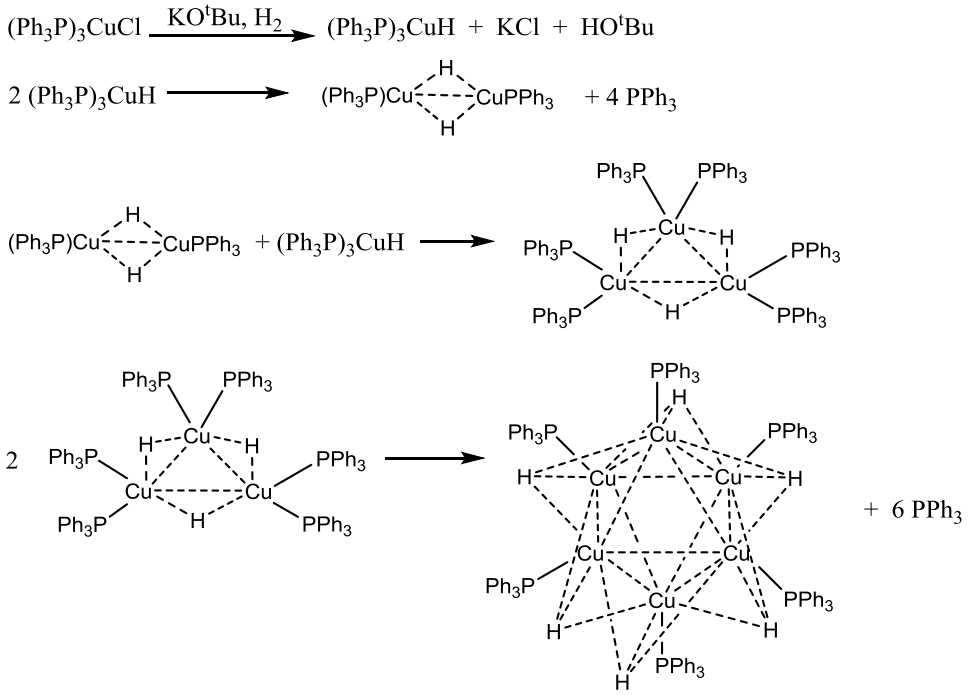

Scheme 1.2. Possible mechanism for the formation of copper hydride hexamers from lower nuclearity copper hydrides.

The location of the hydride ligands in copper hydride hexamers has sparked considerable interest.[13, 20, 22] Caulton, Hoffman and coworkers first determined that the hydride ligands were facially bridging in $H_6Cu_6[P(NMe_2)_3]_6$,[12] using X-ray diffraction techniques. Robert Bau, Thomas Koetzle and coworkers later determined that the hydride ligands in $[tol_3PCuH]_6$ bridged the six smaller faces of a distorted octahedron by a neutron diffraction study[21]. Parker et al. have

recently argued that the hydrides in Stryker's reagent are edge bridging rather than face bridging.[23] The data they have published are consistent with Bau and Koetzle's previous results and it does not appear there are any new data to support a conclusion that the hydrides are not face bridging. Parker et al. have not provided the metrical parameters of their structure. In the Bau and Koetzle neutron diffraction study, the hydride ligands do have modestly longer distances to one of the coppers than the other two (average short Cu-H distance is 1.63(13) Å (range 1.39 Å – 1.88 Å). The longer Cu-H distance averages 1.93(7) Å (range 1.82-2.03). The variability in individually measured bond lengths distances is considerable. However, the difference in the distance between the longer set of Cu-H distances and the shorter Cu-H distances is statistically significant ($P = 0.001$).[24-25] Statistical significance only tells us whether the difference between two populations can be measured (how good is the ruler); statistical analysis cannot say anything about whether or not the difference is important. While the hydride ligand and three bridged copper atoms are not C_3 symmetric, we would expect the hydride ligand not to be sitting so close to the third copper atom if there was no interaction with it. Additionally, the idealized D_{3h} symmetry of copper hydride hexamers precludes a true C_3 axis passing through the hydride capped faces. There is only one C_3 axis in the molecule which passes through the middle of the two Cu_3 faces uncapped by hydride ligands.

By single crystal x-ray diffraction,[26] it was found that $[BnPh_2PCuH]_6$, $[(p\text{-anisyl})_3PCuH]_6$, and $[^iPrPh_2PCuH]_6$ all exist as hexamers similar to other copper hydrides ligated by monodentate phosphines. The hexameric structure of copper hydrides ligated by monodentate phosphine ligands is analogous to the structure of $[nBuLi]_6$.[27] The hydride ligands in $[(p\text{-anisyl})_3PCuH]_6$ and $[^iPrPh_2PCuH]_6$ were found to bridge the six smaller faces of a slightly distorted octahedron. The copper cores of each species form a distorted octahedron. [(*p*-

Anis)$_3$PCuH]$_6$ and [^{i}PrPh$_2$PCuH]$_6$ have six shorter and six longer copper-copper contacts. The shorter copper-copper distances are slightly shorter than copper-copper distances in metallic copper (2.5562 Å). The x-ray structure of [BnPh$_2$PCuH]$_6$ lacks distinct sets of short and long bonds, and has copper-copper bond distances ranging from 2.43 to 2.83 Å. This structure was of relatively poor quality, the crystal was twinned and the hydrides could not be located.

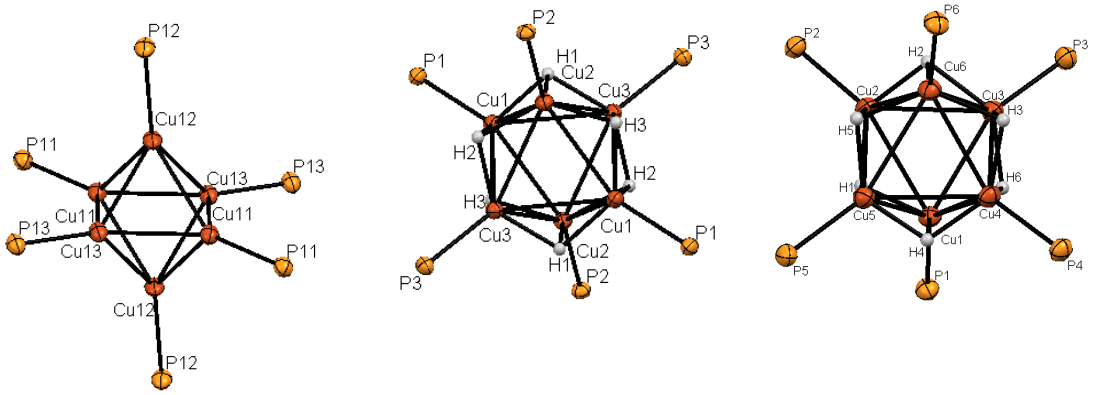

[BnPh$_2$PCuH]$_6$	[^{i}PrPh$_2$PCuH]$_6$	[(p-anisyl)$_3$PCuH]$_6$
Core Ellipsoid Plot	Core Ellipsoid Plot	Core Ellipsoid Plot
P2$_1$/c	P2$_1$/n	P–1
Cu-Cu distances range from 2.43 to 2.83 Å	Average short bond 2.47 Å Average long bond 2.70 Å	Average short bond 2.49 Å Average long bond 2.76 Å

Figure 1.1. Core Ellipsoid Plots for Hexameric Copper Hydrides and Selected Crystallographic Data.

1.4 Solution Structure of Copper Hydrides

The solution structure of copper hydrides had long been a matter of debate and speculation in the literature.[10, 19, 21] This was partially due to an erroneous report that the extinction coefficient of [Ph$_3$PCuH]$_6$ varied with concentration, an observation that was

attributed to "a concentration-dependent distribution of molecular aggregates."[28] Unfortunately this report from Stephens did not detail the concentration range examined or the extinction coefficients for any concentration. Contrary to what had been reported in the literature, the extinction coefficient at 525 nm for $[Ph_3PCuH]_6$ proves to be constant over a wide concentration range (Figure 1.2). An early cryoscopic study of copper hydrides in solution[6] also seemed to suggest various aggregation states; however, Kenneth Caulton has pointed out that the results could also be interpreted in terms of a hexameric copper hydride.[15]

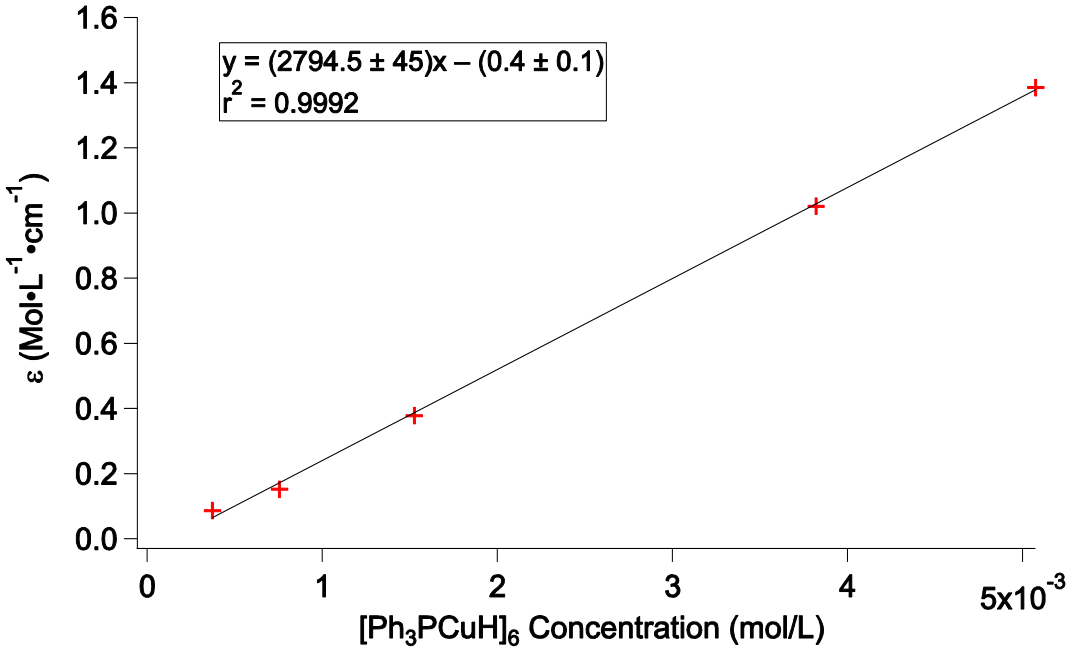

Figure 1.2. Extinction Coefficient Determination for $[Ph_3PCuH]_6$.

The hydride ligands in copper hydrides have a chemical shift downfield of TMS which is consistent with the chemical shifts observed in other d^0 and d^{10} transition metal hydrides. The chemical shifts of copper hydrides or deuterides in the ^1H or ^2H NMR respectively tend to fall between $\delta = 4$ and $\delta = 0$; some representative examples are shown in table 1.1.[12, 15, 29-30]

Table 1.1

Representative Copper Hydrides	CuH ^{1}H or ^{2}H Chemical Shift
$[Ph_3PCuH]_6$	3.50 (^{1}H)[15]
$Cu_2(\mu\text{-}D)_2[\kappa^2\text{-}CH_3C(CH_2PPh_2)_3]_2$	1.83 (^{2}H)[29]
$[P(NMe_2)_3CuD]_6$	2.57 (^{2}H)[12]
$D_8Cu_8(dppp)_4$	1.86 (^{2}H)[12]
$[(dppbz)CuH]_3$	0.60 (^{1}H)
$[(IPr)CuH]_2$ IPr = 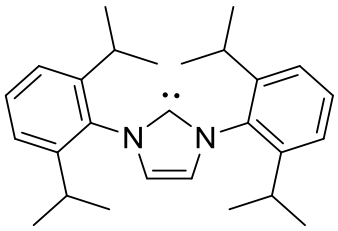	2.46 (^{1}H)[10]

Caulton was the first to identify the ^{1}H NMR resonance of the hydride ligand in $[Ph_3PCuH]_6$ at $\delta = +3.50$ which appeared as "structured multiplet" with "at least five components of a septet" being resolved at reduced temperature. This result suggests the solution structure of $[Ph_3PCuH]_6$ may be hexameric just as in the solid state.[15]

At room temperature, the ^{1}H NMR resonance of the hydride ligand in $[Ph_3PCuH]_6$ appears as a singlet due to residual coupling to copper-63 and copper-65 nuclei and the resulting quadrupolar relaxation of those nuclei (Figure 1.3). At lower temperature, the ^{1}H resonance is sharper and at 263 K is a septet; the hydrides are coupled to six equivalent ^{31}P atoms. At higher temperature, solvent viscosity decreases and molecules tumble at a higher rate. The quadrupolar relaxation mechanism is less effective as the molecule tumbles faster, and thus the spectrum

appears broader due to residual coupling to copper-63 and copper-65 nuclei at higher temperature. The sharpening effect at low temperature should also be achievable by increasing the solvent viscosity.

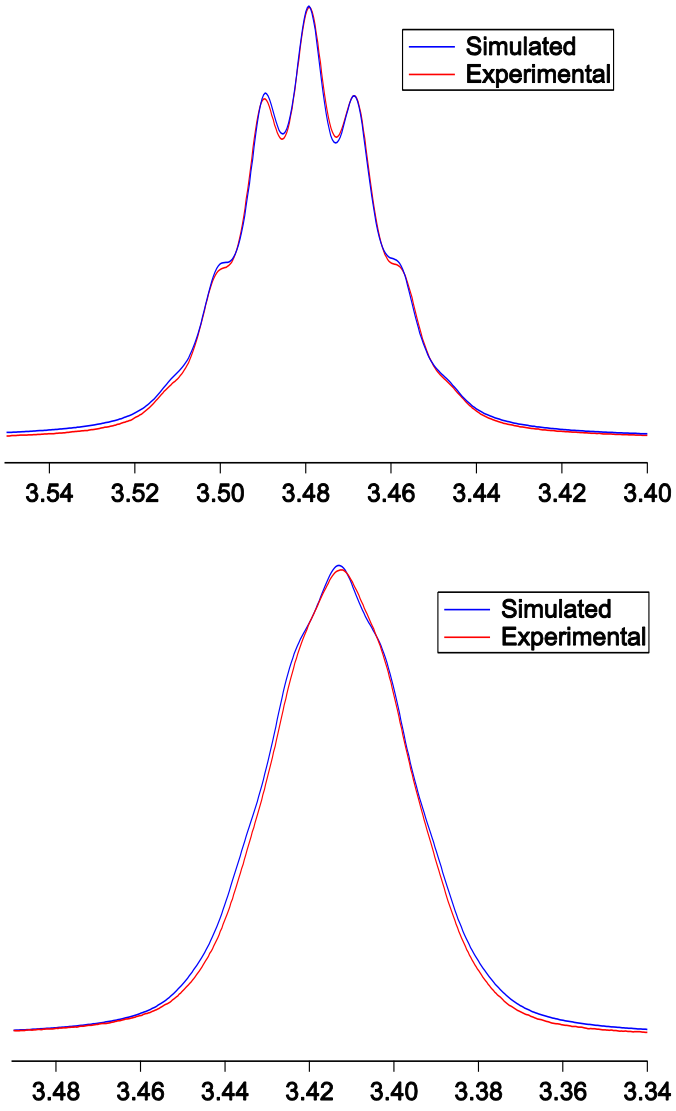

Figure 1.3. 1H NMR showing the resonance of the hydride ligand in $[Ph_3PCuH]_6$ at 263 K (top) and 303 K (bottom). The simulated spectra were generated for a system of six spin 1/2 nuclei

(^{31}P) and six spin 3/2 nuclei (^{63,65}Cu) using MestReNova's "Spin Simulation" feature. The coupling constant between the hydride ligand and the ^{31}P nuclei was iteratively varied on the 263 K spectrum until the best possible match to the experimental spectrum was obtained, the same coupling constant was used for the 303 K simulated spectrum, the line widths differ between the 303 K and 263 K spectra.

Observing this septet at 263 K is only possible because there is rapid intramolecular exchange. The septet occurs because there are six phosphorus-31 atoms, all of which are felt equally by the hydride ligands. Since there are actually eight triangular faces in the hexameric copper hydride structures, six small faces capped with hydride ligands and two larger faces that are uncapped, the most likely mechanism of intramolecular exchange seems to be that the hydrides move over the surface of the Cu_6 core in the cluster leaving capped faces and migrating to uncapped faces allowing all six ^{31}P nuclei to be felt equally. There are actually two competing effects on the broadening of the ^{1}H spectra; as temperature increases spectra broaden as described above and at very low temperature, the ^{1}H resonance of the hydride ligands once again broadens because the intramolecular exchange slows to the point where it is no longer rapid on the NMR time scale. This can be observed in $[p\text{-anisyl})_3PCuH]_6$ when cooled to 200 K in toluene-d_8 (figure 1.4). The impact on the spectrum at intermediate temperatures is similar to that discussed and shown above for $[Ph_3PCuH]_6$.

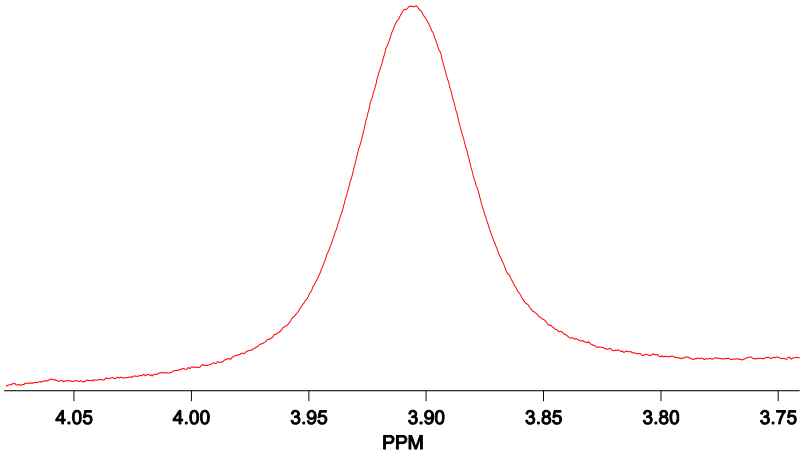

Figure 1.4. ^{1}H NMR Spectrum showing the hydride ligand resonance of $[(p\text{-anisyl})_3PCuH]_6$ at 200 K. The spectrum becomes broad as intramolecular exchange slows.

The hydride ligand being split by six equivalent ^{31}P nuclei along with the concentration independent extinction coefficient proves that not only does a single aggregate predominate in solution, but that the predominant species in solution is hexanuclear as in the solid state structure of $[Ph_3PCuH]_6$.

In contrast to the solution behavior of $[Ph_3PCuH]_6$, which is clearly hexameric under a wide range of conditions, Jeffrey Stryker et al. have described a $[MePh_2PCuH]_n$ species which has proven impossible to crystallize, but yielded a "thermochromic oil" which was red at ambient temperature but became yellow at -40° C.[31-32] Although the aggregation state of this species in the solid state is unknown due to lack of structural data, the thermochromic behavior strongly suggests a change in aggregation state with changing temperature.[31-32] Stryker has suggested that the red species is likely a hexameric copper hydride while the yellow form is a lower aggregate with a likely P:Cu stoichiometry of 2:1.[32] A similar copper hydride containing

the Me_2PhP ligand is yellow in solution and also not crystallographically characterized, but appears to exist in a lower aggregation state based on its color and reactivity.

Phosphine Copper(I) chloride species appear to exhibit behavior analogous to their copper hydride counterparts. In the case of $(MePh_2P)CuCl$, the UV-vis spectrum changes dramatically with concentration. A lesser dependence is observed with $(Ph_3P)_3CuCl$, which does exist in various aggregation states in benzene solution depending on concentration. Several different $(Ph_3P)_xCu_yCl_y$ species have been crystallographically characterized in the solid state including a cubane type tetramer $[Ph_3PCuCl]_4$ and a mononuclear species $(Ph_3P)_3CuCl$.[33]

To see if simple modifications of the phosphine ligand could result in non-hexameric aggregation states, $[^{i}PrPh_2PCuH]_6$ and $[BnPh_2PCuH]_6$ were synthesized. Both of these species proved to be hexameric in the solid state, but at least could be crystallized unlike their $(MePh_2P)CuH$ counterpart. These species are both red solids. In limited testing, these two species had reactivitity similar to other copper hydride species towards N-carbophenoxypyridinium (discussed in chapter 3). These two species also proved to be much more sensitive to water in solution than $[Ph_3PCuH]_6$ or $[(p\text{-anisyl})_3PCuH]_6$. Finally the ^1H NMR spectra of these two species are much broader than their triarylphosphine ligated counterparts. The hydride resonance in the ^1H NMR could not be observed for either species which may indicate aggregation/deaggregation processes occurring on the NMR time scale. Unfortunately many properties of these compounds that may prove interesting could not be investigated due to limited availability of materials to synthesize these two compounds at the time they were being investigated. It would clearly be intriguing to see if the extinction coefficient of these two species shows concentration dependence. It would also be very interesting to see if the hydride ligands in these compounds can be observed by ^1H NMR at lower temperature and examine their

reactivity towards classic copper hydride substrates such as α,β-unsaturated carbonyl compounds.

1.5 Low Nuclearity Copper Hydrides

There has long been a substantial interest in synthesis of lower nuclearity copper hydrides because the nuclearity of these clusters appears to have a dramatic impact on their reactivity. Despite the efforts of many researchers, no crystallographically characterized mononuclear copper hydride has yet been reported. The relationship between copper hydride structure and reactivity is clearly important. Christoper Zall and Aaron Appel have recently suggested a mononuclear copper hydride as an intermediate step in their recently reported hydrogenation of carbon dioxide.[34] However, they have not obtained x-ray data or NMR data that supports this species and cannot rule out a dimeric structure similar to Caulton's discussed later in this section. Low nuclearity copper hydrides may offer reactivity that differs substantially from their higher oligomer counterparts. For example, $[Me_2PhPCuH]_n$ discussed earlier, likely exists as a lower aggregation state and its reactivity towards enones is distinct from most other copper hydrides.[31] Treatment α,β-unsaturated carbonyl compounds with $[Me_2PhPCuH]_n$ results in exclusive formation of the α,β-unsaturated alcohol product while other copper hydrides yield the α,β-saturated carbonyl indicating that the aggregation state could be critical to the reactivity of copper hydrides with organic substrates.[31-32]

Caulton has pointed out that the identity of the phosphine ligand on a copper hydride has a "dramatic influence" on the aggregation state of copper hydrides.[12] Copper hydrides with multidentate phosphines do take a variety of forms,[7, 12] but the structure any of these species will take is difficult to predict with any confidence.[12, 29] In the 1980s, Caulton et al attempted to

synthesize a mononuclear copper hydride using a tripod ligand, but found that only two out of three ligand phosphorous atoms were coordinated to copper in the solid state resulting in the dimer $Cu_2(\mu\text{-}H)_2[\kappa^2\text{-}CH_3C(CH_2PPh_2)_3]_2$ [29] with one uncoordinated phosphorus per ligand. They were also able to observe two chemical shifts in the ^{31}P NMR corresponding to the free and coordinated arms of the phosphine[29] and suggest that the solution structure of this copper hydride is likely to be the same as the solid state structure.

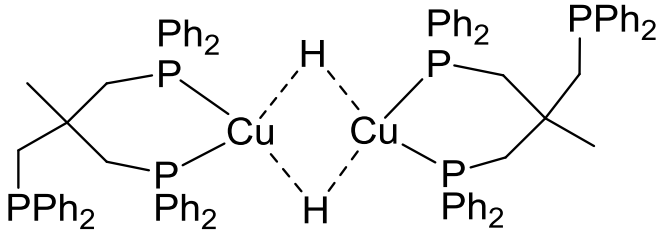

Figure 1.5. Caulton's $Cu_2(\mu\text{-}H)_2[\kappa^2\text{-}CH_3C(CH_2PPh_2)_3]_2$ structure. One arm of each phosphine ligand is not coordinated to copper.

Sadighi et al. have used an N-heterocyclic carbene ligand (NHC) to generate a dimeric copper hydride that was characterized by X-ray crystallography despite its thermal instability.[10] Bertrand et al. have used a very bulky cyclic (alkyl)(amino)carbine (CAAC) ligand[35] to generate a very stable copper hydride, but even this bulky ligand resulted in a copper hydride which is dinuclear in its solid state structure. [36]

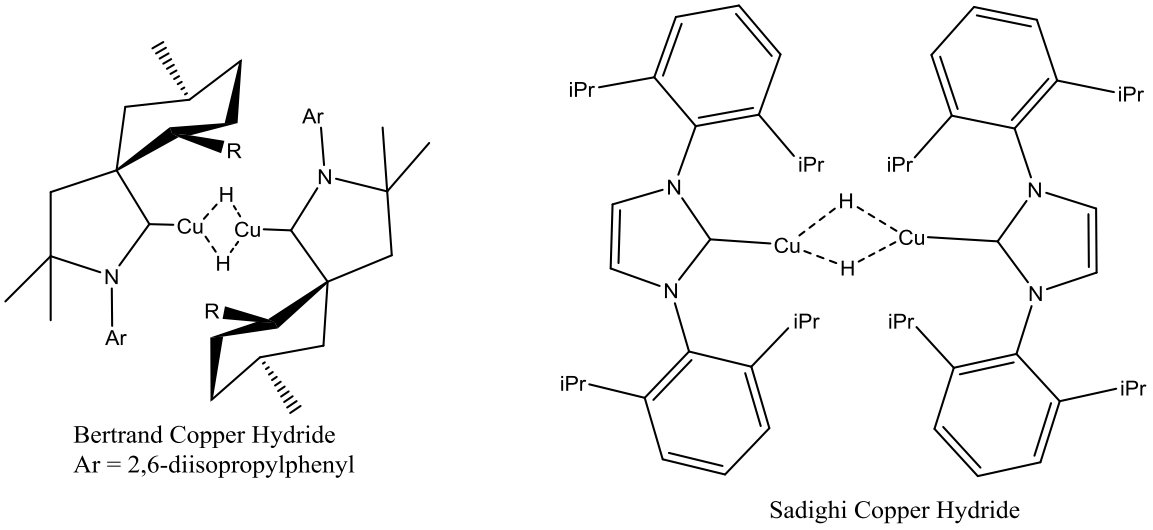

Figure 1.6. Structures of the dimeric Bertrand[36] and Sadighi[10] Copper Hydrides

Steric bulk alone will probably be insufficient to achieve a mononuclear copper hydride since the ligands used by Sidighi and Bertrand are already extremely bulky. Even bulkier ligands run the risk of rendering copper hydrides incompetent as catalysts, which would defeat much of the purpose of studying them. A mononuclear copper hydride would be fascinating from a structural perspective whether or not it can harnessed for any useful purpose.

Caulton's hydride, $Cu_2(\mu\text{-}H)_2[\kappa^2\text{-}CH_3C(CH_2PPh_2)_3]_2$, was investigated by Stryker et al. in the 2000s as a catalyst.[32] Surprisingly, when triphenylphosphine is added to a solution containing $Cu_2(\mu\text{-}H)_2[\kappa^2\text{-}CH_3C(CH_2PPh_2)_3]_2$, the hexameric cluster $[Ph_3PCuH]_6$ is observable by NMR in addition to $Cu_2(\mu\text{-}H)_2[\kappa^2\text{-}CH_3C(CH_2PPh_2)_3]_2$ and free phosphine ligands (both Ph_3P and $CH_3C(CH_2PPh_2)_3$ are observed).[32] One would expect the chelate effect with the tripod ligand to dominate triphenylphosphine's ability to coordinate to copper. Caulton also points out that the Cu-(μ_2-H) bond is favored over an additional P-Cu bond since the third phosphorus atom in

$CH_3C(CH_2PPh_2)_3$ remains uncoordinated to copper (scheme 1.3).[29] This suggests that the P-Cu bond may be unusually weak in this particular case.

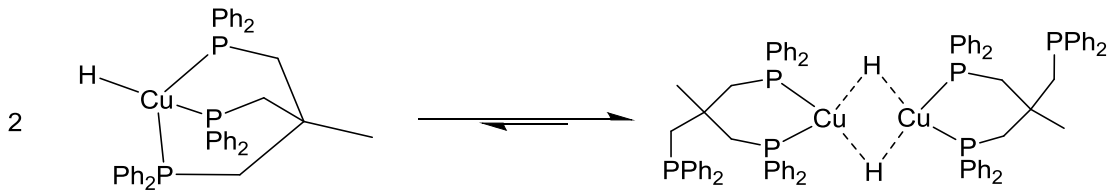

Scheme 1.3. The dimeric structure on the right is favored; there is no evidence for the structure on the left in solution or in the solid state.

A different triphos ligand may yet be capable of producing a mononuclear copper hydride. Anecdotally, triarylphosphines appear to be better ligands for producing stable copper hydrides; although, the reason for this is not clear and may just be coincidental.

The structure of $[(dppbz)CuH]_3$ is quite different from that of $(dppp)_4Cu_8H_8$ which takes on a dodecahedral structure[12] and the earlier discussed $Cu_2(\mu\text{-}H)_2[\kappa^2\text{-}CH_3C(CH_2PPh_2)_3]_2$ suggests that although the phosphine ligand in all three of these species is coordinated to copper in a bidentate fashion, relatively minor differences in the ligand can have a profound impact on the structure of the copper hydride.

With 1,2-bis(diphenylphosphino)benzene (dppbz), a copper hydride trimer $[(dppbz)CuH]_3$ is formed. This species can be synthesized directly using dppbz, CuCl, and KO^tBu under a hydrogen atmosphere (equation 1.2). Additionally, it can be rapidly and irreversibly generated by addition of dppbz to a solution of $[Ph_3PCuH]_6$. Addition of Ph_3P to a solution of $[dppbzCuH]_3$ does not have any impact on the structure of the $[(dppbz)CuH]_3$ by

NMR. Unlike Caulton's $Cu_2(\mu\text{-}H)_2[\kappa^2\text{-}CH_3C(CH_2PPh_2)_3]_2$, $[(dppbz)CuH]_3$ does not exchange the chelating ligand with Ph_3P. This trinuclear species appears to be more stable than many other copper hydrides towards decomposition. Many copper hydrides, including $Cu_2(\mu\text{-}H)_2[\kappa^2\text{-}CH_3C(CH_2PPh_2)_3]_2$ and $[Ph_3PCuH]_6$, are subject to decomposition in solution over prolonged periods of time, often forming a copper mirror. This decomposition is inhibited by the presence of excess phosphine in solution, which indicates that loss of a phosphine ligand is required for decomposition of the copper hydride.[16, 32, 37] This suggests that the phosphine ligand in $[(dppbz)CuH]_3$ is bound more tightly and does not readily dissociate.

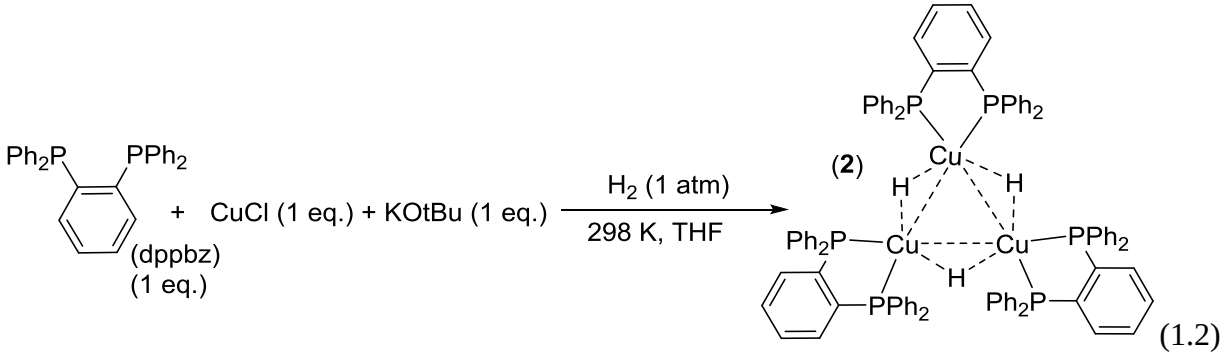

(1.2)

1.6 Electronic Structure of Copper Hydrides - DFT Molecular Orbital Calculations

We have performed DFT calculations on a simplified model of copper hydride with PH_3 in place of more computationally demanding ligands. Calculated Cu-Cu distances correspond well to crystallographically determined distances (short Cu-Cu contacts average 2.54 Å; long Cu-Cu contacts average 2.71 Å). The large HOMO-LUMO gap is to be expected for an 84 e^- six metal cluster and supports the determination that the electrochemistry to be discussed in chapter 2 corresponds to $[Ph_3PCuH]_6^{0/+}$.

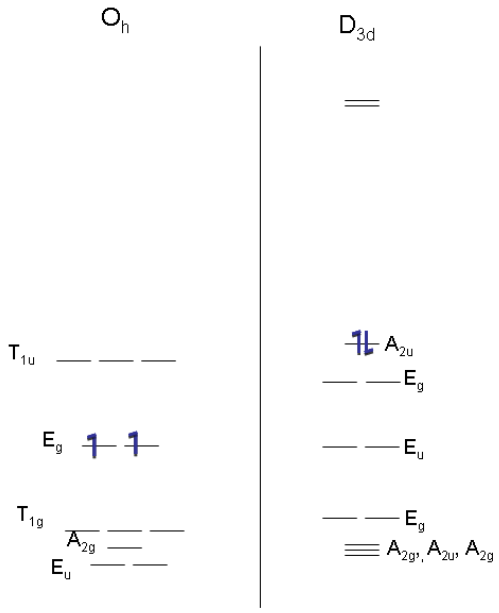

Figure 1.7. Frontier Molecular Orbitals for $[H_3PRhH_2]_6$ (left)[38] and $[H_3PCuH]_6$ (right).

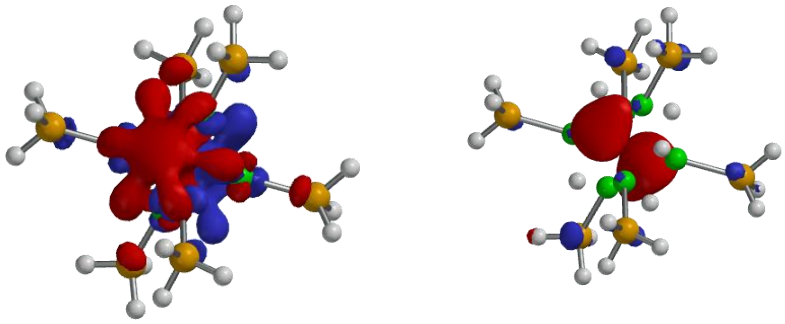

Figure 1.8. HOMO (left) and LUMO (right) Calculated for $[H_3PCuH]_6$

General Procedures

Copper hydrides are slowly oxidized in the presence of oxygen. All manipulations were performed using standard Schlenk techniques or in inert atmosphere glove boxes. Cuprous chloride and KO^{t}Bu (95%) were stored in an inert atmosphere glove box and used as received. Hydrogen gas was >99.998%. CH_2Cl_2 was deoxygenated and dried by two successive columns

(Q-5, activated alumina). CD_2Cl_2 was degassed and distilled from CaH_2. THF and benzene were distilled from sodium/benzophenone under an N_2 atmosphere. THF-d_8 and benzene-d_6 were stirred over sodium/benzophenone and vacuum transferred to a receiving flask. CH_3CN was treated with anhydrous $CuSO_4$ to remove amines, distilled from P_4O_{10} onto CaH_2 and distilled once more from the CaH_2.

^1H and ^{13}C NMR chemical shifts are reported in PPM relative to TMS, peaks are referenced relative to solvent residual peaks in THF-d_8 and benzene-d_6. ^{31}P NMR chemical shifts are reported relative to 85% H_3PO_4 and were determined by the deuterium lock signal.

Samples of $[Ph_3PCuH]_6$ were synthesized as reported in the literature by use of either hydrogen[16] or diphenylsilane[11]. Samples of ($[p\text{-}tol_3PCuH]_6$) were synthesized by a procedure analogous to that used to synthesize $[Ph_3PCuH]_6$,[11] replacing Ph_3P with an equimolar amount of $p\text{-}tol_3P$.

DFT Calculations

Calculations were done using Spartan '10, B3LYP, LACVP*.

Synthesis of $[(p\text{-anisyl})_3PCuH]_6$

Tris(4-methoxy)phenyl phosphine was synthesized as reported in the literature.[39] A Fisher-Porter bottle was charged with 1 gram $(p\text{-anisyl})_3P$ (2.84 mmol), 140 mg CuCl (1.42 mmol), 159 mg KO^tBu (1.42 mmol), and 5.7 mL benzene. This was pressurized to 80 psig H_2 and stirred overnight. The dark red solution was filtered, concentrated to ~2/3 its original volume, and layered with acetonitrile to crystallize the product. Yield 519 mg (88%).

^{1}H NMR (400 MHz, C_6D_6) δ 7.82 (approx. t, *J* = 8.5 Hz, 36H), 7.45 (d, *J* = 8.5 Hz, 36H), 3.71 (broad septet, *J* = 6.8 Hz, 6H (Cu**H)**), 3.28 (s, 54H).

^{31}P NMR (162 MHz, C_6D_6) δ −11.3

^{13}C NMR (125 MHz, C_6D_6) δ 160.5, 136.5, 129.4, 113.9, 54.7

Synthesis of $[^{i}PrPh_2PCuH]_6$

A fisher-porter bottle was charged with 1 gram $iPrPh_2P$ (4.38 mmol), 217 mg anhydrous CuCl (2.19 mmol), 246 mg $KO^{t}Bu$ (2.19 mmol), and 10 mL benzene. This was pressurized to 90 psig H_2. After two hours, a red slurry formed. Approximately half of the benzene was removed under vacuum and acetonitrile was added. The red powder was collected on a Schlenk frit and washed with acetonitrile. Yield 478 mg, 75%. The red solid obtained is insoluble in benzene, but can be purified by dissolution in THF followed by filtration and crystallization by addition of acetonitrile. ^{1}H NMR spectra were broad; the hydride resonance could not be observed in the proton spectrum.

^{1}H NMR (500 MHz, THF-d_8) δ 7.83-6.95 (br, 60 H), 3.05 (br, 6H), 0.99 (d, *J* = 10 Hz, 54H)

^{31}P NMR (162 MHz, THF-d_8) δ 1.59

^{13}C NMR (125 MHz, THF-d_8) δ 136.68, 134.02, 127.92, 127.44, 25.87, 18.71

Synthesis of $[BnPh_2PCuH]_6$

A fisher-porter bottle was charged with 3 grams $BnPh_2P$ (10.86 mmol), 537 mg anhydrous CuCl (5.43 mmol), 609 mg KO^tBu (5.43 mmol), and 23 mL benzene. This was pressurized to 90 psig H_2 (>99.998%) and stirred overnight. The dark red solution was filtered, concentrated to ~2/3 its original volume and layered with acetonitrile. 339 mg of red $[BnPh_2PCuH]_6$ crystals were collected and some decomposition was also observed during the crystallization process. ^{1}H NMR spectra were broad; the hydride resonance could not be observed in the proton spectrum.

^{1}H NMR (400 MHz C_6D_6) δ 7.76 (br), 6.64-7.11, 3.50 (br, C**H**$_2$Ph), 3.18 (br, C**H**$_2$Ph).

^{31}P NMR (162 MHz C_6D_6) δ −7.42

Preparation of $[(dppbz)CuH]_3$ Crystals for X-ray Diffraction

1 gram (2.24 mmol) dppbz (1,2-bis(diphenylphosphino)benzene), 222 mg CuCl (2.24 mmol), 251 mg KO^tBu (2.24 mmol), and 11.7 mL toluene were added to a Schlenk flask and stirred. H_2 was bubbled through the solution for 15 minutes at atmospheric pressure and the reaction was then allowed to stir under 1 atm H_2 for 1 hour. The bright yellow suspension eventually formed a dark yellow solution and finally formed some yellow-brown precipitate which was removed by filtration and extracted with toluene (3x5 mL). Toluene was removed under reduced pressure to yield a yellow solid. The yellow solid obtained was redissolved in a minimal amount of toluene and layered with acetonitrile yielding 189 mg yellow crystals (17%).

^{1}H NMR (500 MHz, C_6D_6) δ 7.68 (br, 24 H), 7.51 (br, 6 H), 6.95 (dd, *J* = 5.5, 3.2 Hz, 6 H), 6.84 (t, *J* = 7.5 Hz, 12 H), 6.68 (t, *J* = 7.5 Hz, 24 H), 0.60 (s 3 H)

^{31}P NMR (162 MHz, C_6D_6) δ −2.75

Improved Procedure for Preparing [(dppbz)CuH]$_3$

The solvent system used in preparing x-ray quality crystals of [(dppbz)CuH]$_3$ is less than ideal for producing larger amounts of material for experiments. The use of acetonitrile can be an issue because its ^{1}H resonance overlaps that of the hydride ligand in many solvents making determination of the hydride content of the product problematic. Additionally, extended reaction times should give improved yield, but [(dppbz)CuH]$_3$ has limited solubility in toluene and often precipitates complicating separation of the desired product from some Cu containing impurities. 1 gram (2.24 mmol) dppbz (1,2-bis(diphenylphosphino)benzene), 222 mg CuCl (2.24 mmol), 251 mg KO^{t}Bu (2.24 mmol), and 25 mL THF were added to a Schlenk flask and stirred. H_2 was bubbled through the solution overnight at atmospheric pressure. A cloudy yellow-brown solution formed which was then filtered to remove insoluble KCl under inert atmosphere using a schlenck filter. The yellow-orange filtrate was concentrated to ~5 mL under reduced pressure and carefully layered with 30 mL hexanes and allowed to stand overnight. The yellow solid was collected on a schlenk frit and washed with pentane to yield 801 mg yellow powder (70%).

^{1}H NMR (500 MHz, C_6D_6) δ 7.68 (br, 24 H), 7.51 (br, 6 H), 6.95 (dd, *J* = 5.5, 3.2 Hz, 6 H), 6.84 (t, *J* = 7.5 Hz, 12 H), 6.68 (t, *J* = 7.5 Hz, 24 H), 0.60 (s 3 H)

^{31}P NMR (162 MHz, C_6D_6) δ −2.75

A Method of Preparing $[(dppbz)CuH]_3$ from $[Ph_3PCuH]_6$

Exploiting the chelate effect, $[(dppbz)CuH]_3$ can be easily synthesized by mixing dppbz with $[Ph_3PCuH]_6$. 500 mg $[Ph_3PCuH]_6$ (0.255 mol) and 683 mg dppbz (1.53 mmol, 6 equiv.) were dissolved in 18 mL toluene under inert atmosphere. This was layered with approximately 35 mL acetonitrile and left to stand for two days. Yield 520 mg (67%).

^{1}H NMR (500 MHz, C_6D_6) δ 7.68 (br, 24 H), 7.51 (br, 6 H), 6.95 (dd, *J* = 5.5, 3.2 Hz, 6 H), 6.84 (t, *J* = 7.5 Hz, 12 H), 6.68 (t, *J* = 7.5 Hz, 24 H), 0.60 (s 3 H)

^{31}P NMR (162 MHz, C_6D_6) δ −2.75

A Method of Preparing $[(dppbz)CuH]_3$ from Copper(II) Acetate and Diphenylsilane

Similar to the method of Yun and Lee for the preparation of $[Ph_3PCuH]_6$,[11] $[(dppbz)CuH]_3$ can be prepared from a copper(II) starting material if a silane is used. The primary advantages of this method are that air stable precursors can be used; copper(II) salts are stable to air. The quality of copper(I) chloride used in other methods of preparing copper hydrides is important. Copper(I) chloride is slowly oxidized in the atmosphere and impractical to purify; fresh preparation of copper(I) chloride by reduction of a copper(II) salt is more practical than attempting to purify copper(I). The other advantage of this route is that fewer filtration steps are required. For the synthesis of both Stryker's reagent and $[(dppbz)CuH]_3$ some insoluble brown material must be removed by filtration before the desired product can be

crystallized when copper(I) and hydrogen gas are used. When reducing a copper(II) salt, no potassium chloride is formed and there are no other insoluble species present that must be removed. 0.5 grams of dppbz (1.12 mmol), 203 mg $Cu(OAc)_2$ (1.12 mmol), and a stirbar were added to a schenck flask. Toluene (5 mL) was then added and reaction was stirred as 1.2 equiv. (1.344 mmol) diphenylsilane were added (0.25 mL) by syringe. The blue/green reaction turned to bright yellow-orange within a few hours and the reaction was stirred for 24 hours. Due to the relatively poor solubility of $[(dppbz)CuH]_3$ in toluene, the product can be collected by filtration directly and washed with hexanes followed by pentane. Yield 278 mg (49%). The yield and purity of $[(dppbz)CuH]_3$ can be improved by using THF in place of toluene and precipitating the copper hydride product with pentane or hexane.

^{1}H NMR (500 MHz, C_6D_6) δ 7.68 (br, 24 H), 7.51 (br, 6 H), 6.95 (dd, *J* = 5.5, 3.2 Hz, 6 H), 6.84 (t, *J* = 7.5 Hz, 12 H), 6.68 (t, *J* = 7.5 Hz, 24 H), 0.60 (s 3 H)

^{31}P NMR (162 MHz, C_6D_6) δ −2.75

Chapter 1 References

1. A portion of this chapter has been published in J. Am. Chem. Soc. 2013, 135 (46), 17262-17265.

2. Wurtz, A., *Ann. Chim. Phys.* **1844,** *3* (11), 250.

3. Dilts, J. A.; Shriver, D. F., Nature of soluble copper(I) hydride. *Journal of the American Chemical Society* **1968,** *90* (21), 5769-5772.

4. Warf, J. C.; Feitknecht, W., Zur Kenntnis des Kupferhydrids, insbesondere der Kinetik des Zerfalls. *Helvetica Chimica Acta* **1950,** *33* (3), 613-639.

5. Whitesides, G. M.; San Filippo, J.; Stredronsky, E. R.; Casey, C. P., Reaction of copper(I) hydride with organocopper(I) compounds. *Journal of the American Chemical Society* **1969,** *91* (23), 6542-6544.

6. Dilts, J. A.; Shriver, D. F., Cryoscopic study of copper(I) hydride-phosphine complexes. *Journal of the American Chemical Society* **1969,** *91* (15), 4088-4091.

7. Lutsenko, I. F.; Kazankova, M. A.; Malykhina, I. G., Complexes of copper hydride with phosphites and phosphines. *Zh. Obshch. Khim.* **1967,** *37*, 2364-5.

8. Malykhina, I. G.; Kazankova, M. A.; Lutsenko, I. F., Preparation of copper hydride complexes with phosphorus(III) compounds. *Zh. Obshch. Khim.* **1971,** *41* (9), 2103-4.

9. Kazankova, M. A.; Malykhina, I. G.; Terenina, M. B.; Lutsenko, I. F., Preparation of copper hydride and its complexes with phosphorus(III) compounds. *Zh. Obshch. Khim.* **1972,** *42* (10), 2133-7.

10. Mankad, N. P.; Laitar, D. S.; Sadighi, J. P., Synthesis, Structure, and Alkyne Reactivity of a Dimeric (Carbene)copper(I) Hydride. *Organometallics* **2004,** *23* (14), 3369-3371.

11. Lee, D.-w.; Yun, J., Direct synthesis of Stryker's reagent from a Cu(II) salt. *Tetrahedron Letters* **2005,** *46* (12), 2037-2039.

12. Lemmen, T. H.; Folting, K.; Huffman, J. C.; Caulton, K. G., Copper polyhydrides. *Journal of the American Chemical Society* **1985,** *107* (25), 7774-7775.

13. Churchill, M. R.; Bezman, S. A.; Osborn, J. A.; Wormald, J., Synthesis and molecular geometry of hexameric triphenylphosphinocopper(I) hydride and the crystal structure of $H_6Cu_6(PPh_3)_6$. $HCONMe_2$ [hexameric triphenylphosphino copper(I) hydride dimethylformamide]. *Inorganic chemistry* **1972,** *11* (8), 1818-1825.

14. Albert, C. F.; Healy, P. C.; Kildea, J. D.; Raston, C. L.; Skelton, B. W.; White, A. H., Lewis-base adducts of Group 11 metal(I) compounds. 49. Structural characterization of hexameric and pentameric (triphenylphosphine)copper(I) hydrides. *Inorganic Chemistry* **1989,** *28* (7), 1300-1306.

15. Goeden, G. V.; Caulton, K. G., Soluble copper hydrides: solution behavior and reactions related to carbon monoxide hydrogenation. *Journal of the American Chemical Society* **1981,** *103* (24), 7354-7355.

16. Brestensky, D. M.; Huseland, D. E.; McGettigan, C.; Stryker, J. M., Simplified, "one-pot" procedure for the synthesis of $[(Ph_3P)CuH]_6$, a stable copper hydride for conjugate reductions. *Tetrahedron Letters* **1988,** *29* (31), 3749-3752.

17. Chiu, P.; Li, Z.; Fung, K. C. M., An expedient preparation of Stryker's reagent. *Tetrahedron Letters* **2003,** *44* (3), 455-457.

18. Lipshutz, B. H.; Chrisman, W.; Noson, K., Hydrosilylation of aldehydes and ketones catalyzed by $[Ph_3P(CuH)]_6$. *Journal of Organometallic Chemistry* **2001,** *624* (1–2), 367-371.

19. Riant, O., Copper(I) Hydride Reagents and Catalysts. In *Chemistry of Organocopper Compounds*, John Wiley & Sons, Ltd: 2009; pp 731-773.

20. Ho, D. M.; Bau, R., The skeletal bonding and structure of $H_6Cu_6(PR_3)_6$ clusters. X-ray and topological studies on the $H_6Cu_6[P(p\text{-tolyl})_3]_6$ molecule. *Inorganica Chimica Acta* **1984,** *84* (2), 213-220.

21. Stevens, R. C.; McLean, M. R.; Bau, R.; Koetzle, T. F., Neutron diffraction structure analysis of a hexanuclear copper hydrido complex, $H_6Cu_6[P(p\text{-tolyl})_3]_6$: an unexpected finding. *Journal of the American Chemical Society* **1989,** *111* (9), 3472-3473.

22. Zerger, R.; Rhine, W.; Stucky, G., Stereochemistry of polynuclear compounds of the main group elements. Bonding and the effect of metal-hydrogen-carbon interactions in the molecular structure of cyclohexyllithium, a hexameric organolithium compound. *Journal of the American Chemical Society* **1974,** *96* (19), 6048-6055.

23. Bennett, E. L.; Murphy, P. J.; Imberti, S.; Parker, S. F., Characterization of the Hydrides in Stryker's Reagent: $[HCu\{P(C_6H_5)_3\}]_6$. *Inorganic Chemistry* **2014,** *53* (6), 2963-2967.

24. The statistical method used was an unpaired t-test

25. This analysis also makes the assumption that each bond length measured is an independent measurement and the variance in the two populations is the same.

26. The x-ray data were collected and the structures were solved by Ashley Zuzek for $[BnPh_2PCuH]_6$ and $[(p\text{-anisyl})_3PCuH]_6$. Wesley Sattler collected the x-ray data and solved the structure for $[^iPrPh_2PCuH]_6$.

27. Kottke, T.; Stalke, D., Structures of Classical Reagents in Chemical Synthesis: $(nBuLi)_6$, $(tBuLi)_4$, and the Metastable $(^tBuLi \cdot Et_2O)_2$. *Angewandte Chemie International Edition in English* **1993,** *32* (4), 580-582.

28. Stephens, R. D., Hydrido(triphenylphosphine)copper(I). *Inorg. Synth.* **1979,** *19*, 87-9.

29. Goeden, G. V.; Huffman, J. C.; Caulton, K. G., A copper-(μ^2-hydrogen) bond can be stronger than an intramolecular phosphorus-copper bond. Synthesis and structure of di-μ-hydridobis[η^2-1,1,1-tris(diphenylphosphinomethyl)ethane]dicopper. *Inorganic Chemistry* **1986,** *25* (15), 2484-2485.

30. Eberhart, M. S.; Norton, J. R.; Zuzek, A.; Sattler, W.; Ruccolo, S., Electron Transfer from Hexameric Copper Hydrides. *Journal of the American Chemical Society* **2013,** *135* (46), 17262-17265.

31. Chen, J.-X.; Daeuble, J. F.; Stryker, J. M., Phosphine Effects in the Copper(I) Hydride-Catalyzed Hydrogenation of Ketones and Regioselective 1,2-Reduction of α,β-Unsaturated Ketones and Aldehydes. Hydrogenation of Decalin and Steroidal Ketones and Enones. *Tetrahedron* **2000,** *56* (18), 2789-2798.

32. Chen, J.-X.; Daeuble, J. F.; Brestensky, D. M.; Stryker, J. M., Highly Chemoselective Catalytic Hydrogenation of Unsaturated Ketones and Aldehydes to Unsaturated Alcohols Using Phosphine-Stabilized Copper(I) Hydride Complexes. *Tetrahedron* **2000,** *56* (15), 2153-2166.

33. Fife, D. J.; Moore, W. M.; Morse, K. W., Solution equilibria of tertiary phosphine complexes of copper(I) halides. *Inorganic Chemistry* **1984,** *23* (12), 1684-1691.

34. Zall, C. M.; Linehan, J. C.; Appel, A. M., A Molecular Copper Catalyst for Hydrogenation of CO_2 to Formate. *ACS Catalysis* **2015,** *5* (9), 5301-5305.

35. Lavallo, V.; Canac, Y.; DeHope, A.; Donnadieu, B.; Bertrand, G., A Rigid Cyclic (Alkyl)(amino)carbene Ligand Leads to Isolation of Low-Coordinate Transition-Metal Complexes. *Angewandte Chemie* **2005,** *117* (44), 7402-7405.

36. Frey, G. D.; Donnadieu, B.; Soleilhavoup, M.; Bertrand, G., Synthesis of a Room-Temperature-Stable Dimeric Copper(I) Hydride. *Chemistry – An Asian Journal* **2011,** *6* (2), 402-405.

37. Mahoney, W. S.; Stryker, J. M., Hydride-mediated homogeneous catalysis. Catalytic reduction of α,β-unsaturated ketones using $[(Ph_3P)CuH]_6$ and H_2. *Journal of the American Chemical Society* **1989,** *111* (24), 8818-8823.

38. Brayshaw, S. K.; Green, J. C.; Hazari, N.; Weller, A. S., A DFT based investigation into the electronic structure and properties of hydride rich rhodium clusters. *Dalton Transactions* **2007,** (18), 1781-1792.

39. Watanabe, Y.; Yamazaki, T., Application of Mitsunobu Reagents to Redox Isomerization of CF_3-Containing Propargylic Alcohols to (E)-α,β-Enones. *The Journal of Organic Chemistry* **2011,** *76* (6), 1957-1960.

Chapter 2 - Electron Transfer from Copper Hydrides[1]

2.1 Motivation to study the electrochemistry of copper hydrides

Electron transfer is a fundamentally important chemical process. Electron transfer reactions are critical to life and electron transfer steps are part of many biological processes including photosynthesis and respiration.[2] In chemistry, electron transfer is particularly important for energy conversion uses such as batteries and fuel cells.

2.2 Electron Transfer in Molecular Transformations

Electron transfer reactions can also be useful for molecular transformations; for example, a Birch reduction involves electron transfer to an arene.[3-7] Transition metals complexes frequently participate in electron transfer reactions because they have multiple oxidation states that are energetically accessible. In particular, first-row transition metals are well known for participating in single-electron chemistry.[8] Understanding the single-electron redox chemistry of catalysts is also important to understanding how they perform even when electron transfer reactions are undesirable. Platinum group metals are particularly useful for reactions which formally require cycles with oxidation states differing by two (M^n-M^{n+2}). Replacement of platinum group metals with first row metals is a popular research objective,[9-12] but many important catalytic reactions do not involve unpaired electrons. Election transfer reactions that lead to radicals may pose problems when earth-abundant metals are used to replace precious metals.

Aside from organic molecules, electron transfer has important ramifications for inorganic species. For example, cobalt coordination complexes in the cobalt(III) oxidation state are substitutionally inert, although reduction to cobalt(II) makes the ligands in such species labile. Tris(ethylenediamine)cobalt(III) is a classic case. In the cobalt(III) oxidation state, an enantiopure sample of tris(ethylenediamine)cobalt(III) retains its optical purity, but addition of a small amount of reducing agent converts some of the tris(ethylenediamine)cobalt(III) to tris(ethylenediamine)cobalt(II), which then racemizes. Since the tris(ethylenediamine)cobalt(II/III) species participate in electron transfer self-exchange, the entire population of tris(ethylenediamine)cobalt(II/III) will eventually become racemic (scheme 2.1).[13]

Δ-$Co(en)_3^{3+}$ + reductant $\longrightarrow$ $Co(en)_3^{2+}$ (not exchange inert)

Δ-$Co(en)_3^{2+}$ $\longrightarrow$ rac-$Co(en)_3^{2+}$ fast

rac-$Co(en)_3^{2+}$ + Δ-$Co(en)_3^{3+}$ $\longrightarrow$ rac-$Co(en)_3^{3+}$ + Δ-$Co(en)_3^{2+}$

Scheme 2.1. Steps in the racemization of optically pure $Co(en)_3^{3+}$.

This is an elegant example where the electron transfer self-exchange rate can be easily measured simply by monitoring the rate at which optical purity is lost. In this chapter, we will see how NMR line broadening methods of measuring electron transfer self-exchange rates can be employed to determine the electron transfer self-exchange rate for $[Ph_3PCuH]_6$. The rate of electron transfer self-exchange is important for determining when electron transfer steps may be mechanistically relevant since electron transfer depends not only on thermodynamics which can be determined electrochemically, but also on the kinetics. Rates and mechanisms of electron transfer have been the subject of decades of research and a few Nobel Prizes, including that awarded to Rudolph A. Marcus in 1992 “for his contributions to the theory of electron transfer

reactions in chemical systems." Taube won the Nobel Prize in 1983 "for his work in the mechanisms of electron-transfer reactions, especially in metal complexes."

In addition to the changes that impact ligand exchange, a change in redox state can have other dramatic impacts in inorganic chemistry. The Norton group has diverse interests, but transition metal hydride chemistry is the unifying theme. When transition-metal hydrides are oxidized, they become more acidic, typically by 15-30 pKa units.[14] All crystallographically characterized copper hydrides are polynuclear, as we have seen in chapter 1. This tendency to form polynuclear species leads to a variety of additional reaction types on the part of copper hydrides; some of these reactions will be the subject of chapter 4. In this chapter, we will see that copper hydrides are good single electron reducing agents.

2.3 Electron Transfer for Energy Conversion

Currently, platinum is used in fuel cells as the catalyst for hydrogen oxidation; however, platinum's high cost and rarity are barriers to widespread adoption of fuel cell technology. Compared to platinum, which costs $991.50 per ounce, copper costs only $2.32 per pound. Platinum fuel cell catalysts are vulnerable to poisoning by carbon monoxide,[15-16] while copper hydride based catalysts may be less susceptible to carbon monoxide poisoning. Copper carbonyl species are known to not be very stable and dissociation of CO is typically facile.[17-18] When $[Ph_3PCuH]_6$ was examined as a possible catalyst for CO and CO_2 hydrogenation, Sneeden and coworkers found that treatment of $[Ph_3PCuH]_6$ with carbon dioxide resulted in a copper formate that was identical to that formed by formate reduction of a copper(II) salt in the presence of triphenylphosphine.[19] Upon treatment of $[Ph_3PCuH]_6$ with carbon monoxide, Sneeden and

coworkers found that the same copper formate species was formed although much more slowly than with carbon dioxide and the reaction was inhibited by H_2.[19] This suggests that $[Ph_3PCuH]_6$ would probably not react with trace quantities of CO in hydrogen rapidly enough to be of major consequence. Even if copper formats did form in a copper hydride fuel cell from CO or CO_2 impurities, such a copper formate may be relatively stable. Appel et al have recently demonstrated that a copper hydride catalyst can be regenerated from a copper formate is capable of hydrogenating CO_2 catalytically, proving that a copper formate species is not necessarily a dead end.[20] This is an important practical advantage for a copper hydride based fuel cell. Platinum fuel cells must be either engineered to withstand small amounts of CO contaminants or use only hydrogen sources that are free of any CO contamination.

The thermodynamic potential of a hydrogen/oxygen fuel cell is 1.23 V.[21] Determining the practical cell voltage that could be achieved using a copper hydride based fuel cell is complicated by acid-base chemistry. In non-aqueous solvents, O_2 can be reduced to a superoxide radical anion ($O_2^{-\bullet}$)with reversible electrochemistry.[22] The $O_2^{-\bullet}/O_2$ redox potential in methylene chloride is -0.79 V vs SCE[23] (-1.19 V vs. Fc/Fc^+); the potential of $O_2^{-\bullet}/O_2$ is -0.18 V vs NHE in water.[24] The potential of the $O_2^{-\bullet}/O_2$ redox potential is not dramatically impacted by changes in solvent. At this potential, electron transfer from $[Ph_3PCuH]_6$ to oxygen would be modestly uphill and electron transfer from $[(p\text{-Anisyl})_3PCuH]_6$ and $[tol_3PCuH]_6$ would be approximately thermoneutral. As a result, it would be impossible to derive useful energy from a fuel cell under these conditions (no proton transfer to accompany redox events). It is clear that the role of protons in this reaction is critical. Protons are necessary to make oxygen reduction more thermodynamically favorable and removal of protons from copper hydride after oxidation is also necessary to regenerate copper hydrides using hydrogen gas as we will see in chapter 4.

In protic solvents, the protonanted superoxide radical anion disproportionates to form O_2 and H_2O_2.[22] The thermodynamic potential of a hydrogen/oxygen fuel cell is essentially the four electron, four proton reduction of O_2 which occurs at 1.23 V vs SHE since the redox potential of hydrogen/H^+ is defined as zero on this scale. Unfortunately, this potential for oxygen reduction depends on acidic aqueous conditions. Copper hydrides are not stable to strong acids although they do have good stability towards water and similarly weak acids. Comparing potentials for oxygen reduction under acidic conditions with the redox potentials of copper hydrides determined under aprotic conditions is unreasonable.

Many catalysts for hydrogen oxidation have been reported in the literature. Morris Bullock et al have reported several first-row metal catalysts with $P^R_2N^{R'}_2$ (cyclic 1,5-diaza-3,7-diphosphacyclooctane) ligands for hydrogen oxidation.[25-28] These $P^R_2N^{R'}_2$ catalysts model the active site of hydrogenase enzymes which use iron and/or nickel. The $P^R_2N^{R'}_2$ ligand in these catalysts functions as a proton relay to facilitate acid-base chemistry that must accompany the electron transfer reactions analogously to proton relays in natural hydrogenase enzymes which are very efficient catalysts for the oxidation of hydrogen and the reduction of protons.[29-31]

2.4 Determining Redox Potentials

The most common method of determining a redox potential is by cyclic voltammetry with a three electrode setup containing a working electrode, a counter electrode, and a reference electrode.[32] Cyclic voltammetry is a standard method, sometimes also called linear sweep voltammetry because the potential of the working electrode is swept across a range of potentials at a programmed rate. The potential is generally swept from a starting potential to a potential at

which the sweep direction is reversed and swept back to the starting potential at the same scan rate (mV/s), Figure 2.1. For a reversible system, both the oxidation and reduction events can be observed, demonstrating that the correct thermodynamic potential has been found.

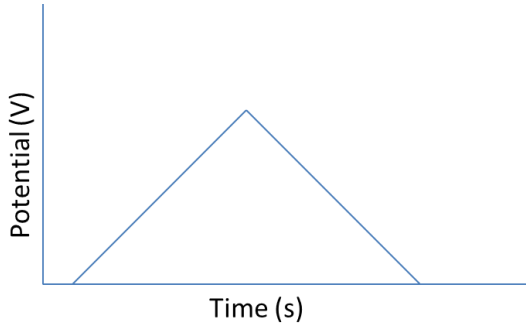

Figure 2.1. Potential as a function of time in a cyclic voltammetry experiment.

In this setup, the potential of the working electrode is varied while the current passed is measured. An opposing chemical reaction occurs at the counter electrode to balance the overall charge; however, this reaction is not necessarily the reverse of the reaction occurring at the working electrode. Often, solvent molecules may be oxidized or reduced at the counter electrode in order to compensate for the current of a reduction or oxidation reaction respectively at the working electrode. For this reason, the counter electrode is sometimes separated from the analyte solution by a porous frit to limit the impact these species could have on the analyte solution.

Ideally, the reference electrode consists of a redox couple with a reliable potential to which the potential of the working electrode can be compared. Historically, chemical potentials have been referenced to a normal hydrogen electrode (NHE)[33] or a standard hydrogen electrode (SHE)[34] with the thermodynamic hydrogen potential being defined as zero on these scales. However, in practice, a SHE electrode is difficult to implement in the laboratory, so other types

of electrodes are often used and the potentials converted to the desired scale. In aqueous electrochemistry, a saturated calomel electrode (SCE)[35] is typically the preferred reference electrode and potentials are frequently reported vs. SCE.

2.5 Non-aqueous Redox Potentials

Copper hydrides are not soluble in water and as a result their electrochemistry can only be investigated in non-aqueous solvent. Non-aqueous electrochemistry is somewhat less established than its aqueous counterpart, although it has been studied since the 1950s and presents some particular challenges.[36] In particular, non-aqueous solvents generally have lower dielectric constants than water, causing solution conductivity and ion pairing to be more common problems in non-aqueous electrochemistry.[37-39] However, non-aqueous electrochemistry has many advantages including larger electrochemical windows, aprotic solvents, and non-coordinating solvents. Unlike aqueous electrochemistry where there are plenty of well-behaved reference electrodes such as SCE, there is no equivalent for non-aqueous electrochemistry. A SCE can be used as a reference electrode for non-aqueous systems; however, there are plenty of drawbacks to doing so.[40] Most importantly, there can be a substantial junction potential between the aqueous solvent in the SCE and the non-aqueous analyte solution, especially in cases where the non-aqueous solvents used are immiscible with water. Failing to address this junction potential can lead to a sizeable error in determining the correct redox potential of the species being investigated. Preferably, a non-aqueous reference electrode is used instead. Among the few options for non-aqueous reference electrodes, an acetonitrile Ag/Ag^+ reference electrode[41] is the most popular choice. Even this reference electrode has drawbacks. Silver nitrate, typically used to prepare the electrode, is insoluble in many organic solvents including methylene

chloride. The electrode is most commonly prepared using acetonitrile which may still cause significant junction potentials when other solvents are used for the analyte. Despite all the drawbacks of reference electrodes in non-aqueous electrochemistry, many of them can be overcome by simply using an internal reference. Ferrocene can be added to the analyte solution and the potentials of the analyte can then be directly compared to ferrocene's redox couple which is reversible under nearly all conditions.[42] Other metallocenes such as decamethylferrocene or cobaltocene can be used in order to avoid overlapping important redox events. A metallocene reference species can be added to the analyte solution after investigation of the analyte redox chemistry, as was done in the case of copper hydrides, to be certain the reference species is not altering the chemistry of the desired analyte. Directly referencing measured potentials to ferrocene is advantageous in that it reduces error in comparing potentials; converting potentials between solvents and reference electrodes often depends on the redox potential for ferrocene and the assumption that it does not vary with solvent,[40, 43] which is not correct.[44-45]

2.6 Voltammetry of Hexameric Copper Hydrides

The $[Ph_3PCuH]_6/[Ph_3PCuH]_6^{+\bullet}$ electrochemical couple has a half-cell potential of -1.01 V vs Fc/Fc^+. With this strongly reducing potential, copper hydrides in conjunction with another half-cell where a reduction (such as that of oxygen) takes place can provide a useful voltage difference in a fuel cell or transfer an electron to a substrate molecule. $[Ph_3PCuH]_6$, $[tolyl_3PCuH]_6$, and $[(p\text{-anisyl})_3PCuH]_6$, were characterized by cyclic voltammetry and all found to have reversible redox potentials in methylene chloride (Figures 2.2-4). Respective $E_{1/2}$ values are −1.01 V, −1.12 V, and −1.15 V vs. Fc/Fc^+. With these potentials, hexameric copper hydrides are excellent single electron reductants with potentials similar to Co(II)/Co(III) in

cobaltocene/cobalticenium[46]; $[(p\text{-anisyl})_3PCuH]_6$ is only 180 mV less reducing than cobaltocene in methylene chloride.

The cyclic voltammograms of $[Ph_3PCuH]_6$, $[tolyl_3PCuH]6$, and $[(p\text{-anisyl})_3PCuH]_6$ are reversible with reduction/oxidation peak separations of 67 mV, 69 mV, and 66 mV respectively, slightly larger than the 59 mV separation expected for an ideal reversible single electron process. The larger than theoretical peak separation is caused by uncompensated solution resistance which was confirmed by varying the scan rate (Figure 2.5). A larger than theoretical separation was also observed for ferrocene.

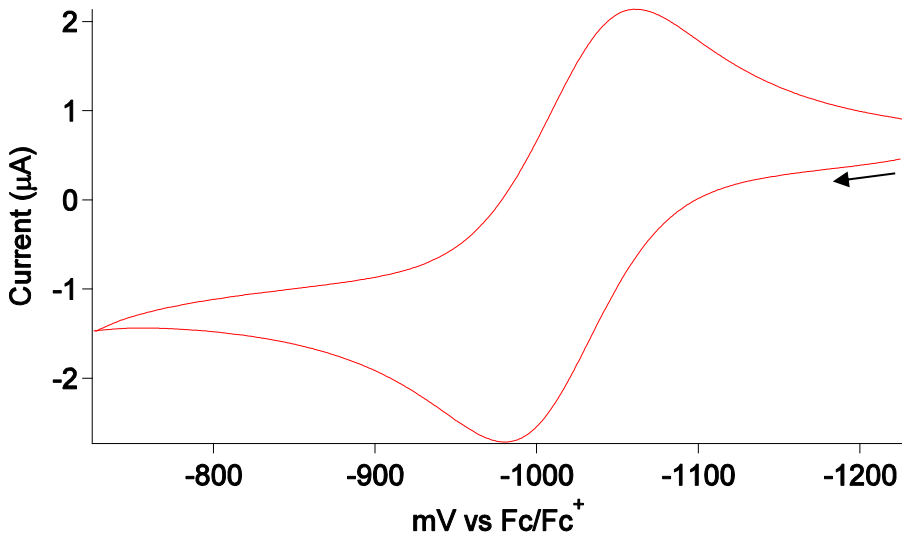

Figure 2.2. – Cyclic voltammogram of $[Ph_3PCuH]_6$. 0.001 Mol/L $[Ph_3PCuH]_6$, 0.1 Mol/L $[NBu_4][(C_6F_5)_4B]$ in CH_2Cl_2, 50 mV/s.

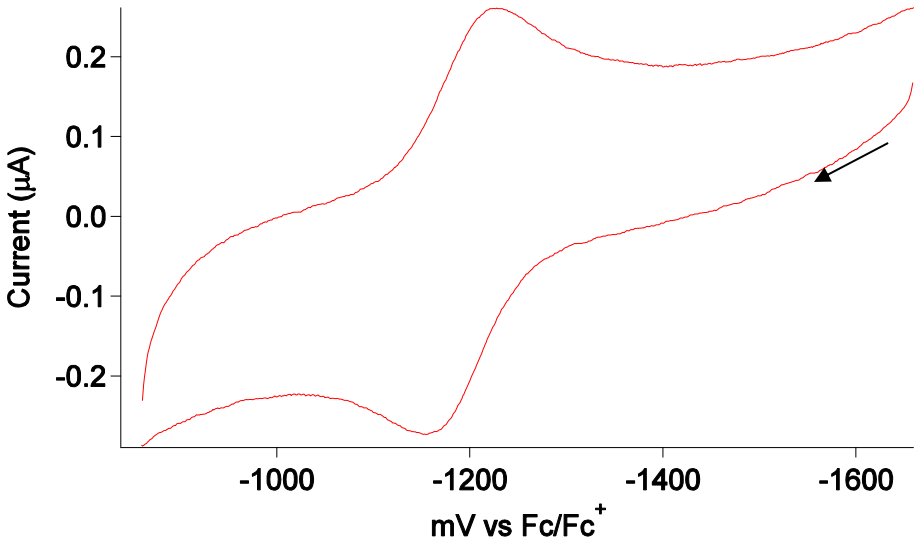

Figure 2.3. Cyclic voltammogram of $[tolyl_3PCuH]_6$. 0.001 Mol/L $[tolyl_3PCuH]_6$, 0.1 Mol/L $[NBu_4][(C_6F_5)_4B]$ in CH_2Cl_2, 100 mV/s.

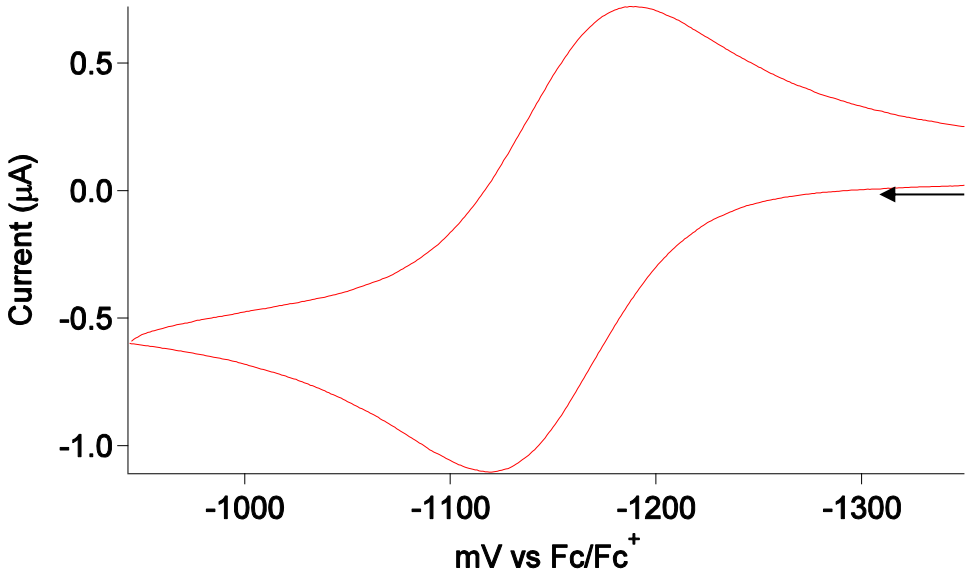

Figure 2.4. Cyclic voltammogram of $[(p\text{-anisyl})_3PCuH]_6$. 0.001 Mol/L $[(p\text{-anisyl})_3PCuH]_6$, 0.1 Mol/L $[NBu_4][(C_6F_5)_4B]$ in CH_2Cl_2, 25 mV/s.

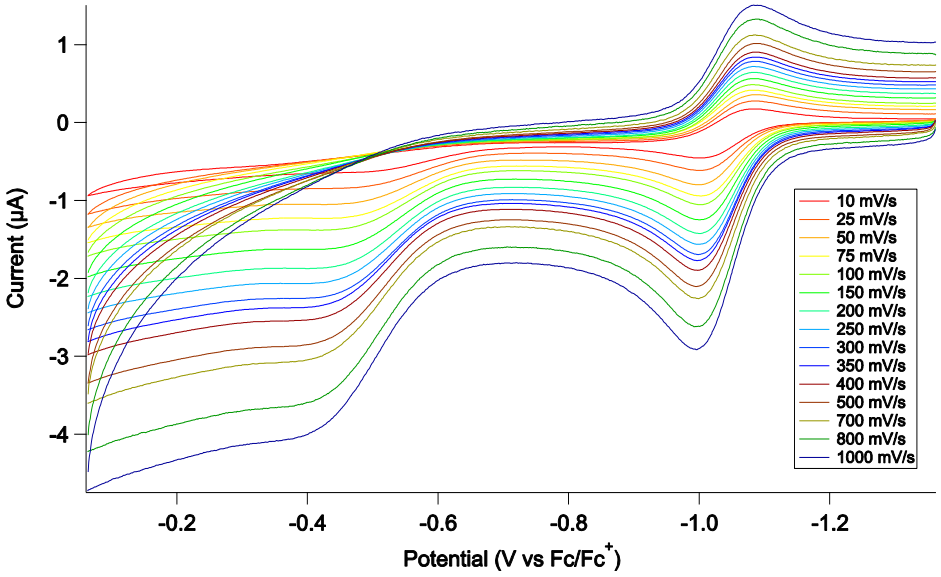

Figure 2.5. Increasing Scan rate causes an increase in ΔE for $[Ph_3PCuH]_6$. 0.001 Mol/L $[Ph_3PCuH]_6$, 0.1 Mol/L $[NBu_4][(C_6F_5)_4B]$ in CH_2Cl_2.

$[Tolyl_3PCuH]_6$ shows good solution stability like the other two hexameric clusters investigated electrochemically. However, when tetrabutylammonium tetrakis(pentafluorophenyl)borate is added as an electrolyte, $[tolyl_3PCuH]_6$ begins to decompose for reasons that are unclear. The solution turns from red to yellow/brown and the peak currents observed for a given scan rate decrease concurrently with the color change, indicating that the concentration of the copper hydride in solution is decreasing over time. The same behavior is observed in other solvents suitable for electrochemistry, such as α,α,α-trifluorotoluene. This more inert solvent for electrochemistry has otherwise similar properties to methylene chloride[47-48] (although its solvating ability is worse than methylene chloride and it is a poor solvent for copper hydrides). THF also showed similar behavior. The fact that $[tolyl_3PCuH]_6$ is stable without the electrolyte indicates that the electrolyte must be the problem despite careful preparation and purification by literature methods.[38] The more conventional electrolyte

tetrabutylammonium hexafluorophosphate which was obtained commercially also resulted in decomposition of $[tolyl_3PCuH]_6$ in solution. In spite of these problems, a reversible wave was observed by rapidly preparing a solution containing $[tolyl_3PCuH]_6$ in methylene chloride with tetrabutylammonium tetrakis(pentafluorophenyl)borate. The cyclic voltammogram in figure 2.3 appears to have more steeply sloped changes in current as potential changes (away from the redox events, near the potential limits at -900 mV and -1600 mV vs Fc/Fc^+), but this slope appearance is an artifact of the graph scaling; the current passed in the $[tolyl_3PCuH]_6^{0/+}$ redox couple is much smaller than the analogous current with $[Ph_3PCuH]_6$ and $[(p\text{-anisyl})_3PCuH]_6$. The change in current with change in potential at the edges of the graph is small and similar to that in figures 2.2 and 2.4.

The reversible electrochemistry of these species demonstrates that there is little structural change upon oxidation. The rest potential of the solution used in our electrochemical experiments proved to be −1.09 V vs Fc/Fc+ for $[Ph_3PCuH]_6$, which demonstrates that the cyclic voltammograms show oxidation of the neutral species. The fact that little current flows at the beginning of the scans reflects the fact that they start near the rest potential. The first wave observed is anodic, clearly indicating that the electrochemical process is $[Ph_3PCuH]_6/[Ph_3PCuH]_6^{+\bullet}$ rather than $[Ph_3PCuH]_6/[Ph_3PCuH]_6^{-\bullet}$. The strongly reducing potential of these three copper hydride clusters is unusual for being so negative relative to Fc/Fc^+, but not unique since there are other organometallic species with more reducing potentials.[46]

Two oxidations can be observed for $[Ph_3PCuH]_6$ and $[tolyl_3PCuH]_6$ (Figures 2.6 and 2.7) and four successive oxidations (Figure 2.8) can be observed by cyclic voltammetry experiments

with [(*p*-anisyl)$_3$PCuH]$_6$. These additional oxidations are irreversible, indicating that they are accompanied by irreversible chemical changes. Faster scan rates up to 1 V/s did not lead to reversible waves, the currents increased as anticipated with scan rate. When the turnaround potential is increased to more oxidizing values, the waves assigned to the [Ar$_3$PCuH]$_6$/[Ar$_3$PCuH]$_6^{+\bullet}$ couples become more irreversible.

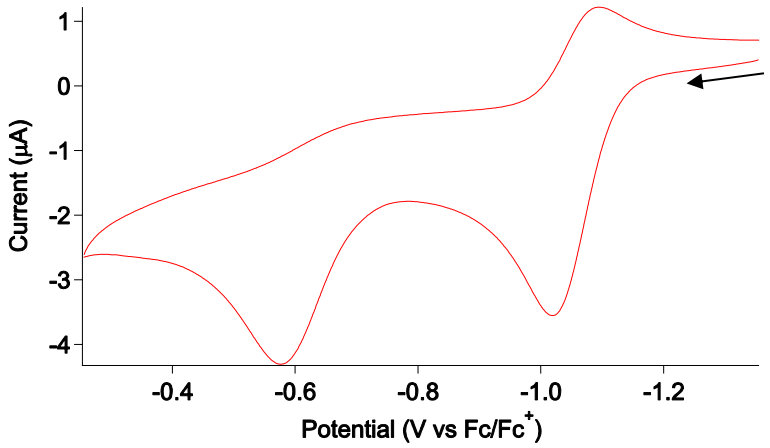

Figure 2.6. Cyclic Voltammogram of [Ph$_3$PCuH]$_6$ showing second (irreversible) oxidation. 0.001 Mol/L [Ph$_3$PCuH]$_6$, 0.1 Mol/L [NBu$_4$][(C$_6$F$_5$)$_4$B] in CH$_2$Cl$_2$, 100 mV/s.

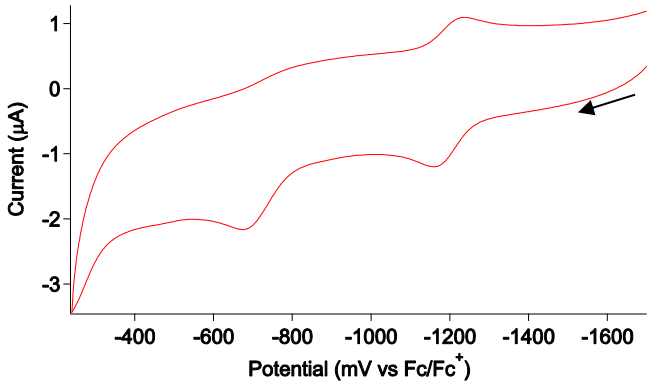

Figure 2.7. Cyclic Voltammogram of [tolyl$_3$PCuH]$_6$ showing second (irreversible) oxidation. 0.001 Mol/L [(*p*-anisyl)$_3$PCuH]$_6$, 0.1 Mol/L [NBu$_4$][(C$_6$F$_5$)$_4$B] in CH$_2$Cl$_2$, 25 mV/s.

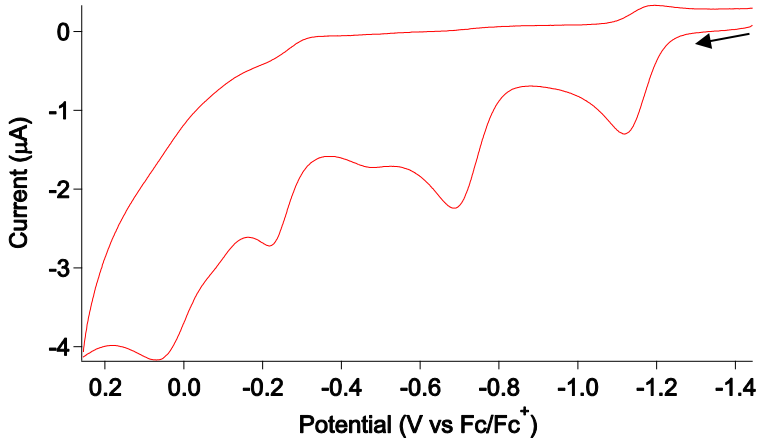

Figure 2.8. Cyclic Voltammogram of $[(p\text{-anisyl})_3PCuH]_6$ showing multiple oxidations. 0.001 Mol/L $[(p\text{-anisyl})_3PCuH]_6$, 0.1 Mol/L $[NBu_4][(C_6F_5)_4B]$ in CH_2Cl_2, 100 mV/s.

The reversible electrochemistry of these three hexameric clusters suggests that the corresponding radical cations $[Ar_3PCuH]_6^{+\bullet}$ are stable, at least on the time scale of the cyclic voltammetry measurements which take tens of seconds. The radical cation $[Ph_3PCuH]_6^{+\bullet}$ (figure 2.9) can be obtained by chemical oxidation with $Cp^*_2Fe[PF_6]$, which confirms that the $[Ph_3PCuH]_6/[Ph_3PCuH]_6^{+\bullet}$ potential is more negative than that of $Cp^*_2Fe/Cp^*_2Fe^+$ ($E_{1/2}$ = −590 mV vs Fc/Fc^+)[46].

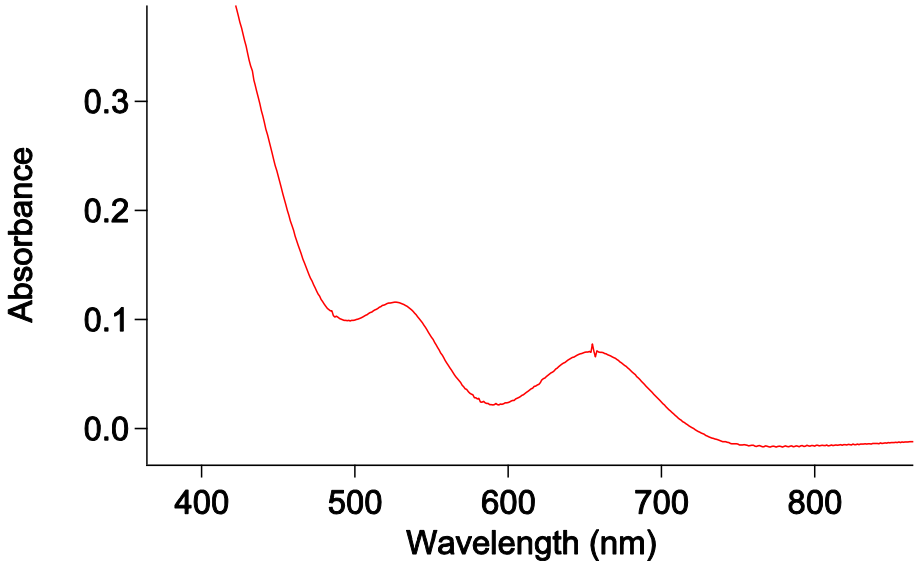

Figure 2.9. $[Ph_3PCuH]_6^{+\bullet}$ with λmax = 655 nm. The spectrum was observed after reacting 5.7 mg $[Ph_3PCuH]_6$ (2.9×10^{-6} mol) with 0.3 mg $[Cp^*_2Fe][PF_6]$ (6×10^{-7} mol, 0.2 equiv.) in methylene chloride.

2.7 Spectroelectrochemistry of $[Ph_3PCuH]_6$

To confirm that the product produced by chemical oxidation of $[Ph_3PCuH]_6$ by decamethylferrocenium is the same species that is formed electrochemically in the cyclic voltammetry experiments on the previous pages, UV-vis spectroelectrochemistry was used to observe $[Ph_3PCuH]_6^{+\bullet}$ formed by electrochemical oxidation of $[Ph_3PCuH]_6$ at -800 mV vs Fc/Fc^+(figure 2.10). Ideally, it should be possible to observe an EPR signal from $[Ph_3PCuH]_6^{+\bullet}$. However, attempts to observe it at room temperature and 77 K were unsuccessful, liquid helium temperatures may be required. The EPR spectrum would be complicated since there are six

copper nuclei with two different isotopes, ^{63}Cu and ^{65}Cu present with 69% and 31% respective abundances each being spin –3/2, along with six ^{1}H nuclei and six ^{31}P nuclei. In chapter 3, we will see this radical cation species appear as an intermediate in reactions with several different substrates.

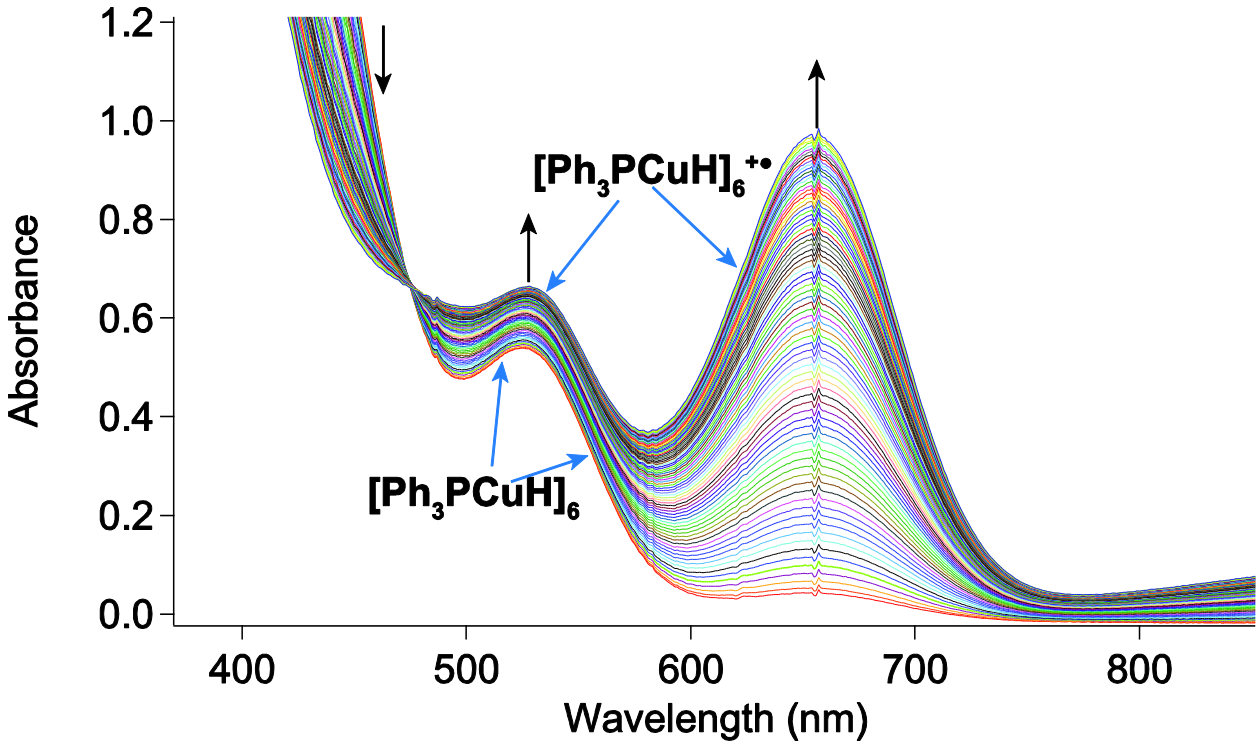

Figure 2.10. Spectroelectrochemical oxidation of $[Ph_3PCuH_6]$. $[Ph_3PCuH]_6^{+\bullet}$ with λ_{max} = 655 nm is observed by oxidizing $[Ph_3PCuH]_6$ in a methylene chloride solution containing 0.1 Mol/L $[nBu_4N][(C_6F_5)_4B]$ as an electrolyte at -800 mV vs. Fc/Fc^+.

2.8 Voltammetry of $[(dppbz)CuH]_3$

The trinuclear copper hydride $[(dppbz)CuH]_3$ was also investigated by cyclic voltammetry. In contrast to the behavior of its hexameric relatives, only a single irreversible oxidation wave is observed in its cyclic voltammogram (Figure 2.11).

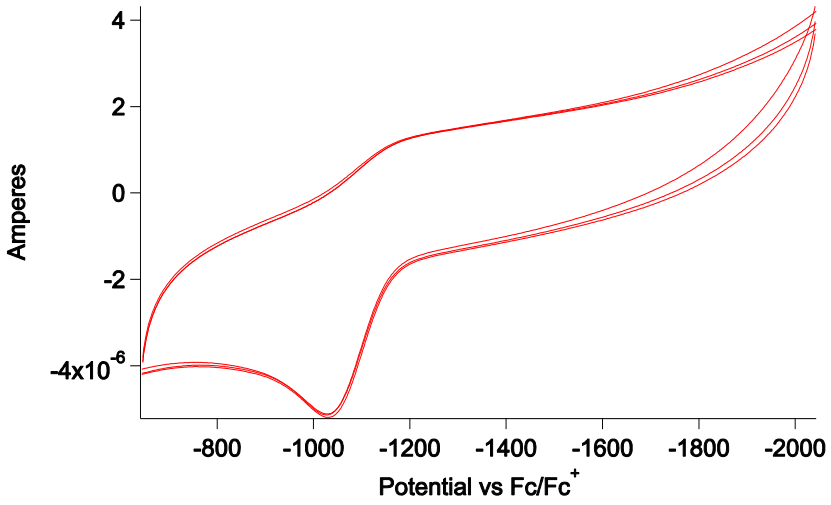

Figure 2.11. Cyclic voltammogram of $[(dppbz)CuH]_3$. 0.001 Mol/L $[(dppbz)CuH]_3$, 0.1 Mol/L $[NBu_4][(C_6F_5)_4B]$ in CH_2Cl_2, 100 mV/s.

In figure 2.11, six sweeps across the potential range are shown (three in each direction). The reproducibility of the scans demonstrates that the starting position of the scan does not impact the cyclic voltammogram despite the most reducing potential (more negative) being relatively far from the rest potential of the solution. This fact is apparent from the non-zero current at the most negative potentials which is approaching the window of the solvent electrolyte combination (0.1 Mol/L $[nBu_4N][(C_6F_5)_4B]$ in methylene chloride).

The irreversibility of the cyclic voltammogram indicates that the $[(dppbz)CuH]_3^{+\bullet}$ radical cation is not stable. Due to the dramatic increase in acidity of hydride ligands upon oxidation, many transition metal radical cations have irreversible cyclic voltammograms because they

rapidly transfer a proton after oxidation.[14] The M-H bond strength is often weakened by one electron oxidation of the neutral parent complex. In chapter 3, we will see evidence that the M-H bonds are much weaker in $[Ph_3PCuH]_6^{+\bullet}$ than in $[Ph_3PCuH]_6$. One method of overcoming these problems and obtaining reversible potentials is to increase the scan rate. Within the limits of our experimental setup, increasing the scan rate did not result in a more reversible wave. In some cases, ultramicroelectrodes can be used to achieve reversible cyclic voltammograms; however, our lab does not have an ultramicroelectrode. Radical reactions, particularly in methylene chloride solvent are also of concern due to its reactivity towards radicals.

The cyclic voltammogram of $[(dppbz)CuH]_3$ is also irreversible in 1,2-difluorobenzene (Figure 2.12). This solvent is much less prone to radical reactions than methylene chloride and unlike α,α,α-trifluorotoluene, 1,2-difluorobenzene is an excellent solvent for neutral copper hydrides. In addition to being more inert than methylene chloride, 1,2-difluorobenzene also has a high dielectric constant and good electrochemical properties. In 1,2-difluorobenzene, the oxidation wave was observed at -0.87 mV vs Fc/Fc^+.

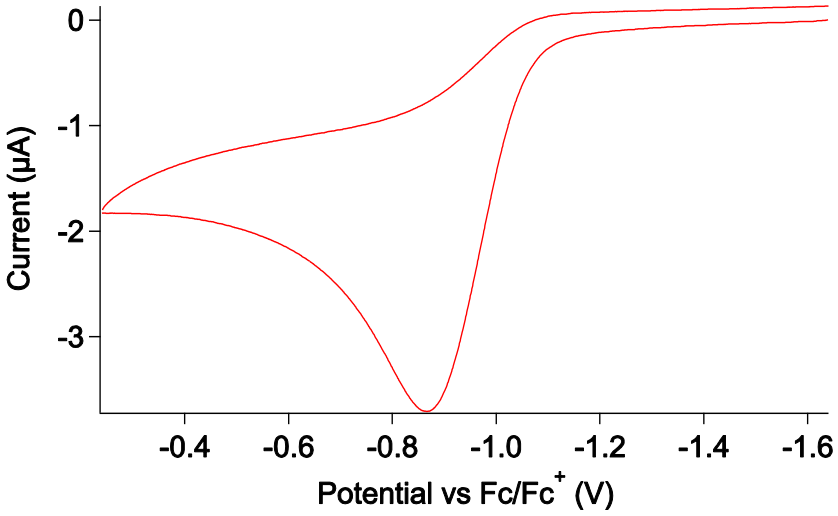

Figure 2.12. Cyclic voltammogram of $[(dppbz)CuH]_3$ in 1,2-difluorobenzene. 0.001 Mol/L $[(dppbz)CuH]_3$, 0.1 Mol/L $[NBu_4][(C_6F_5)_4B]$ in CH_2Cl_2, 100 mV/s.

2.9 Determining the Electron Transfer Self-Exchange Rate for $[Ph_3PCuH]_6$.

Voltammetry typically only measures the thermodynamics of an electron transfer. However, both the kinetics and the thermodynamics of an electron transfer reaction determine whether or not it will actually occur in a reaction sequence. There are several methods available for measuring electron transfer self-exchange rates. A particularly favorable case is tris(ethylenediamine)cobalt(II/III), discussed earlier in this chapter. However, the majority of chemical systems are not amenable to such a strategy.

Radioisotopic labeling has been a useful method of determining electron transfer self-exchange rates. Some early examples measured by this method include an earlier measurement, using ^{60}Co, of the tris(ethylenediamine)cobalt(II/III) self-exchange rate and

hexamminecobalt(II/III).[49] Electron transfer self-exchange between thallous and thallic ions in aqueous solution has been studied using ^{204,206}Tl.[50-51] This method has obvious drawbacks as well, including the limited availability of suitable radionuclides if isotopes with suitable half-lives even exist for the element of interest. The biggest drawback to radioisotopic labeling is that it is only aplicable to relatively slow reactions, since chemical separations are necessary before the tracer is quantified; the approach to equilibrium cannot be faster than the chemist doing the experiment.

Determining electron transfer self-exchange rates by line broadening methods is presently the preferred technique. Line broadening methods by either EPR or NMR can be used. The concentration of at least one species present in solution must be accurately known, under favorable circumstances, only the concentration of one species needs to be known as we will soon see. The equations relating NMR line width to electron transfer-self exchange rates were first derived by de Boer and MacLean[52-53] and the relationship between line width, concentrations, and the electron transfer self-exchange rate is given by equation 2.1. In equation 2.1, f_N and f_R are the mole fractions of the neutral species and radical species respectively, τ_R is the lifetime of the radical, a is the hyperfine coupling constant, T_{1e} is the spin lattice relaxation time and T_{2ex}^{-1} is the line broadening due to electron transfer self-exchange.[54]

$$\Delta(T_{2ex}^{-1}) = \frac{f_R \tau_R a^2 / 4}{1 + f_N \tau_R a^2 / 4 + 2\tau_R T_{1e}^{-1}} \quad (2.1)$$

There are two limiting cases of equation 2.1. In the large hyperfine limit:[52-53, 55-56]

$$f_R \tau_R a^2 / 4 \gg 1 + 2\tau_R T_{1e}^{-1}$$

This leads to the simplification of equation 2.1 to equation 2.2.[54]

$$\Delta(T_{2ex}^{-1}) = k[\text{Radical}] \quad (2.2)$$

In the small hyperfine limit: [53, 55]

$$f_R \tau_R a^2 / 4 + 2\tau_R T_{1e}^{-1} \ll 1$$

which leads to equation 2.3.[54]

$$\Delta(T_{2ex}^{-1}) = \left(\frac{a^2}{4k}\right)\left(\frac{[radical]}{[neutral]}\right)^2 \quad (2.3)$$

Systems in the large hyperfine limit are much easier to deal with experimentally, because only the concentration of radical species in solution needs to be known. It can be easily determined whether a system is in the large hyperfine limit or the small hyperfine limit by the effect on line width of temperature. In the large hyperfine limit, line width increases because k (the rate constant) is directly proportional to the excess line width; as temperature increases, k increases. In the small hyperfine limit, k is inversely proportional to the excess line width; so as k increases with increasing temperature, the excess line width decreases.

In the case of $[Ph_3PCuH]_6/[Ph_3PCuH]_6^{+\bullet}$, the system is in the large hyperfine limit. Figure 2.13 shows the impact of temperature on the line width of the ^1H resonance assigned to the hydride ligands in $[Ph_3PCuH]_6$.

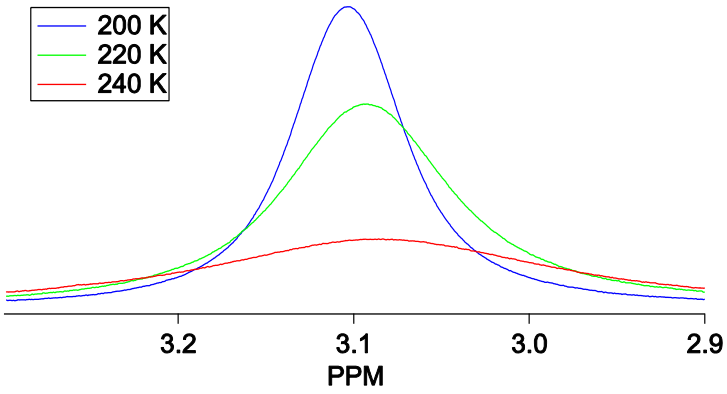

Figure 2.13. Effects of temperature on the NMR line width of the hydride ligands in $[Ph_3PCuH]_6/[Ph_3PCuH]_6^{+\bullet}$ in THF-d_8. The solution contains 6.1×10^{-4} Mol/L $[Ph_3PCuH]_6^{+\bullet}$.

The concentration of copper hydride radical cation in solution, $[Ph_3PCuH]_6^{+\bullet}$, is determined by the amount of decamethylferrocenium added as an oxidant. The oxidation of $[Ph_3PCuH]_6$ by decamethylferrocenium is assumed to be quantitative. However, the instability of $[Ph_3PCuH]_6^{+\bullet}$ at room temperature (discussed further in chapter 4) is a significant source of error in the experiment. Samples were prepared and cooled in a dry ice/acetone bath as quickly as possible before being transferred to the NMR. Figure 2.14 shows the effects of concentration on the NMR line width.

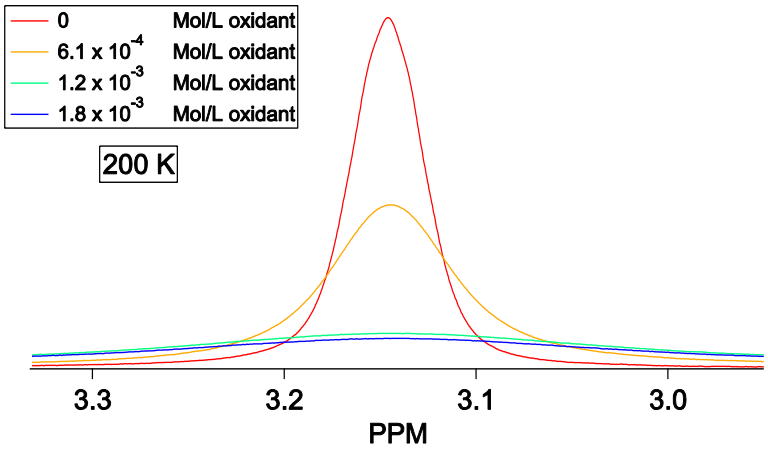

Figure 2.14. NMR line width of the hydride ligands in $[Ph_3PCuH]_6$ in THF-d_8 with four different concentrations of $[Ph_3PCuH]_6^{+\bullet}$.

Line widths were measured by iteratively modeling line width in a simulated spectrum until the best possible fit to the experimental data could be obtained using MestReNova's "Spin Simulation" feature. A plot of measured line widths vs. concentration is shown in Figure 2.15. The slope of the linear least squares regression line gives the rate constant for electron transfer self-exchange. Activation parameters were determined to be $\Delta H^{\ddagger} = 2.0$ kcal/mol and $\Delta S^{\ddagger} = -23$ cal•mol^{-1}K^{-1}, which are similar to other activation parameters reported in the literature for other homogeneous outer-sphere electron transfer self-exchange reactions.[57]

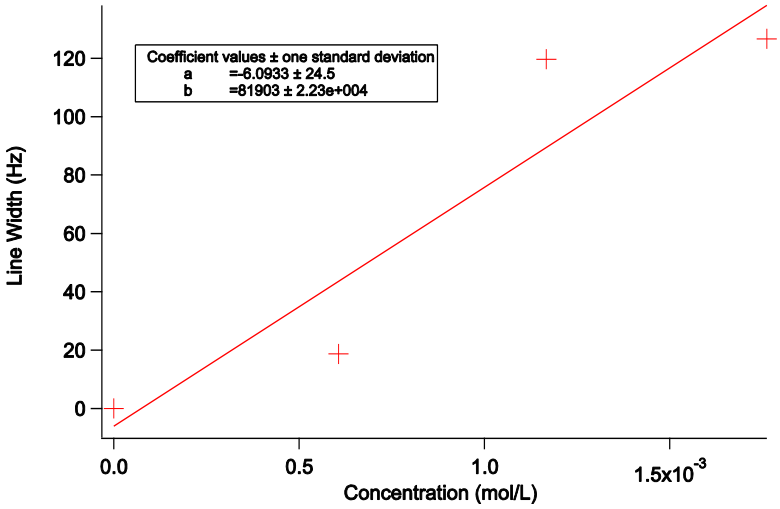

Figure 2.15. Measured NMR line width as a function of concentration of $[Ph_3PCuH]_6^{+\bullet}$ in solution at 200 K.

The measured rate constants are shown in table 2.1 along with the rate constant extrapolated to 298 K. The 298 K rate constant was determined using KINPAR, a program for determining activation parameters.

Table 2.1. Rate constants for electron transfer self-exchange in $[Ph_3PCuH]_6/[Ph_3PCuH]_6^{+\bullet}$ at low temperature.

Temperature (K)	**Rate constant ($M^{-1}s^{-1}$)**
180	9.13×10^4
200	1.96×10^5
220	3.13×10^5
298	1.5×10^6 (extrapolated)

With an extrapolated electron transfer self-exchange rate constant of 1.5×10^6 $M^{-1}s^{-1}$, $[Ph_3PCuH]_6/[Ph_3PCuH]_6^{+\bullet}$ has a respectable self-exchange rate, though it is not close to the fastest measured. This along with the strongly reducing redox potentials discussed earlier make copper hydride clusters good candidates for electron transfer to other species of interest, as will be discussed in chapter 3. The rate of electron transfer self-exchange is determined by how much reorganization is required to undergo a redox process; most importantly, Marcus has described the relationship between the electron transfer self-exchange rates of two species and the rate of electron transfer between them (equation 2.4).[58] K_{12} is the equilibrium constant for electron transfer between two species, k_{11} and k_{22} are the self-exchange rates, *f* is a factor which is frequently close to 1 (the physical meaning of *f* is defined in equation 2.5, z is the collisional frequency).[58]

$$k_{12} = \sqrt{K_{12} k_{11} k_{22} f} \quad (2.4)$$

$$\log(f) = \frac{(\log K_{12})^2}{4\log\left(\frac{k_{11}k_{22}}{z^2}\right)} \quad (2.5)$$

Because copper hydride clusters have many bonds and many metal atoms related to each other by symmetry, the charge distribution is presumably well distributed over the six atoms in the copper core upon oxidation; therefore, each bond should require little rearrangement leading to an overall fast electron transfer self-exchange rate especially for a molecule of its size, 1961.1 Da.

General Experimental Procedures

CH_2Cl_2 was deoxygenated and dried by two successive columns (Q-5, activated alumina). 1,2-difluorobenzene was dried by stirring over CaH_2 and vacuum transferred to a receiving flask followed by three freeze-pump-thaw cycles to remove oxygen. THF-d_8 and C_6D_6 were dried over potassium benzophenone ketyl and vacuum transferred to a receiving flask. All solutions were prepared under inert atmosphere in a glovebox.

Cyclic Voltammetry

Electrochemical experiments for all species were carried out in methylene chloride containing 0.1 mol/L tetrabutylammonium tetrakis(pentafluorophenyl)borate as a supporting electrolyte (synthesized by literature procedures[38]). The reference electrode was Ag/Ag^+ in CH_3CN, and was separated from the analyte solution by a vycor frit; the counter electrode was not isolated from the analyte solution. The potentials were referenced to Fc/Fc^+ by adding ferrocene at the end of each experiment.

General Procedures for Electron Transfer Self-Exchange Measurements

Quantities of solvent and solution at all stages of the experiment were determined by mass, not volume. A stock solution of decamethylferrocenium tetrakis(pentafluorophenyl)borate was prepared (2.78×10^{-2} mol/kg). A sample containing a known concentration of $[Ph_3PCuH]_6$ in THF-d_8 was prepared (6.01×10^{-3} mol/kg). A portion of this $[Ph_3PCuH]_6$ solution was transferred to a J-Young tube and the exact amount of solution transferred was determined by mass (0.997 g), when molarity is listed, it is assumed to be equal to molality divided by the room temperature density of THF-d_8 although this is not entirely accurate since the experiments are

conducted well below room temperature and the volumes change with temperature. This conversion also assumes the change in density of THF-d_8 is negligible when small amounts of $[Ph_3PCuH]_6$ and decamethylferrocenium tetrakis(pentafluorophenyl)borate are dissolved in it. ^{1}H NMR spectra were recorded at each of the temperatures used in a particular experimental run (ranging from 180 K to 300 K) to determine the line width of the ^{1}H resonance assigned to the hydride ligands in $[Ph_3PCuH]_6$ for later comparison to the electron transfer self-exchange broadened line widths. A small aliquot of the decamethylferrocenium stock solution was added and the ^{1}H NMR spectra recorded at each of the experimental temperatures. The sample was then returned to the glovebox for addition of subsequent aliquots of decamethylferrocenium followed by recording of the ^{1}H NMR spectra at each temperature. The decamethylferrocenium aliquots were 15.8 mg, 14.7 mg, and 15.6 mg of decamethylferrocenium stock solution in the experimental run from which the experimental rate constants are listed.

Chapter 2 References

1. A portion of this chapter has been published in J. Am. Chem. Soc. 2013, 135 (46), 17262-17265. Sophie Rubashkin, an undergraduate student from Barnard College I mentored helped prepare the solutions for the cyclic voltammetry experiments in 1,2-difluorobenzene and collaborated in the cyclic voltammetry experiments in that solvent.

2. Moser, C. C.; Keske, J. M.; Warncke, K.; Farid, R. S.; Dutton, P. L., Nature of biological electron transfer. *Nature* **1992,** *355* (6363), 796-802.

3. Birch, A. J., 117. Reduction by dissolving metals. Part I. *Journal of the Chemical Society (Resumed)* **1944**, 430-436.

4. Birch, A. J., 212. Reduction by dissolving metals. Part II. *Journal of the Chemical Society (Resumed)* **1945**, 809-813.

5. Birch, A. J., 119. Reduction by dissolving metals. Part III. *Journal of the Chemical Society (Resumed)* **1946**, 593-597.

6. Birch, A. J., 327. Reduction by dissolving metals. Part V. *Journal of the Chemical Society (Resumed)* **1947**, 1642-1648.

7. Birch, A. J., 25. Reduction by dissolving metals. Part IV. *Journal of the Chemical Society (Resumed)* **1947**, 102-105.

8. Mousseau, J. J.; Charette, A. B., Direct Functionalization Processes: A Journey from Palladium to Copper to Iron to Nickel to Metal-Free Coupling Reactions. *Accounts of Chemical Research* **2013,** *46* (2), 412-424.

9. Chirik, P. J.; Wieghardt, K., Radical Ligands Confer Nobility on Base-Metal Catalysts. *Science* **2010,** *327* (5967), 794-795.

10. Zuo, W.; Lough, A. J.; Li, Y. F.; Morris, R. H., Amine(imine)diphosphine Iron Catalysts for Asymmetric Transfer Hydrogenation of Ketones and Imines. *Science* **2013,** *342* (6162), 1080-1083.

11. Friedfeld, M. R.; Shevlin, M.; Hoyt, J. M.; Krska, S. W.; Tudge, M. T.; Chirik, P. J., Cobalt Precursors for High-Throughput Discovery of Base Metal Asymmetric Alkene Hydrogenation Catalysts. *Science* **2013,** *342* (6162), 1076-1080.

12. Jagadeesh, R. V.; Surkus, A.-E.; Junge, H.; Pohl, M.-M.; Radnik, J.; Rabeah, J.; Huan, H.; Schünemann, V.; Brückner, A.; Beller, M., Nanoscale Fe_2O_3-Based Catalysts for Selective Hydrogenation of Nitroarenes to Anilines. *Science* **2013,** *342* (6162), 1073-1076.

13. Dwyer, F. P.; Sargeson, A. M., The Rate of Electron Transfer Between the Tris-(Ethylenediamine)-Cobalt(II) and Cobalt(III) Ions. *The Journal of Physical Chemistry* **1961,** *65* (10), 1892-1894.

14. Tilset, M., 1.11 - Organometallic Electrochemistry: Thermodynamics of Metal–Ligand Bonding. In *Comprehensive Organometallic Chemistry III*, Editors-in-Chief: Robert, H. C.; Mingos, D. M. P., Eds. Elsevier: Oxford, 2007; pp 279-305.

15. Carrette, L.; Friedrich, K.; Stimming, U., Fuel cells–fundamentals and applications. *Fuel cells* **2001,** *1* (1), 5-39.

16. Winter, M.; Brodd, R. J., What Are Batteries, Fuel Cells, and Supercapacitors? *Chemical Reviews* **2004,** *104* (10), 4245-4270.

17. Churchill, M. R.; DeBoer, B. G.; Rotella, F. J.; Abu Salah, O. M.; Bruce, M. I., Determination of the crystal structure and molecular geometry of [hydrotris(1-pyrazolyl)borato]copper(I) carbonyl. Unique structural investigation of a copper-carbonyl linkage. *Inorganic Chemistry* **1975,** *14* (9), 2051-2056.

18. Bruce, M. I., Carbonyl chemistry of the group IB metals. *Journal of Organometallic Chemistry* **1972,** *44* (2), 209-226.

19. Beguin, B.; Denise, B.; Sneeden, R. P. A., Hydrocondensation of CO2 : II. Reaction of carbon dioxide and carbon monoxide with [HCuPPh3]6. *Journal of Organometallic Chemistry* **1981,** *208* (1), C18-C20.

20. Zall, C. M.; Linehan, J. C.; Appel, A. M., A Molecular Copper Catalyst for Hydrogenation of CO_2 to Formate. *ACS Catalysis* **2015,** *5* (9), 5301-5305.

21. Yeager, E., Dioxygen electrocatalysis: mechanisms in relation to catalyst structure. *Journal of Molecular Catalysis* **1986,** *38* (1–2), 5-25.

22. Huang, X.-J.; Rogers, E. I.; Hardacre, C.; Compton, R. G., The Reduction of Oxygen in Various Room Temperature Ionic Liquids in the Temperature Range 293−318 K: Exploring the Applicability of the Stokes−Einstein Relationship in Room Temperature Ionic Liquids. *The Journal of Physical Chemistry B* **2009,** *113* (26), 8953-8959.

23. Peover, M. E.; White, B. S., Electrolytic reduction of oxygen in aprotic solvents: The superoxide ion. *Electrochimica Acta* **1966,** *11* (8), 1061-1067.

24. Koppenol, W. H.; Stanbury, D. M.; Bounds, P. L., Electrode potentials of partially reduced oxygen species, from dioxygen to water. *Free Radical Biology and Medicine* **2010,** *49* (3), 317-322.

25. Liu, T.; DuBois, D. L.; Bullock, R. M., An iron complex with pendent amines as a molecular electrocatalyst for oxidation of hydrogen. *Nat Chem* **2013,** *5* (3), 228-233.

26. Yang, J. Y.; Chen, S.; Dougherty, W. G.; Kassel, W. S.; Bullock, R. M.; DuBois, D. L.; Raugei, S.; Rousseau, R.; Dupuis, M.; DuBois, M. R., Hydrogen oxidation catalysis by a nickel diphosphine complex with pendant tert-butyl amines. *Chemical Communications* **2010,** *46* (45), 8618-8620.

27. Yang, J. Y.; Bullock, R. M.; Shaw, W. J.; Twamley, B.; Fraze, K.; DuBois, M. R.; DuBois, D. L., Mechanistic Insights into Catalytic H_2 Oxidation by Ni Complexes Containing a Diphosphine Ligand with a Positioned Amine Base. *Journal of the American Chemical Society* **2009,** *131* (16), 5935-5945.

28. Hulley, E. B.; Helm, M. L.; Bullock, R. M., Heterolytic cleavage of H_2 by bifunctional manganese(i) complexes: impact of ligand dynamics, electrophilicity, and base positioning. *Chemical Science* **2014,** *5* (12), 4729-4741.

29. Vincent, K. A.; Parkin, A.; Armstrong, F. A., Investigating and Exploiting the Electrocatalytic Properties of Hydrogenases. *Chemical Reviews* **2007,** *107* (10), 4366-4413.

30. Fontecilla-Camps, J. C.; Volbeda, A.; Cavazza, C.; Nicolet, Y., Structure/Function Relationships of [NiFe]- and [FeFe]-Hydrogenases. *Chemical Reviews* **2007,** *107* (10), 4273-4303.

31. Tard, C.; Liu, X.; Ibrahim, S. K.; Bruschi, M.; Gioia, L. D.; Davies, S. C.; Yang, X.; Wang, L.-S.; Sawers, G.; Pickett, C. J., Synthesis of the H-cluster framework of iron-only hydrogenase. *Nature* **2005,** *433* (7026), 610-613.

32. Bard, A. J.; Faulkner, L. R., *Electrochemical Methods: Fundamentals and Applications*. Wiley: 2000.

33. Ramette, R. W., Outmoded terminology: The normal hydrogen electrode. *Journal of Chemical Education* **1987,** *64* (10), 885.

34. Trasatti, S., The absolute electrode potential: an explanatory note (Recommendations 1986). In *Pure and Applied Chemistry*, 1986; Vol. 58, p 955.

35. Banus, M. G., A Design for a Saturated Calomel Electrode. *Science* **1941,** *93* (2425), 601-602.

36. Izutsu, K., Polarography and Voltammetry in Non-Aqueous Solutions. In *Electrochemistry in Nonaqueous Solutions*, Wiley-VCH Verlag GmbH & Co. KGaA: 2003; pp 223-267.

37. LeSuer, R. J.; Geiger, W. E., Improved Electrochemistry in Low-Polarity Media Using Tetrakis(pentafluorophenyl)borate Salts as Supporting Electrolytes. *Angewandte Chemie International Edition* **2000,** *39* (1), 248-250.

38. LeSuer, R. J.; Buttolph, C.; Geiger, W. E., Comparison of the Conductivity Properties of the Tetrabutylammonium Salt of Tetrakis(pentafluorophenyl)borate Anion with Those of Traditional Supporting Electrolyte Anions in Nonaqueous Solvents. *Analytical Chemistry* **2004,** *76* (21), 6395-6401.

39. Barrière, F.; Geiger, W. E., Use of Weakly Coordinating Anions to Develop an Integrated Approach to the Tuning of $\Delta E_{1/2}$ Values by Medium Effects. *Journal of the American Chemical Society* **2006,** *128* (12), 3980-3989.

40. Pavlishchuk, V. V.; Addison, A. W., Conversion constants for redox potentials measured versus different reference electrodes in acetonitrile solutions at 25°C. *Inorganica Chimica Acta* **2000,** *298* (1), 97-102.

41. Butler, J. N., Reference electrodes. *Advances in Electrochemistry and Electrochemical Engineering* **1970,** *7*, 77-175.

42. Gagne, R. R.; Koval, C. A.; Lisensky, G. C., Ferrocene as an internal standard for electrochemical measurements. *Inorganic Chemistry* **1980,** *19* (9), 2854-2855.

43. Koepp, H. M., *Z. Elektrochem.* **1960**, 483-491.

44. Alexander, R.; Parker, A. J.; Sharp, J. H.; Waghorne, W. E., Solvation of ions. XVI. Solvent activity coefficients of single ions. Recommended extrathermodynamic assumption. *Journal of the American Chemical Society* **1972,** *94* (4), 1148-1158.

45. McDevitt, M. R.; Addison, A. W., Medium effects on the redox properties of tris(2,2′-bipyridyl)ruthenium complexes. *Inorganica Chimica Acta* **1993,** *204* (2), 141-146.

46. Connelly, N. G.; Geiger, W. E., Chemical Redox Agents for Organometallic Chemistry. *Chemical Reviews* **1996,** *96* (2), 877-910.

47. Ohrenberg, C.; Geiger, W. E., Electrochemistry in Benzotrifluoride: Redox Studies in a "Noncoordinating" Solvent Capable of Bridging the Organic and Fluorous Phases. *Inorganic chemistry* **2000,** *39* (13), 2948-2950.

48. LeSuer, R. J.; Geiger, W. E., Approaches to analytical and synthetic electrochemistry in fluorous solvent-containing media. *Journal of Electroanalytical Chemistry* **2006,** *594* (1), 20-26.

49. Lewis, W. B.; Coryell, C. D.; Irvine, J. W., S 81. The electron transfer (exchange) between cobaltous and cobaltic amine complexes. *Journal of the Chemical Society (Resumed)* **1949,** (0), S386-S392.

50. Harbottle, G.; Dodson, R. W., The Exchange Reaction Between the Two Oxidation States of Thallium in Perchloric Acid Solutions. *Journal of the American Chemical Society* **1948,** *70* (2), 880-880.

51. Prestwood, R. J.; Wahl, A. C., Exchange Reaction Between Thallium (I) and Thallium (III) Ions in Perchloric and Nirtic Acid Solutions. *Journal of the American Chemical Society* **1948,** *70* (2), 880-881.

52. de Boer, E.; MacLean, C., NMR Study of Electron Transfer Rates and Spin Densities in p-Xylene and p-Diethylbenzene Anions. *The Journal of Chemical Physics* **1966,** *44* (4), 1334-1342.

53. de Boer, E.; Van Willigen, H., Chapter 3 Nuclear magnetic resonance of paramagnetic systems. *Progress in Nuclear Magnetic Resonance Spectroscopy* **1967,** *2* (0), 111-161.

54. Harlan, C. J.; Hascall, T.; Fujita, E.; Norton, J. R., The One-Electron Oxidation of an Azazirconacyclobutene in the Presence of $B(C_6F_5)_3$. *Journal of the American Chemical Society* **1999,** *121* (31), 7274-7275.

55. McConnell, H. M.; Berger, S. B., Rates of Paramagnetic Pulse Reactions by Nuclear Magnetic Resonance. *The Journal of Chemical Physics* **1957,** *27* (1), 230-234.

56. Solomon, I.; Bloembergen, N., Nuclear Magnetic Interactions in the HF Molecule. *The Journal of Chemical Physics* **1956,** *25* (2), 261-266.

57. Weaver, M. J.; Yee, E. L., Activation parameters for homogeneous outer-sphere electron-transfer reactions. Comparisons between self-exchange and cross reactions using Marcus' theory. *Inorganic Chemistry* **1980,** *19* (7), 1936-1945.

58. Marcus, R. A., On the Theory of Electron-Transfer Reactions. VI. Unified Treatment for Homogeneous and Electrode Reactions. *The Journal of Chemical Physics* **1965,** *43* (2), 679-701.

Chapter 3 Copper Hydride Reagents for Small Molecule Transformations

3.1 Introduction

The copper hydride cluster $[Ph_3PCuH]_6$ is a textbook reagent in organic chemistry. We have already examined the structural aspects of this compound in chapter 1 and its electrochemistry in chapter 2. This compound, popularly known as "Stryker's Reagent" or the "Osborn complex," was developed as a reagent for the selective 1,4-hydrogenation of α,β-unsaturated carbonyls by Jeff Stryker in the late 1980s.[1-7] Stryker's reagent has since become commercially available through Aldrich and Fisher and we have found the purity of commercial samples to be of generally acceptable quality. However, some commercial samples do have large amounts of free triphenylphosphine, which can impact the reactivity. The air sensitivity of the compound can also be an issue, depending on how it is packaged. Many researchers, including ourselves, prefer to prepare it in the laboratory.[8-9]

In the 1990s and 2000s, Buchwald and Lipshutz were instrumental in developing highly enantioselective copper hydride mediated reductions using chiral phosphines, with ee's reaching 99%.[10-14] Lipshutz also investigated organosilanes as stoichiometric reagents to regenerate copper hydrides,[15-16] including some inexpensive silanes such as polymethylhydrosiloxane (PMHS) to regenerate copper hydrides. The ability to use organosilanes to make copper hydride reactions catalytic has made the application of copper hydrides in synthetic chemistry more practical, particularly when expensive chiral ligands are employed.

Outside of organic chemistry, copper hydrides have also attracted interest as catalysts for CO_2 reduction chemistry.[17] Copper hydrides readily react with carbon dioxide; however,

regenerating copper hydrides from the copper containing products of this reaction is a formidable challenge.[18] After a two-and-a-half decade hiatus in CO_2 chemistry with copper hydrides, in the past few years copper hydrides have once again emerged as a system of interest for CO_2 hydrogenation.[18-20] Due to the high thermodynamic stability of carbon dioxide, catalytically converting it to anything else requires significant driving force. Typically, the necessary driving force for an overall catalytic reaction will require stoichiometric amounts of base; or stoichiometric use of a silane or borohydride reagent as the hydride source to form a strong bond such as B-O or Si-O.

Christopher Zall and Aaron Appel have recently demonstrated that a system related to Caulton's copper hydride $Cu_2(\mu\text{-}H)_2[\kappa^2\text{-}CH_3C(CH_2PPh_2)_3]_2)]$ (discussed in chapter 1)[21] is capable of catalytically hydrogenating CO_2 in the presence of a base.[18] Rather than using Caulton's hydride, Zall and Appel used $[LCuNCH_3]^+$ ($L = CH_3C(CH_2PPh_2)_3$) as a precursor and propose that a mononuclear copper hydride (Figure 3.1) LCuH is formed as an intermediate, although their experimental evidence does not rule out a dinuclear species such as that reported by Caulton.

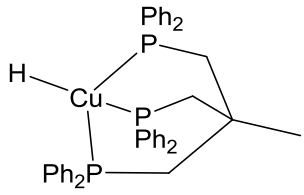

Figure 3.1. A possible structure for a mononuclear copper hydride [LCuH] ($L = CH_3C(CH_2PPh_2)_3$)

In this system, no ^1H resonance for a hydride ligand was observed and the resting state of the catalyst was found to be $[LCuDBU]^+$ ($L = CH_3C(CH_2PPh_2)_3$, DBU = 1,8-

diazabicyclo[5.4.0]undec-7-ene) in the presence of DBU, which was used as the base in this system. The catalyst turnover rate was independent of the base concentration and less nucleophilic bases did not perform as well. This suggests that the copper hydride is not regenerated by a classic mechanism where a cationic dihydrogen complex is deprotonated by exogenous base, but rather that the base must be coordinated to the metal before H_2 is deprotonated. This mechanism where base must be coordinated to the metal prior to the reaction with H_2 is analogous to the hydrogenolysis of Cu-O^{t}Bu bonds, a useful method of synthesizing copper hydrides.

3.2 Electron Transfer to Small Molecules

Our interests involve electron transfer to small molecules. In particular, we are interested in determining when electron transfer is a step in net hydride transfer and what effect such a step has in determining the final small molecule products. We want to determine when electron transfer from transition metal hydrides is mechanistically relevant.

The Norton group's interest in copper hydride chemistry was sparked by a report from Commins et al. in 1984 that demonstrated that a "copper hydride" species could be used to selectively obtain a 1-acyl-1,4-dihydropyridine by hydrogenating pyridine in the presence of a chloroformate (equation 3.1).[22] The "copper hydride" mixture they used consisted of 4.4 equiv CuBr and 3 equiv LiAl(O^{t}Bu)$_3$H. While the product of this reaction is very interesting, the copper hydride mixture is not amenable to the types of mechanistic experiments we were interested in using to probe the reaction.

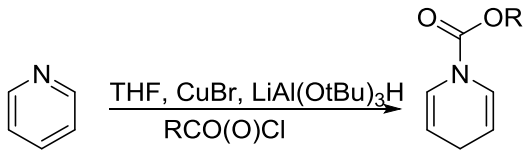

(3.1)

3.3 Electron Transfer to Pyridinium Cations

Anthony Shaw investigated a series of ruthenium hydrides (Cp(dppe)RuH, Cp(dppf)RuH, Cp*(dppe)RuH, and Cp*(dppf)RuH) for this reaction and showed that electron transfer as an initial step in the hydride transfer may lead to exclusive formation of a 1,4-dihydropyridine product from a pyridinium cation.[23] As the Ru(II/III) redox potentials become more negative (more reducing) in the series of ruthenium hydrides studied, the ratio of 1,4-dihydropyridine to 1,2-dihydropyridine products increased until the most reducing ruthenium hydride in the series, Cp*(dppf)RuH, produced exclusively the 1,4-dihydropyridine product (equation 3.2).

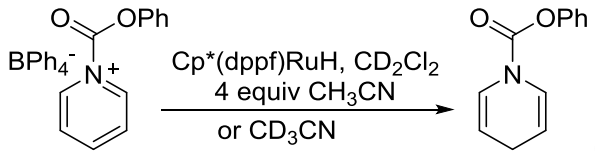

(3.2)

It appears that the mechanism of hydride transfer (concerted H^- transfer, electron-proton-electron transfer, or electron transfer followed by hydrogen atom transfer) may govern the regiochemistry of hydride transfer. [23]

During the reaction of Cp*(dppf)RuH with N-carbophenoxypyridinium, Shaw et al. were able to observe the X-band EPR spectrum of $Cp^*(dppf)RuH^{+\bullet}$ confirming that electron transfer does occur in this reaction.[23] The increasing ratio of 1,4-dihydropyridine product (right of scheme 3.1) to 1,2-dihydropyridine product (left of scheme 3.1) as the ruthenium hydrides

become more reducing suggests that the product distribution may arise from competing pathways for net hydride transfer (scheme 3.1).[23]

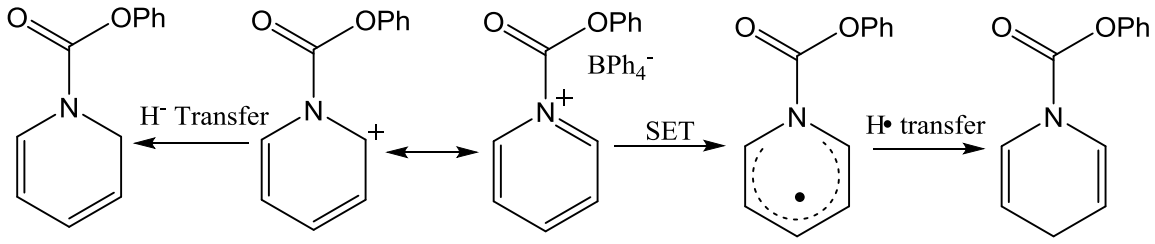

Scheme 3.1. Mechanistic pathways leading to different products from net hydride transfer to a N-acyl pyridinium cation. Concerted hydride transfer leads to the predominant formation of a 1,2-dihydropyridine product, while stepwise hydride transfer (electron transfer followed by hydrogen atom transfer) may lead to a 1,4-dihydropyridine.

Computational results reported by Shaw et al. also support this explanation of the observed regioselectivity and indicate that the spin density in the pyridine radical resides primarily at the para position.[23]

In view of these results, a variety of $[R_3PCuH]_6$ species were treated with N-carbophenoxypyridinium. With redox potentials around -1.1 V vs Fc/Fc^+ as discussed in chapter 2, electron transfer from a copper hydride to N-carbophenoxypyridinium (E_{pc} = -0.87 V vs Fc/Fc^+)[23] is thermodynamically downhill. The products of these reactions were mixtures of 1,2 and 1,4-dihydropyridines formed quantitatively, in a ratio that varied only slightly among the five $[R_3PCuH]_6$ copper hydrides tested (table 3.1). However, the redox potentials are also similar where they are known. The redox potentials of $[BnPh_2PCuH]_6$ and $[^iPrPh_2PCuH]_6$ were not measured because of the high reactivity of these species in solution; the cost of materials required for synthesis of larger quantities was also unpalatable at the time when their reactivity

did not seem to differ greatly from $[Ph_3PCuH]_6$ in terms of the 1,2 and 1,4-dihydropyridine product ratio. Sadighi's copper hydride ($[IPrCuH]_2$, the structure of this species is shown in chapter 1, figure 1.6) was also tested and gave similar product distributions to the other copper hydrides.

Table 3.1. Dihydropyridine product ratios obtained when an N-acyl pyridinium cation is treated with various transition metal hydrides.

Metal Hydride	**1,4:1,2-dihydropyridine**	M-H/M-H$^+$ potential (V vs. Fc/Fc$^+$)
$[Ph_3PCuH]_6$	65:35	-1.01
$[tolyl_3PCuH]_6$	80:20	-1.12
$[iPrPh_2PCuH]_6$	75:25	
$[BnPh_2PCuH]_6$	75:25	
$[(p\text{-anisyl})_3PCuH]_6$	80:20	-1.15
$[(NHC)CuH]_2$	80:20	

One factor in the poorer selectivity of the copper hydrides compared with ruthenium hydride systems is the greater reactivity of copper hydrides and N-carbophenoxypyridinium. The reaction with Cp*dppfRuH took several minutes during which color change was observed at –50 °C, before it was quenched with liquid nitrogen Cp*dppfRuH$^{+\bullet}$ was observed by EPR (it is possible that the radical cation could have been observed earlier in the reaction, but the color change took several minutes indicating that the reaction takes that long at low temperature). The reactions between $[R_3PCuH]_6$ and N-carbophenoxypyridinium gave an instantaneous color

change from the red solution of the copper hydride to an intense green solution. The reaction was so fast that the rate of formation of the green solution (containing $[Ph_3PCuH]_6^{+\bullet}$) could not be measured with our stopped-flow instrument that is equipped with a rapid scanning spectrometer capable of collecting spectra every millisecond. It is possible that the rate of this reaction could be measured at low temperature; however, leaks in the stopped-flow circuit have delayed additional stopped-flow experiments on this system. The high reactivity of the copper hydride system may account to the erosion in selectivity compared to ruthenium hydrides.

Figure 3.2 shows the spectra obtained in a stopped-flow reaction between $[Ph_3PCuH]_6$ and N-carbophenoxypyridinium. The copper hydride radical cation $[Ph_3PCuH]_6^{+\bullet}$ is clearly visible with $\lambda_{max} = 655$. From our spectroelectrochemistry experiments in chapter 2, we estimate the extinction coefficient at 655 nm of the copper hydride radical cation to be 5600 $L \bullet mol^{-1}cm^{-1}$. At the concentration of copper hydride used in the experiment shown in figure 3.2, quantitative electron transfer using this estimate for the extinction coefficient of $[Ph_3PCuH]_6^{+\bullet}$ should result in an absorbance of 2.30 at 655 nm using those concentrations, the observed absorbance was about 1.5 which equates to a $[Ph_3PCuH]_6^{+\bullet}$ yield of 65%. This yield is the same as the observed 65% yield of 1,4-dihydropyridine, a product that appears to be formed by the two-step pathway discussed earlier. The observation $[Ph_3PCuH]_6^{+\bullet}$ of proves that $[Ph_3PCuH]_6$ transfers an electron to N-carbophenoxypyridinium. The fact that $[Ph_3PCuH]_6^{+\bullet}$ is readily observed also demonstrates that a subsequent hydrogen atom transfer step from $[Ph_3PCuH]_6^{+\bullet}$ to the pyridine radical is slower than electron transfer. The presence of $[Ph_3PCuH]_6^{+\bullet}$ proves electron transfer, but its absence wouldn't prove the negative.

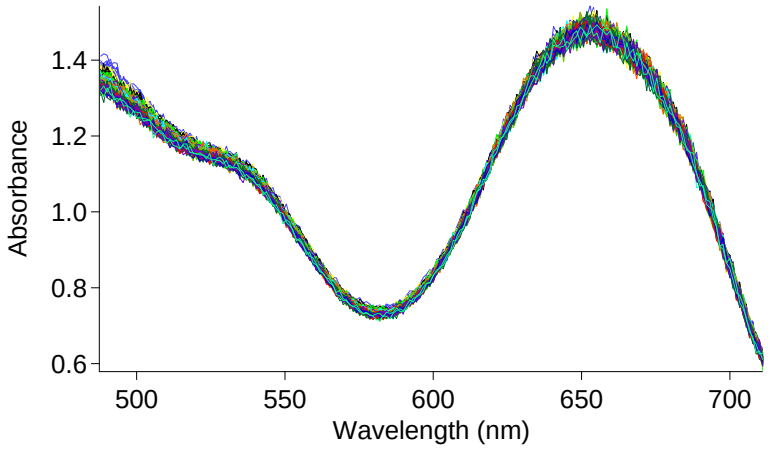

Figure 3.2. UV-vis spectra obtained from reaction of $[Ph_3PCuH]_6$ and N-carbophenoxypyridinium in a stopped-flow. A solution containing $[Ph_3PCuH]_6$ = 8.20 x 10^{-4} Mol/L was mixed with an equal amount of a solution containing 3.37 x 10^{-3} Mol/L N-carbophenoxypyridinium tetraphenylborate. Over a period of three seconds, there is no significant change in the spectra (multiple spectra over about 300 ms are shown in the graph), indicating that the electron transfer step is much faster than subsequent steps.

3.4 Attempts to Open Epoxides to Primary Alcohols

Controlling the regioselectivity of epoxide opening is an important problem in organic chemistry. Our objective is to transfer an electron to terminal epoxides which we hypothesize will open to the more stable radical and eventually lead to primary alcohol products. In general, this should give complementary regioselectivity to other methods of opening epoxides.

A reaction opening epoxides to primary alcohols must overcome some drawbacks. The most obvious of these is that epoxides are generally more expensive than the primary alcohol products that would be formed so if the reaction worked, it would still be turning a more valuable

starting material into a less valuable product. This issue could be potentially overcome by an industrial route where a terminal olefin is efficiently epoxidized before a different chemical process is used to open the epoxide. The production of primary alcohols by a hydroformylation route is also an excellent industrial method which would be hard to compete with, but there are many basic science questions that investigation of epoxide opening can answer.

Having demonstrated that hydride transfer from copper hydrides to pyridinium cations occurs by an electron transfer mechanism, we targeted a more challenging substrate. Opening of terminal epoxides by a transition metal hydrides typically leads to a secondary alkoxide products.[24] Catalysts for the homogeneous hydrogenation of epoxides also typically lead to secondary alcohols, examples include a rhodium catalyzed reaction[25] (equation 3.3, from ^{i}PrOH) and a ruthenium catalyzed reaction[26] (equation 3.4, with H_2).

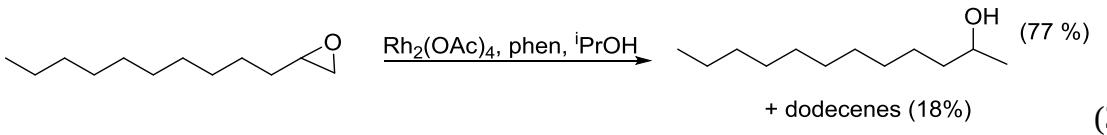

(3.3)

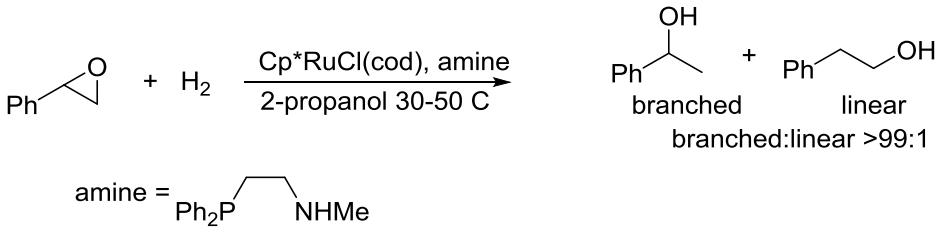

(3.4)

However, electron transfer should lead to the opposite regioselectivity. Transfer of an electron to a terminal epoxide should lead to the more stable radical and subsequent transfer of H• would then give the primary alkoxide (scheme 3.2).[27-28]

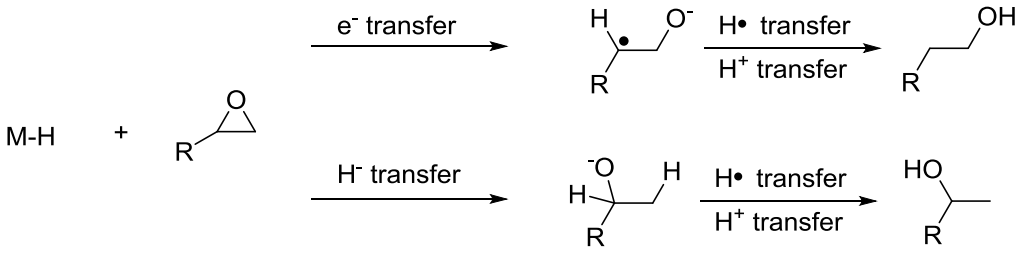

Scheme 3.2. Electron transfer to a terminal epoxide should result in a primary alcohol while hydride transfer leads to a secondary alcohol.

We selected styrene oxide as a model epoxide to study. Styrene oxide is a commonly reported substrate in papers that have investigated epoxide opening which makes comparisons of the results more meaningful. The possible products of the reaction are simple and distinctive by NMR, and the phenyl substituent should help stabilize radical intermediates, making an electron transfer pathway more favorable. Perhaps unsurprisingly, $[Ph_3PCuH]_6$ was unable to directly transfer an electron to styrene oxide (no reaction occurred between $[Ph_3PCuH]_6$ and styrene oxide). Typical potentials necessary to reduce an epoxide by one electron are around –2.0 V vs Fc/Fc^+.[29] We considered activating the epoxide by protonation or activation with a Lewis acid. However, protonating an epoxide is perilous because epoxides open and rearrange under acid conditions.[30] The hydride ligands in copper hydride can also be quantitatively protonated to yield H_2;[31] in my experience this reaction is rapid. $[Ph_3PCuH]_6$ was also found to react with many Lewis acids including BF_3 and $(C_6F_5)_3B$ to lose H_2.

Interestingly, $[Ph_3PCuH]_6$ is capable of transferring an electron to $(C_6F_5)_3B$ in CH_2Cl_2 (Figure 3.3). The Norton group previously estimated the redox potential of $(C_6F_5)_3B$ by determining the redox potentials of $(C_6F_5)_n(mesityl)_{3-n}B$.[32] The redox potential of $(C_6F_5)_3B$ could not be determined itself due to irreversibility, but was estimated to be -1.17 V vs Fc/Fc^+ in

THF.[32] More recently, Wildgoose et al. have measured the redox potential of $(C_6F_5)_3B$ in methylene chloride and 1,2-difluorobenzene, finding it to be -1.79 V vs Fc/Fc^+ and -1.65 V vs Fc/Fc^+ respectively in those solvents; this potential would seem to suggest that $[Ph_3PCuH]_6$ should not be able to transfer an electron to $(C_6F_5)_3B$ if the reported potentials are correct. Wildgoose has stated that the role of THF as a donor solvent may have a significant impact in the redox potential explaining why the estimated potential in THF is much different from the potential they have reported in methylene chloride.[33] However, as a donor solvent, THF should make reducing BAr_3 more difficult.

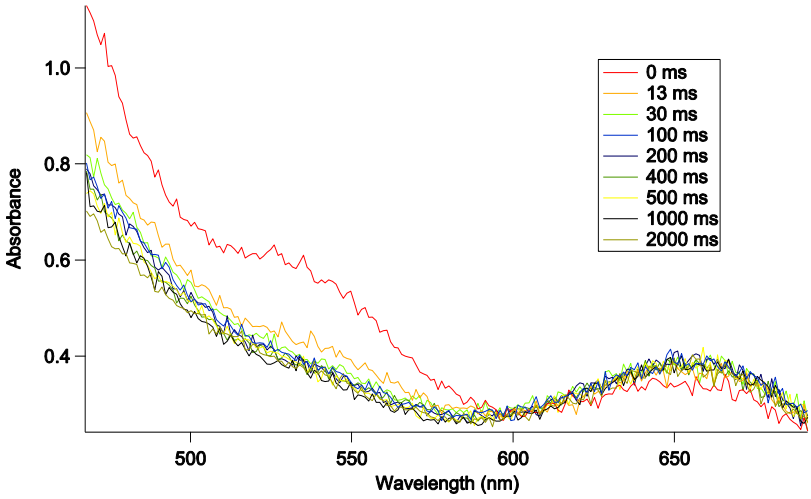

Figure 3.3. $[Ph_3PCuH]_6^{+\bullet}$ is observed in a stopped flow reaction between $[Ph_3PCuH]_6$ and $(C_6F_5)_4B$. A solution containing 1.13 mMol/L $[Ph_3PCuH]_6$ was mixed with an equal amount of a solution containing 26.47 mMol/L $(C_6F_5)_3B$.

Based on the estimated extinction coefficient of 5600 $L \bullet mol^{-1}cm^{-1}$ for $[Ph_3PCuH]_6^{+\bullet}$, the maximum obtained concentration of $[Ph_3PCuH]_6^{+\bullet}$ appears to be 6.8×10^{-5} Mol/L in this reaction between $[Ph_3PCuH]_6$ and $(C_6F_5)_3B$. The $(C_6F_5)_3B$ is in large excess in this reaction; lower concentrations (but still in large excess) of $(C_6F_5)_3B$ resulted in lower observed concentrations of

$[Ph_3PCuH]_6^{+\bullet}$. This result makes sense if electron transfer from $[Ph_3PCuH]_6$ to $(C_6F_5)_3B$ is slightly uphill.

Because of the reactivity between copper hydrides and Lewis acids, this route proved to not be a feasible method of opening epoxides. In test reactions that used $[Ph_3PCuH]_6$ and Lewis acids (including $Al(OTf)_3$ and BF_3) in combination, the styrene oxide was untouched.

Another approach we tried to reduce epoxides to primary alcohols was to use $[Ph_3PCuH]_6$ to reduce Cp_2TiCl_2. Cp_2TiCl_2 is reduced at about -1.2 V vs Fc/Fc^+ and rapidly loses Cl^- upon reduction to give Cp_2TiCl.[34] Cp_2TiCl reduces epoxides by an inner-sphere electron transfer mechanism.[35] At least theoretically, a system using Cp_2TiCl_2 and $[Ph_3PCuH]_6$ could be made catalytic. $[Ph_3PCuH]_6$ could be regenerated with H_2 and a base. Our collaborator Andreas Gansäuer has shown that Cp_2TiCl can be used to catalytically open epoxides forming a primary alcohol. This system used manganese metal to reduce titanium(IV) back to titanium(III) and collidine hydrochloride to remove the alkoxide from the metal.[36]

By treating $[Ph_3PCuH]_6$ with Cp_2TiCl_2, the copper hydride radical cation $[Ph_3PCuH]_6^{+\bullet}$ is observed. Again indicating that an electron is transferred to Cp_2TiCl_2. The 655 nm absorbance of $[Ph_3PCuH]_6^{+\bullet}$ disappears rather quickly (within 1.5 seconds) indicating that there must be a relatively rapid follow up reaction involving the copper hydride radical cation (Figure 3.4). When reduced, Cp_2TiCl_2 generally loses Cl^- as discussed earlier. In chapter 4, we will see that some copper hydride oxidation products can be trapped by Cl^- which may be one explanation for the fate of the copper hydride radical cation in this reaction.

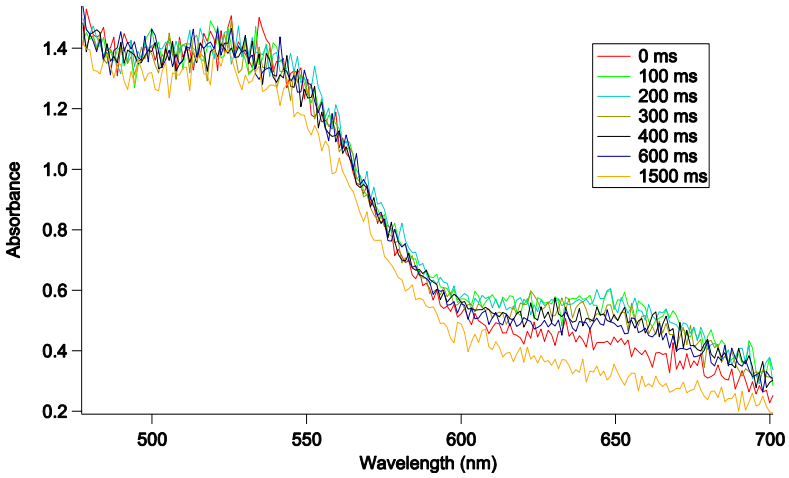

Figure 3.4. $[Ph_3PCuH]_6^{+\bullet}$ is observed in a stopped flow reaction between $[Ph_3PCuH]_6$ and Cp_2TiCl_2. A solution containing 8.82 x 10^{-4} Mol/L $[Ph_3PCuH]_6$ was mixed with an equal amount of a solution containing 5.58 x 10^{-3} Mol/L Cp_2TiCl_2. The stopped flow spectra suggest a maximum concentration of 1.1 x 10^{-4} Mol/L $[Ph_3PCuH]_6^{+\bullet}$ is obtained. In this case, the electron transfer reaction is approximately thermoneutral (based on the electrochemical potentials), the maximum concentration of $[Ph_3PCuH]_6^{+\bullet}$ is also observed only briefly. Therefore, a subsequent reaction involving $[Ph_3PCuH]_6^{+\bullet}$ is occurring at a rate comparable to the formation of $[Ph_3PCuH]_6^{+\bullet}$.

The preliminary data suggested that the Cp_2TiCl_2/$[Ph_3PCuH]_6$ system was sufficiently promising to attempt to open styrene oxide. Unlike the earlier attempts with lewis acids, this system did result in reactivity in the epoxide. However the organic products of these reactions were an intractable mixture. Upon acidification of the reaction mixture, neither 1-phenylethanol nor 2-phenylethanol were detectible products of the reaction by NMR.

3.2 Is Electron Transfer Relevant in the Hydrogenation of α,β-Unsaturated Carbonyl Compounds?

In this chapter we have seen how electron transfer reactions might be used to alter the regioselectivity of hydrogenation reactions. As copper hydrides are most famously reagents for the selective hydrogenation of α,β-unsaturated carbonyl compounds, the question of whether electron transfer could play a role in this important reaction is an obvious one to ask.

In the case of α,β-unsaturated nitriles which have chemistry similar to their enone cousins, Paquette et al. have observed that a copper hydride system has selectivity for only reducing the C=C bond in α,β-unsaturated nitriles. This reaction produces results similar to an earlier method of using magnesium in methanol.[37] However, magnesium in methanol also results in dimerized products (shown in left portion of scheme 3.3) and clearly goes by an electron transfer mechanism. Paquette proposed that the copper hydride reduction of α,β-unsaturated nitriles occurs by an analogous electron transfer mechanism (right portion of scheme 3.3).[38]

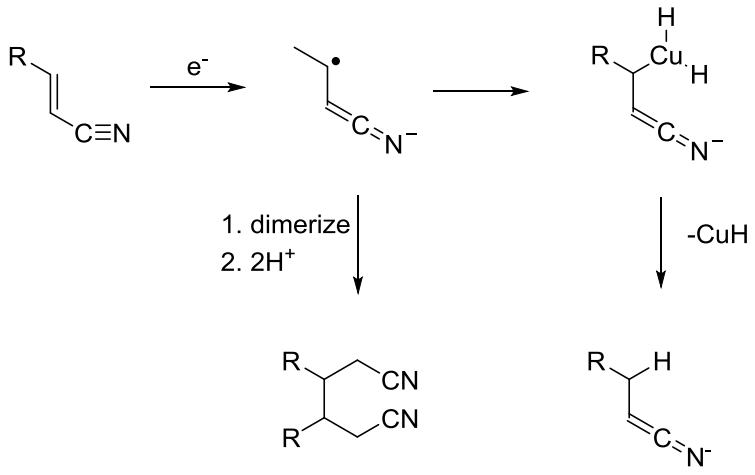

Scheme 3.3. An electron transfer mechanism proposed for the selective reduction of the C=C bond in α,β-unsaturated nitriles. This scheme is redrawn from reference 38. The middle portion shows a dimerized product that is formed in reference 37 and the right shows the product from a reaction with a copper hydride which does not include any dimerized product.

Unlike with magnesium in methanol, the copper hydride reduction does not result in detectable dimerization, perhaps because copper rapidly bonds with any free radical. House,[39-40] along with Semmelhack and Stauffer[41-42] have proposed electron transfer to α,β-unsaturated carbonyls from copper hydride or organocuprates. Semmelhack and Stauffer proposed that mixtures consisting of CuBr and either $LiAlH(OCH_3)_3$ or $NaAlH_2(OCH_2CH_2OCH_3)_2$, which are referred to as the "Li complex" and "Na complex" respectively, most likely transferred an electron to α,β-unsaturated carbonyls. However, in more recent years, the idea that well-defined copper hydride reagents such as $[Ph_3PCuH]_6$ transfer an electron to enones has fallen out of favor. Stryker et al. tested an enone with a thiophenoxy substituent in the γ position.[4] Stryker et al. argue that the thiophenoxy substituent should not survive an electron transfer mechanism instead resulting in the loss of PhS•. When tested, this substrate did easily survive the reaction

with $[Ph_3PCuH]_6$ (scheme 3.4) suggesting that electron transfer is not involved in hydrogenation of α,β-unsaturated carbonyls with $[Ph_3PCuH]_6$.[4] However, it did appear that $[Ph_3PCuH]_6$ initiated the isomerization of 5-hexenyl iodide to cyclopentylmethyl iodide.[4] Presumably, $[Ph_3PCuH]_6$ is able to transfer an electron to an alkyl iodide.

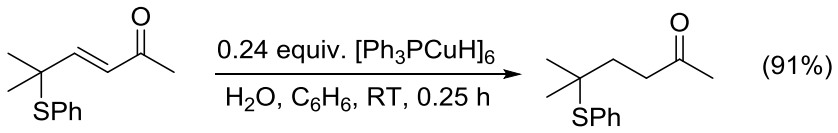

Scheme 3.4. An α,β-unsaturated carbonyl compound with a δ thiophenoxy substituent which Stryker et al. argue would not survive an electron transfer mechanism.

When we reacted $[Ph_3PCuH]_6$ with cyclohexenone in a stopped flow, we did not observe $[Ph_3PCuH]_6^{+\bullet}$ (figure 3.5). This could just mean that follow-up reactions of the copper hydride radical cation (such as H• transfer or proton transfer) are faster than the initial electron transfer.

We have found that the rate $[Ph_3PCuH]_6$ reacts with cyclohexenone is slowed by adding free triphenylphosphine to the reaction (figure 3.6). The rate does increase slightly as the concentration of cyclohexenone increases; however, the reaction is less than first order in cyclohexenone (figure 3.7). Phosphine dissociation is approximately the rate determining step. The observed kinetics are not zero order in cyclohexenone because coordination of cyclohexenone to copper occurs at a rate that is competitive with phosphine dissociation. At higher concentrations of cyclohexenone the kinetics should approach a limit where they are zero order in cyclohexenone, and at very low concentrations of cyclohexenone, the kinetics should approach a limit where the rate law is first order in cyclohexenone. The mechanism appears to be dissociative ligand substitution.

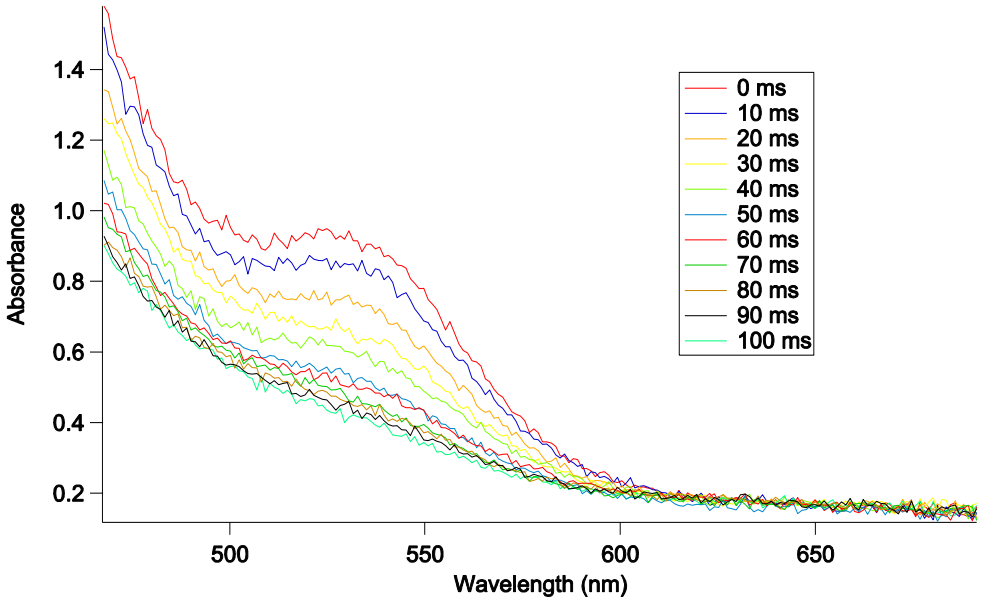

Figure 3.5. The disappearance of $[Ph_3PCuH]_6$ is observed over time as it reacts with cyclohexenone. $[Ph_3PCuH]_6^{+\bullet}$ is not observed in a stopped flow reaction between $[Ph_3PCuH]_6$ and cyclohexenone. A solution containing 8.51 x 10^{-4} Mol/L $[Ph_3PCuH]_6$ was mixed with an equal volume of solution containing 3.22 x 10^{-2} Mol/L cyclohexenone. Observed rates were determined by monitoring the disappearance of $[Ph_3PCuH]_6$; global fitting was used to model the change in absorbance across all wavelengths observed.

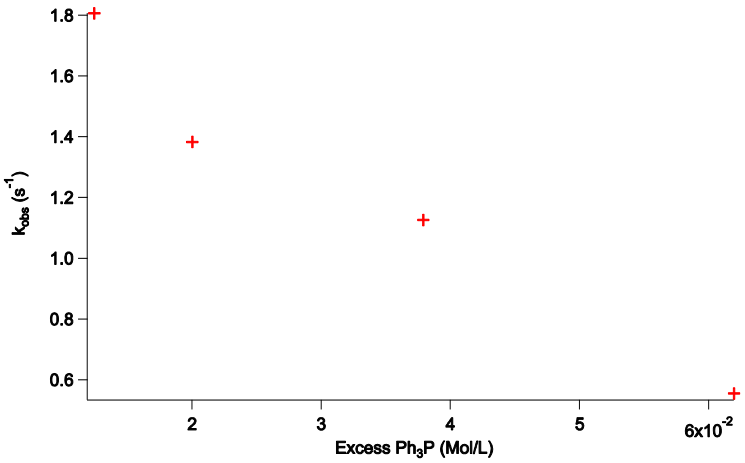

Figure 3.6. Observed rate constants of the disappearance of $[Ph_3PCuH]_6$ reacting with cyclohexenone vs concentration of excess phosphine. A solution containing 8.13×10^{-4} Mol/L $[Ph_3PCuH]_6$ in CH_2Cl_2 was mixed with an equal amount of CH_2Cl_2 solution containing 42.6 mMol/L cyclohexenone. The excess phosphine was added to the $[Ph_3PCuH]_6$ solutions rather than the cyclohexenone solutions because the concentration of the limiting reagent does not need to be known precisely under pseudo first-order conditions. All concentrations shown are before mixing so the reaction concentrations are half concentration after mixing.

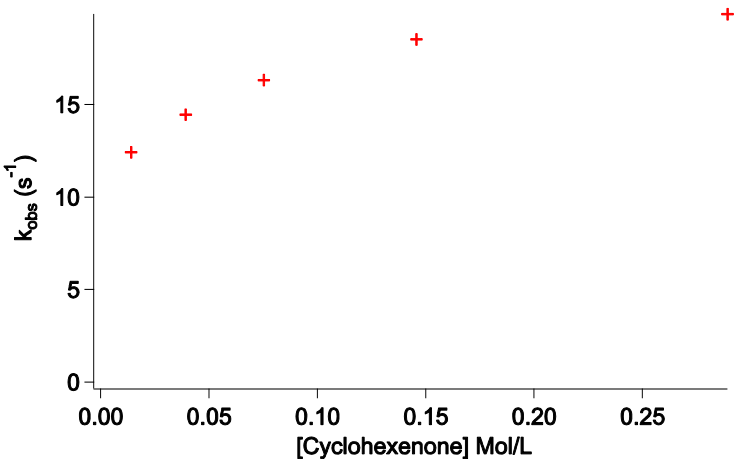

Figure 3.7. Observed rate constants of the disappearance of $[Ph_3PCuH]_6$ vs concentration of cyclohexenone. A solution containing 8.55×10^{-4} Mol/L $[Ph_3PCuH]_6$ in CH_2Cl_2 was mixed with CH_2Cl_2 solution of cyclohexenone. The concentrations of cyclohexenone shown on the x-axis are the concentrations before mixing.

These results suggest that a phosphine ligand must dissociate from a copper hydride hexamer before it can react with cyclohexenone. Observed rates of electron transfer from copper hydride to oxidants are generally much faster (faster than can be observed in our stopped flow) than the reaction with enones. This seems to suggest that electron transfer from $[Ph_3PCuH]_6$ to an oxidant is probably much faster than phosphine dissociation and suggests that phosphine dissociation is not required for an electron transfer, much as one might expect.

While we have yet to determine the rate of phosphine exchange in $[Ph_3PCuH]_6$, it is clear that the phosphine ligands do exchange. Addition of free triphenylphosphine to a sample of $[Ph_3PCuH]_6$ in C_6D_6 only results in the ^1H NMR resonances of both free Ph_3P and $[Ph_3PCuH]_6$, the peaks do not broaden. This demonstrates that the rate of phosphine exchange is slow on the NMR time scale. In studying the formation of $[(dppbz)CuH]_3$ from $[Ph_3PCuH]_6$, it was possible

to observe an intermediate with a ^{1}H NMR Cu-H resonance of $\delta = 1.83$ (A resonance Lipshutz previously observed and attributed to a dppbzCuH species)[43] when a solution of $[Ph_3PCuH]_6$ was reacted with free dppbz. This reaction presumably occurs by dissociation of Ph_3P ligands from $[Ph_3PCuH]_6$ which are then replaced by dppbz ligands. The fact that intermediates can be observed suggests that the phosphine dissociation rate is not that fast.

It appears that hydrogenation of α,β-unsaturated carbonyl compounds by $[Ph_3PCuH]_6$ does not occur by an outer-sphere electron transfer mechanism.

3.3 Reactions of $[Ph_3PCuH]_6$ with Trityl Cations and Trityl Radicals.

In an effort to better understand the follow-up reactions to electron transfer, triarylmethyl cations (Ar_3C^+), often referred to as "trityl cations" were reacted with copper hydrides. These species are examples of stable carbocations. Upon reduction by a single electron, trityl radicals are formed which are good examples of stable carbon based radicals[44-45] (although they are photosensitive). Two trityl cations are commonly used. The first is a triphenylmethyl cation; upon reduction, the triphenylmethyl radical exists in a monomer-dimer equilibrium. The dimer, known as "Gomberg's dimer" after its discoverer, is a head to tail dimer with the structure shown in scheme 3.5.

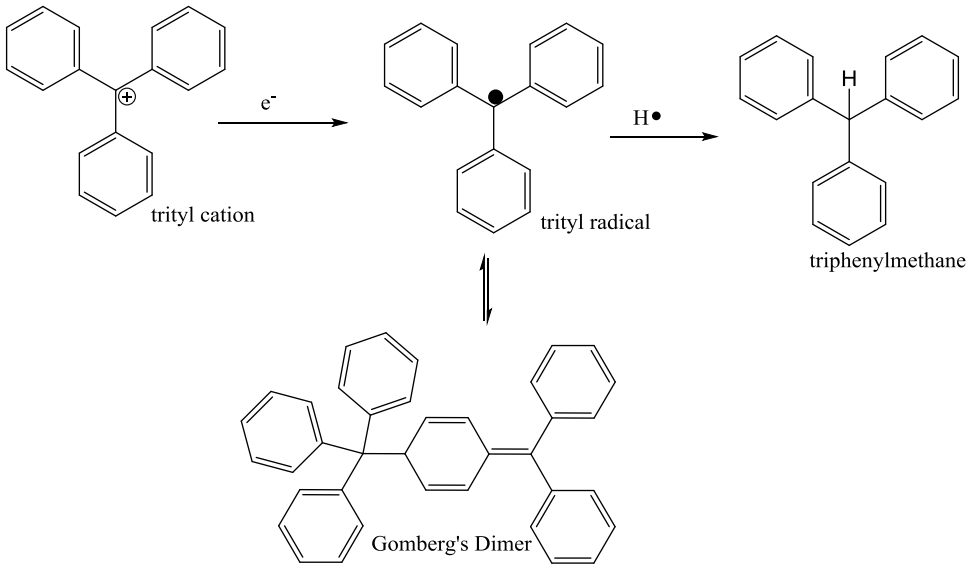

Scheme 3.5. Reactions of triphenylmethyl cations and triphenylmethyl radicals.

This dimerization can be blocked by adding para t-butyl substituents to the aryls[46-47] which can be useful for quantifying the amount of radical present by UV-vis spectroscopy since the extinction coefficient of the radical is known to be 825 $M^{-1}cm^{-1}$.[48] The Norton group has previously demonstrated the use of trityl radicals to abstract hydrogen atoms from transition metal hydrides.[48-49] Trityl cations have also been used to demonstrate that hydride transfer can occur by a two-step mechanism previously. Hembre treated Cp*dppfRuH with triphenylmethyl cations and Gomberg's dimer was observed, demonstrating that the hydride transfer goes by a radical mechanism.[50] The redox potential of the $Ph_3C^{+/\bullet}$ is +0.11 V vs Fc/Fc^+ in acetonitrile[51-52] meaning trityl cations are fairly good oxidants, comparable to the strength of ferrocenium. Many transition metal hydrides can be oxidized by a reagent having this potential so presumably hydride transfer to trityl cations frequently occurs by a two-step mechanism. If hydrogen atom transfer subsequent to electron transfer is faster than dimerization of $Ph_3C\bullet$, it is not unlikely that

relying on observation of the dimer would fail detect cases of electron transfer. Detection of $Ph_3C\bullet$ or $(p\text{-}^tBuPh)_3C\bullet$ by UV-visible spectroscopy is a more reliable method.

In a stopped flow reaction we have observed that $(p\text{-}^tBuPh)_3C\bullet$ is formed in an intermediate in the reaction between $(p\text{-}^tBuPh)_3C^+$ and $[Ph_3PCuH]_6$ (eq. 3.1, figure 3.8). The $(p\text{-}^tBuPh)_3C\bullet$ radical has a sharp absorbance at 523 nm. This sharp absorbance is observed even though it overlaps with the broad absorbance peak at 525 nm of $[Ph_3PCuH]_6$. By NMR we also observe that hydride transfer is eventually completed by observing the $(p\text{-}^tBuPh)_3C\textbf{-H}$ resonance in ^1H NMR (eq. 3.2). The source of this hydrogen atom was confirmed to have come from $[Ph_3PCuH]_6$ by treating $(p\text{-}^tBuPh)_3C^+$ with $[Ph_3PCuD]_6$, which allowed us to observe $(p\text{-}^tBuPh)_3C\textbf{-D}$ by ^2H NMR.

$$[Ph_3PCuH]_6 + (p\text{-}^tBu)_3C^+ \longrightarrow [Ph_3PCuH]_6^{+\bullet} + (p\text{-}^tBu)_3C\bullet \qquad (3.1)$$

$$[Ph_3PCuH]_6^{+\bullet} + (p\text{-}^tBu)_3C\bullet \longrightarrow (Ph_3P)_6Cu_6H_5^{+} + (p\text{-}^tBu)_3C\text{-}H \qquad (3.2)$$

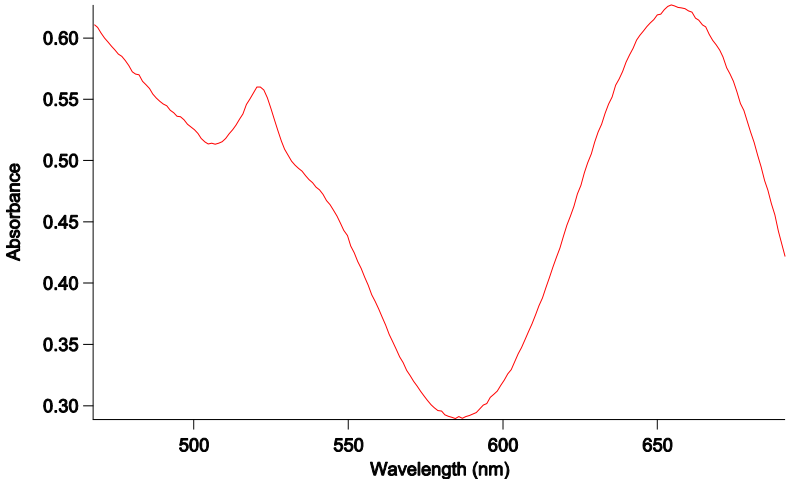

Figure 3.8. Calculated infinite time spectra determined by global fitting of multiwavelength stopped-flow data to a kinetic model for a second order reaction of unequal concentrations. The

solution concentrations used were 1.008 mMol/L $[Ph_3PCuH]_6$ and 0.542 mMol/L $[(p\text{-}{}^tBuPh)_3C]^+[(C_6F_5)_4B]^-$.

The calculated spectra obtained (Figure 3.8) are consistent with quantitative electron transfer from $[Ph_3PCuH]_6$ to $(p\text{-}{}^tBuPh)_3C^+$ based on known extinction coefficients for $[Ph_3PCuH]_6$ and $(p\text{-}{}^tBuPh)_3C\bullet$. The extinction coefficient of $[Ph_3PCuH]_6^{+\bullet}$ at λ_{max} = 655 nm has been estimated to be 5600 $L^{-1}mol^{-1}cm^{-1}$ based on the spectroelectrochemical data in chapter 2.

Chapter 3 References

1. Brestensky, D. M.; Stryker, J. M., Regioselective conjugate reduction and reductive silylation of α,β-unsaturated aldehydes using [(Ph3P)CuH]6. *Tetrahedron Letters* **1989,** *30* (42), 5677-5680.

2. Chen, J.-X.; Daeuble, J. F.; Brestensky, D. M.; Stryker, J. M., Highly Chemoselective Catalytic Hydrogenation of Unsaturated Ketones and Aldehydes to Unsaturated Alcohols Using Phosphine-Stabilized Copper(I) Hydride Complexes. *Tetrahedron* **2000,** *56* (15), 2153-2166.

3. Daeuble, J. F.; Stryker, J. M. In *Hexa-m-hydrohexakis(triphenylphosphine)hexacopper*, John Wiley & Sons, Ltd.: 2001; p No pp. given.

4. Koenig, T. M.; Daeuble, J. F.; Brestensky, D. M.; Stryker, J. M., Conjugate reduction of polyfunctional α,β-unsaturated carbonyl compounds using [(Ph3P)CuH]6. Compatibility with halogen, sulfonate, and γ-oxygen and sulfur substituents. *Tetrahedron Letters* **1990,** *31* (23), 3237-3240.

5. Mahoney, W. S.; Brestensky, D. M.; Stryker, J. M., Selective hydride-mediated conjugate reduction of α,β-unsaturated carbonyl compounds using [(Ph3P)CuH]6. *Journal of the American Chemical Society* **1988,** *110* (1), 291-293.

6. Mahoney, W. S.; Stryker, J. M., Hydride-mediated homogeneous catalysis. Catalytic reduction of α,β-unsaturated ketones using $[(Ph_3P)CuH]_6$ and H_2. *Journal of the American Chemical Society* **1989,** *111* (24), 8818-8823.

7. Riant, O., Copper(I) Hydride Reagents and Catalysts. In *Chemistry of Organocopper Compounds*, John Wiley & Sons, Ltd: 2009; pp 731-773.

8. Chiu, P.; Li, Z.; Fung, K. C. M., An expedient preparation of Stryker's reagent. *Tetrahedron Letters* **2003,** *44* (3), 455-457.

9. Lee, D.-w.; Yun, J., Direct synthesis of Stryker's reagent from a Cu(II) salt. *Tetrahedron Letters* **2005,** *46* (12), 2037-2039.

10. Moritani, Y.; Appella, D. H.; Jurkauskas, V.; Buchwald, S. L., Synthesis of β-Alkyl Cyclopentanones in High Enantiomeric Excess via Copper-Catalyzed Asymmetric Conjugate Reduction. *Journal of the American Chemical Society* **2000,** *122* (28), 6797-6798.

11. Appella, D. H.; Moritani, Y.; Shintani, R.; Ferreira, E. M.; Buchwald, S. L., Asymmetric Conjugate Reduction of α,β-Unsaturated Esters Using a Chiral Phosphine−Copper Catalyst. *Journal of the American Chemical Society* **1999,** *121* (40), 9473-9474.

12. Lipshutz, B. H., Rediscovering organocopper chemistry through copper hydride. It's all about the ligand. *Synlett* **2009,** (Copyright (C) 2012 American Chemical Society (ACS). All Rights Reserved.), 509-524.

13. Lipshutz, B. H.; Frieman, B. A., CuH in a Bottle: A Convenient Reagent for Asymmetric Hydrosilylations. *Angewandte Chemie International Edition* **2005,** *44* (39), 6345-6348.

14. Lipshutz, B. H.; Noson, K.; Chrisman, W.; Lower, A., Asymmetric Hydrosilylation of Aryl Ketones Catalyzed by Copper Hydride Complexed by Nonracemic Biphenyl Bis-phosphine Ligands. *Journal of the American Chemical Society* **2003,** *125* (29), 8779-8789.

15. Lipshutz, B. H.; Keith, J.; Papa, P.; Vivian, R., A convenient, efficient method for conjugate reductions using catalytic quantities of Cu(I). *Tetrahedron Letters* **1998,** *39* (26), 4627-4630.

16. Lipshutz, B. H.; Chrisman, W.; Noson, K.; Papa, P.; Sclafani, J. A.; Vivian, R. W.; Keith, J. M., Copper Hydride-Catalyzed Tandem 1,4-Reduction/Alkylation Reactions. *Tetrahedron* **2000,** *56* (18), 2779-2788.

17. Beguin, B.; Denise, B.; Sneeden, R. P. A., Hydrocondensation of CO2 : II. Reaction of carbon dioxide and carbon monoxide with [HCuPPh3]6. *Journal of Organometallic Chemistry* **1981,** *208* (1), C18-C20.

18. Zall, C. M.; Linehan, J. C.; Appel, A. M., A Molecular Copper Catalyst for Hydrogenation of CO_2 to Formate. *ACS Catalysis* **2015,** *5* (9), 5301-5305.

19. Zhang, L.; Cheng, J.; Hou, Z., Highly efficient catalytic hydrosilylation of carbon dioxide by an N-heterocyclic carbene copper catalyst. *Chemical Communications* **2013,** *49* (42), 4782-4784.

20. Nakamae, K.; Kure, B.; Nakajima, T.; Ura, Y.; Tanase, T., Facile Insertion of Carbon Dioxide into $Cu_2(\mu\text{-H})$ Dinuclear Units Supported by Tetraphosphine Ligands. *Chemistry – An Asian Journal* **2014,** *9* (11), 3106-3110.

21. Goeden, G. V.; Huffman, J. C.; Caulton, K. G., A copper-(μ^2-hydrogen) bond can be stronger than an intramolecular phosphorus-copper bond. Synthesis and structure of di-μ-hydridobis[η^2-1,1,1-tris(diphenylphosphinomethyl)ethane]dicopper. *Inorganic Chemistry* **1986,** *25* (15), 2484-2485.

22. Comins, D. L.; Abdullah, A. H., Synthesis of 1-acyl-1,4-dihydropyridines via copper hydride reduction of 1-acylpyridinium salts. *The Journal of Organic Chemistry* **1984,** *49* (18), 3392-3394.

23. Shaw, A. P.; Ryland, B. L.; Franklin, M. J.; Norton, J. R.; Chen, J. Y. C.; Hall, M. L., Using a Two-Step Hydride Transfer To Achieve 1,4-Reduction in the Catalytic Hydrogenation of an Acyl Pyridinium Cation. *The Journal of Organic Chemistry* **2008,** *73* (24), 9668-9674.

24. Murai, S.; Murai, T.; Kato, S., Reduction of Epoxides. In *Comprehensive Organic Synthesis*, 1st ed.; Trost, B. M., Ed. Pergamon Press: Oxford, 1991; Vol. 9, pp 871-893.

25. Ricci, M.; Slama, A., Transfer Hydrogenation of Simple Epoxides. *Journal of Molecular Catalysis* **1994,** *89* (1-2), L1-L4.

26. Ito, M.; Hirakawa, M.; Osaku, A.; Ikariya, T., Highly Efficient Chemoselective Hydrogenolysis of Epoxides Catalyzed by a (η^5-$C_5(CH_3)_5$)Ru Complex Bearing a 2-(diphenylphosphino)ethylamine Ligand. *Organometallics* **2003,** *22* (21), 4190-4192.

27. Daasbjerg, K.; Svith, H.; Grimme, S.; Gerenkamp, M.; Muck-Lichtenfeld, C.; Gansäuer, A.; Barchuk, A.; Keller, F., Elucidation of the mechanism of titanocene-mediated epoxide opening by a combined experimental and theoretical approach. *Angewandte Chemie-International Edition* **2006,** *45* (13), 2041-2044.

28. LeSuer, R. J.; Buttolph, C.; Geiger, W. E., Comparison of the Conductivity Properties of the Tetrabutylammonium Salt of Tetrakis(pentafluorophenyl)borate Anion with Those of Traditional Supporting Electrolyte Anions in Nonaqueous Solvents. *Analytical Chemistry* **2004,** *76* (21), 6395-6401.

29. Boujlel, K.; Simonet, J., Cathodic cleavage of carbon-oxygen bonds (V). direct and indirect electrochemical reduction of epoxides. *Electrochimica Acta* **1979,** *24* (5), 481-487.

30. Olah, G. A.; Szilagyi, P. J., Stable carbonium ions. CIV. Protonated alicyclic ethers and sulfides. *The Journal of Organic Chemistry* **1971,** *36* (8), 1121-1126.

31. Churchill, M. R.; Bezman, S. A.; Osborn, J. A.; Wormald, J., Synthesis and molecular geometry of hexameric triphenylphosphinocopper(I) hydride and the crystal structure of $H_6Cu_6(PPh_3)_6$. $HCONMe_2$ [hexameric triphenylphosphino copper(I) hydride dimethylformamide]. *Inorganic chemistry* **1972,** *11* (8), 1818-1825.

32. Cummings, S. A.; Iimura, M.; Harlan, C. J.; Kwaan, R. J.; Trieu, I. V.; Norton, J. R.; Bridgewater, B. M.; Jäkle, F.; Sundararaman, A.; Tilset, M., An Estimate of the Reduction Potential of B(C6F5)3 from Electrochemical Measurements on Related Mesityl Boranes. *Organometallics* **2006,** *25* (7), 1565-1568.

33. Lawrence, E. J.; Oganesyan, V. S.; Wildgoose, G. G.; Ashley, A. E., Exploring the fate of the tris(pentafluorophenyl)borane radical anion in weakly coordinating solvents. *Dalton Transactions* **2013,** *42* (3), 782-789.

34. Gansäuer, A.; Kube, C.; Daasbjerg, K.; Sure, R.; Grimme, S.; Fianu, G. D.; Sadasivam, D. V.; Flowers, R. A., Substituent Effects and Supramolecular Interactions of Titanocene(III) Chloride: Implications for Catalysis in Single Electron Steps. *Journal of the American Chemical Society* **2014,** *136* (4), 1663-1671.

35. RajanBabu, T. V.; Nugent, W. A., Selective Generation of Free Radicals from Epoxides Using a Transition-Metal Radical. A Powerful New Tool for Organic Synthesis. *Journal of the American Chemical Society* **1994,** *116* (3), 986-997.

36. Gansäuer, A.; Bluhm, H.; Pierobon, M., Emergence of a Novel Catalytic Radical Reaction: Titanocene-Catalyzed Reductive Opening of Epoxides. *Journal of the American Chemical Society* **1998,** *120* (49), 12849-12859.

37. Profitt, J. A.; Watt, D. S.; Corey, E. J., Reagent for the α,β reduction of conjugated nitriles. *The Journal of Organic Chemistry* **1975,** *40* (1), 127-128.

38. Osborn, M. E.; Pegues, J. F.; Paquette, L. A., Reduction of α,β-unsaturated nitriles with a copper hydride complex. *The Journal of Organic Chemistry* **1980,** *45* (1), 167-168.

39. House, H. O.; Umen, M. J., Chemistry of carbanions. XXV. Reaction of various organocopper reagents with α,β-unsaturated carbonyl compounds. *The Journal of Organic Chemistry* **1973,** *38* (22), 3893-3901.

40. House, H. O., Use of lithium organocuprate additions as models for an electron-transfer process. *Accounts of Chemical Research* **1976,** *9* (2), 59-67.

41. Semmelhack, M. F.; Stauffer, R. D., Reductions with copper hydride. New preparative and mechanistic aspects. *The Journal of Organic Chemistry* **1975,** *40* (24), 3619-3621.

42. Semmelhack, M. F.; Stauffer, R. D.; Yamashita, A., Reductions of conjugated carbonyl compounds with copper hydride - preparative and mechanistic aspects. *The Journal of Organic Chemistry* **1977,** *42* (19), 3180-3188.

43. Baker, B. A.; Boskovic, Z. V.; Lipshutz, B. H., (BDP)CuH: A "Hot" Stryker's Reagent for Use in Achiral Conjugate Reductions. *Organic Letters* **2007,** *10* (2), 289-292.

44. Tidwell, T. T., Triarylmethyl and Related Radicals. In *Stable Radicals*, John Wiley & Sons, Ltd: 2010; pp 1-31.

45. Gomberg, M., An Instance of Trivalent Carbon: Triphenylmethyl. *Journal of the American Chemical Society* **1900,** *22* (11), 757-771.

46. Colle, K. S.; Glaspie, P. S.; Lewis, E. S., Equilibrium dissociation of triphenylmethyl dimer. *Journal of the Chemical Society, Chemical Communications* **1975,** (7), 266-267.

47. Dünnebacke, D.; Neumann, W. P.; Penenory, A.; Stewen, U., Über sterisch gehinderte freie Radikale, XIX. Stabile 4,4′,4″-trisubstituierte Triphenylmethyl-Radikale. *Chemische Berichte* **1989,** *122* (3), 533-535.

48. Eisenberg, D. C.; Lawrie, C. J. C.; Moody, A. E.; Norton, J. R., Relative rates of hydrogen atom (H●) transfer from transition-metal hydrides to trityl radicals. *Journal of the American Chemical Society* **1991,** *113* (13), 4888-4895.

49. Rodkin, M. A.; Abramo, G. P.; Darula, K. E.; Ramage, D. L.; Santora, B. P.; Norton, J. R., Isotope Effects on Hydrogen Atom Transfer from Transition Metals to Carbon. *Organometallics* **1999,** *18* (6), 1106-1109.

50. Hembre, R. T.; McQueen, J. S., "Redox-Switch" Catalysis of C□C Bond Formation with H2: One-Electron Reduction of the Trityl Cation. *Angewandte Chemie International Edition in English* **1997,** *36* (1-2), 65-67.

51. Volz, H.; Lotsch, W., Polarographische reduktion von triarylmethylkationen. *Tetrahedron Letters* **1969,** *10* (27), 2275-2278.

52. Connelly, N. G.; Geiger, W. E., Chemical Redox Agents for Organometallic Chemistry. *Chemical Reviews* **1996,** *96* (2), 877-910.

Chapter 4 – Regeneration of Copper Hydrides in Catalysis

4.1 Introduction

Copper hydrides are important catalysts for the selective hydrogenation of α,β-unsaturated carbonyl substrates and catalysis using copper hydrides for this purpose has been demonstrated by Stryker, Buchwald, Lipshutz, Lalic, and many others as discussed earlier in chapter 3. Two general strategies for catalysis have been detailed in the literature using either a silane or hydrogen gas and a suitable base. Shortly after their first report that $[Ph_3PCuH]_6$ was completely selective for the hydrogenation of α,β-unsaturated carbonyl substrates to the corresponding saturated carbonyl compounds, Stryker et al reported that $[Ph_3PCuH]_6$ could be used to catalytically hydrogenate α,β-unsaturated carbonyl compounds with hydrogen gas as the only stoichiometric reagent.[1] Recently, most reports have used a silane as the stoichiometric reagent to regenerate such copper hydrides.[2]

The regeneration of a copper hydride in the catalytic hydrogenation of enones is presumed to occur by a mechanism where a copper enolate is formed after transfer of hydride from $[Ph_3PCuH]_6$. This copper enolate then undergoes hydrogenolysis in a reaction analogous to the formation of $[Ph_3PCuH]_6$ from $[CuO^tBu]_4$ in the presence of triphenylphosphine (scheme 4.1). While Stryker et al. have said that they intended to study copper enolates;[1] they have not published on this subject. There are now some examples of copper enolates in the literature that are important intermediates in catalysis. The copper in these species can be bound to either C or O depending on the particular example.[3]

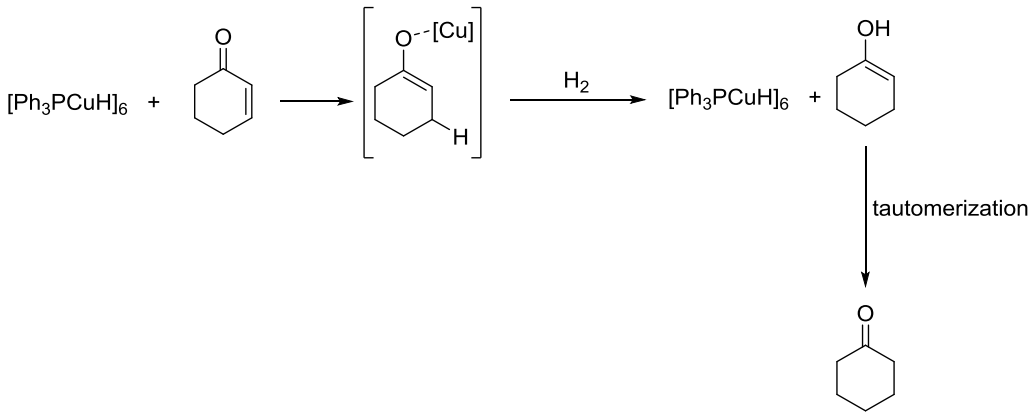

Scheme 4.1. Proposed mechanism for hydrogenation of cyclohexenone by $[Ph_3PCuH]_6$.

In cases where a silane is used instead of hydrogen gas, the copper enolate and the silane undergo a transmetallation reaction to yield a silylated enol. From a laboratory and synthetic standpoint this can be convenient since a protected substrate is obtained directly without the need for an additional protection step.

A critically important aspect of successful catalysis with copper hydrides is the stability of the copper hydrides in solution. While copper(I) is a relatively good electron donor, copper(I) species also are often subject to decomposition by formation of a copper mirror. Stryker has noted that an excess of triphenylphosphine is helpful for preventing decomposition of solutions during catalysis. It is apparent that phosphine ligands can dissociate from a copper hydride hexamer. One method of preparing $[(dppbz)CuH]_3$ is by treatment of $[Ph_3PCuH]_6$ with dppbz, which irreversibly forms $[(dppbz)CuH]_3$ as discussed previously in chapter 1. The sterically congested structure of $[Ph_3PCuH]_6$ presumably encourages dissociation of one triphenylphosphine ligand from $[Ph_3PCuH]_6$, the place of which can then be occupied by a dppbz ligand. In the absence of excess phosphine ligand, the transiently phosphine deficient cluster is subject to decomposition. In my experience, solutions of highly pure $[Ph_3PCuH]_6$ with very low

or no measurable excess triphenylphosphine present are subject to slow decomposition by formation of a copper mirror or a black non-homogeneous solution.

Under catalytic conditions, particularly with enones, use of tert-butanol can be important to improve the stability of copper hydride catalyzed hydrogenations. Stryker has suggested that the tert-butanol helps improve stability by protonating more basic species which may form copper enolates that are less stable than $[CuOtBu]_4$. In cases where a silane is used, Lipshutz has reported that the presence of tert-butanol speeds up catalytic reactions which can also ameliorate stability issues by increasing turnover rates.

4.2 Regeneration of Copper Hydrides following Electron Transfer

While other groups have focused on the use of copper hydride for catalytic hydrogenation of neutral organic substrates, the catalytic regeneration of copper hydrides after electron transfer is intriguing in other regards. In principle, copper hydrides can be used as catalysts for oxidation of hydrogen in a fuel cell. After single electron oxidation copper hydrides can arguably be regenerated by hydrogen gas.

Cationic species are more likely to react with copper hydrides by an electron transfer mechanism. As discussed in chapters 2 and 3, $[Ph_3PCuH]_6$ is capable of transferring an electron to triarylmethyl cations, pyridinium cations, and cationic metallocenes such as ferrocenium and bis(benzene)chromium(I). While an electron can be transferred to some neutral species, as discussed in chapter 3, these cationic species are the most useful for probing the conditions required to catalytically obtain electrons from copper hydride. After transferring an electron or hydride to a neutral substrate, the substrate becomes an anion that can act as a base in the

regeneration of copper hydride. An example of this is copper hydride catalyzed hydrogenation of enones where H_2 is the only stoichiometric reagent.[1]

4.3 Catalytic Reduction of decamethylferrocenium

When $[Ph_3PCuH]_6$ transfers an electron to decamethylferrocenium, $[Ph_3PCuH]_6^{+\bullet}$ is formed. In principle there are several different ways this species could regenerate the original neutral copper hydride. The copper hydride radical cation $[Ph_3PCuH]_6^{+\bullet}$ could be deprotonated to form a neutral radical of the form $(Ph_3P)_6Cu_6H_5^{\bullet}$ and two of these neutral radical species could split H_2 to regenerate the neutral hexamer $[Ph_3PCuH]_6$ in a reaction analogous to the reaction of $CpCr(CO)_3$ with H_2 (scheme 4.2).[4]

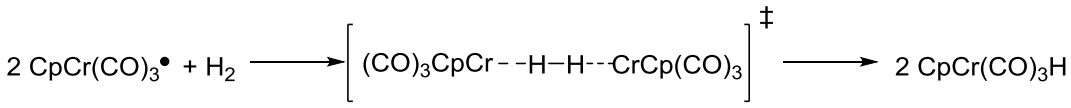

Scheme 4.2. Mechanism by which two metalloradicals react with H_2 to give two metal hydrides.

Upon oxidation, transition metal hydrides are known to become substantially more acidic[5] making this route plausible. Indeed, addition of KO^tBu to a solution containing $[Ph_3PCuH]_6^{+\bullet}$ leads to rapid disappearance of the absorbance at 655 nm which corresponds to $[Ph_3PCuH]_6^{+\bullet}$. The color of the solution changes of the solution changes from green to red, the color of $[Ph_3PCuH]_6$ (equation 4.1).

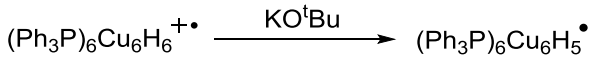

(4.1)

Another possible mechanism is loss of a hydrogen atom from $[Ph_3PCuH]_6^{+\bullet}$ to form a cationic species $(Ph_3P)_6Cu_6H_5^{+}$ which could then coordinate H_2. Deprotonation by a base would

again result in regeneration of $[Ph_3PCuH]_6$ in a reaction that has the same overall stoichiometry as the previously discussed possibility of deprotonation of $[Ph_3PCuH]_6^{+\bullet}$ (scheme 4.3).

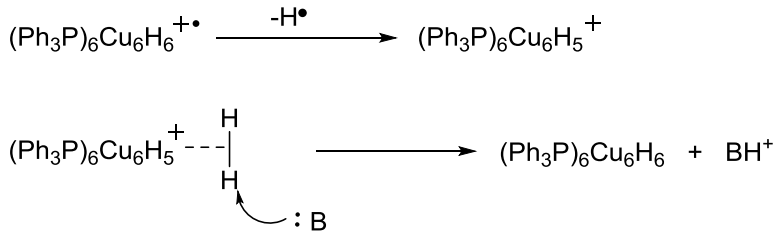

Scheme 4.3. Regeneration of a neutral copper hydride by hydrogen atom loss and deprotonation of a dihydrogen complex.

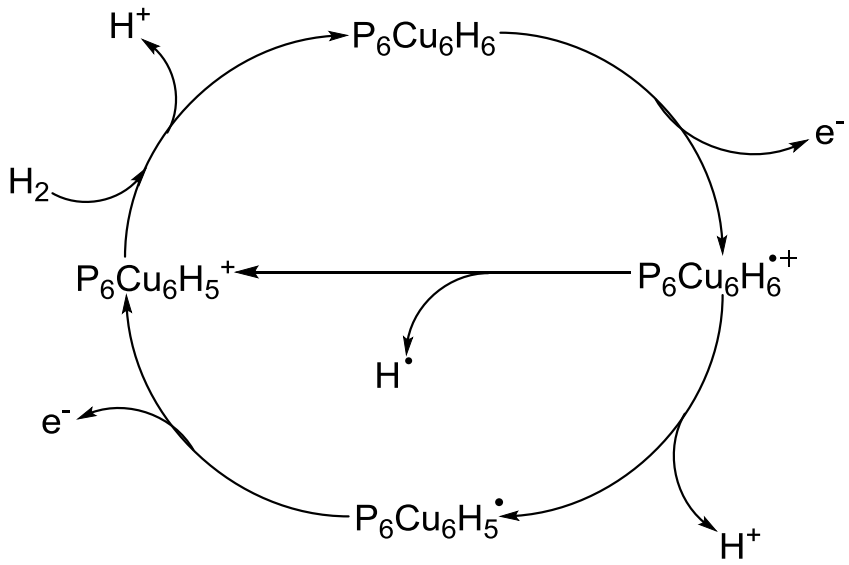

Scheme 4.4. Possible routes by which $[Ph_3PCuH]_6$ could be regenerated after electron transfer.

To probe these routes, a number of experiments were performed. Under 80 psig H_2 and excess triethylamine, 3.64×10^{-5} mol $[Ph_3PCuH]_6$ was able to fully reduce 2.86×10^{-4} mol (7.86 equiv) decamethylferrocenium overnight as confirmed by the absence of decamethylferrocenium

by UV-vis. At the end of this experiment there was no remaining $[Ph_3PCuH]_6$ meaning these conditions are not capable of regenerating $[Ph_3PCuH]_6$ from the final products produced (although the solution is homogeneous and there is no evidence of Cu^0 formation), but it is likely the conditions can reform $[Ph_3PCuH]_6$ from an unstable intermediate. This demonstrates that it is possible to catalytically oxidize hydrogen using a copper hydride catalyst and a base beyond merely transferring one electron per copper(I). Unfortunately, large quantities of triethylamine are required to make this system work at all suggesting that triethylamine may be an insufficiently strong base. The low nucleophilicity of triethylamine could also explain this result; we will see the importance of Cl^- and $tBuO^-$ acting as nucleophiles later in this chapter. It is also not possible to increase the turnover number to more significant values; more decamethylferrocenium always results in some remaining decamethylferrocenium that is unreacted indicating that although it is possible to turn over the catalyst with triethylamine and hydrogen gas, these conditions are not a particularly effective way to do it. Proton sponge (1,8-bis(dimethylamino)naphthalene) has similar thermodynamic basicity to triethylamine and proved to be unable to deprotonate $[Ph_3PCuH]_6^{+\bullet}$. This may be due to the kinetically slow nature of 1,8-bis(dimethylamino)naphthalene. This base also had no impact on the final (stable) copper containing products arising from oxidation of $[Ph_3PCuH]_6$. The pK_a of the conjugate acid (BH^+) is 18.62 for 1,8-bis(dimethylamino)naphthalene and 18.82 for triethylamine in acetonitrile.[6]

I then tried potassium tert-butoxide, since this base is used in the synthesis of $[Ph_3PCuH]_6$. The pK_a of tert-butanol is significantly higher than that of protonated triethylamine. The pK_a of tert-butanol is 19.2 in water[7-8] meaning that KOtBu is a much stronger base than NEt_3 or proton sponge. The radical cation, $[Ph_3PCuH]_6^{+\bullet}$ formed by single electron oxidation of $[Ph_3PCuH]_6$ rapidly disappears when KO^tBu is added to the solution and the red

color of $[Ph_3PCuH]_6$ reappears. Cyclic voltammetry experiments on $[Ph_3PCuH]_6$ in the presence of KO^tBu show an irreversible wave with oxidation at the same potential as the oxidation wave in the $[Ph_3PCuH]_6/[Ph_3PCuH]_6^{+\bullet}$ electrochemical couple (Figure 4.1). It is well known that transition metal hydrides often become 15-30 pKa units more acidic upon oxidation,[5] the resultant facile rapid deprotonation of many oxidized metal hydrides is a major reason why many of them have irreversible electrochemistry. Apparently, KO^tBu can deprotonate $[Ph_3PCuH]_6^{+\bullet}$. However this deprotonation only answers part of the question about how to regenerate copper hydrides under catalytic conditions with hydrogen. Copper hydrides pose an interesting situation, because of their cluster nature; there are more options for structural rearrangement and follow-up reactions than with mononuclear transition metal hydrides.

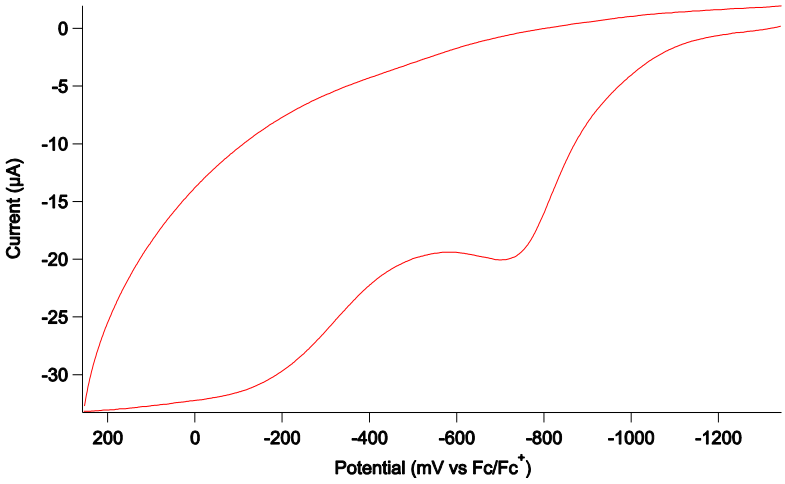

Figure 4.1. Cyclic Voltammogram of $[Ph_3PCuH]_6$ in the presence of KO^tBu. 0.001 Mol/L $[Ph_3PCuH]_6$, 0.035 Mol/L KO^tBu, 0.1 Mol/L $[NBu_4][(C_6F_5)_4B]$ in THF, 100 mV/s. The electrochemistry of $[Ph_3PCuH]_6$ is reversible in THF in the absence of base.

The copper hydride radical cation $[Ph_3PCuH]_6^{+\bullet}$ is unstable in solution at room temperature. This species has been found to decay with a first-order rate constant of about 1 ×

10^{-3} s^{-1} at room temperature in THF. This rate of decomposition varies modestly with solvent and is invariant with concentration of the reaction components. The decomposition of $[Ph_3PCuH]_6^{+\bullet}$ is clearly first order (Figure 4.2) as successive half-lives are the same. Varying the initial quantities of neutral copper hexamer or the amount of oxidant used also does not impact the rate constant for decay of $[Ph_3PCuH]_6^{+\bullet}$.

Table 4.1. Rates of $[Ph_3PCuH]_6^{+\bullet}$ decomposition.

k_{obs} 655 nm (s^{-1})	$[Ph_3PCuH]_6$	[Oxidant]	Oxidant Identity	Solvent
0.00104	1.44 mmol/L	1.08 mmol/L	$Cp^*_2Fe(PF_6)$	THF
0.00109	1.47 mmol/L	0.509 mmol/L	$Cp^*_2Fe(PF_6)$	THF
0.00151	3.23 mmol/L	0.615 mmol/L	$Cp^*_2Fe(PF_6)$	THF
0.00121	2.11 mmol/L	0.631 mmol/L	$Cp^*_2Fe(PF_6)$	THF
0.00079	0.88 mmol/L	0.348 mmol/L	$Cp^*_2Fe(C_6F_5)_4B$	THF
0.000823	1.63 mmol/L	0.965 mmol/L	$Cp^*_2Fe(C_6F_5)_4B$	THF

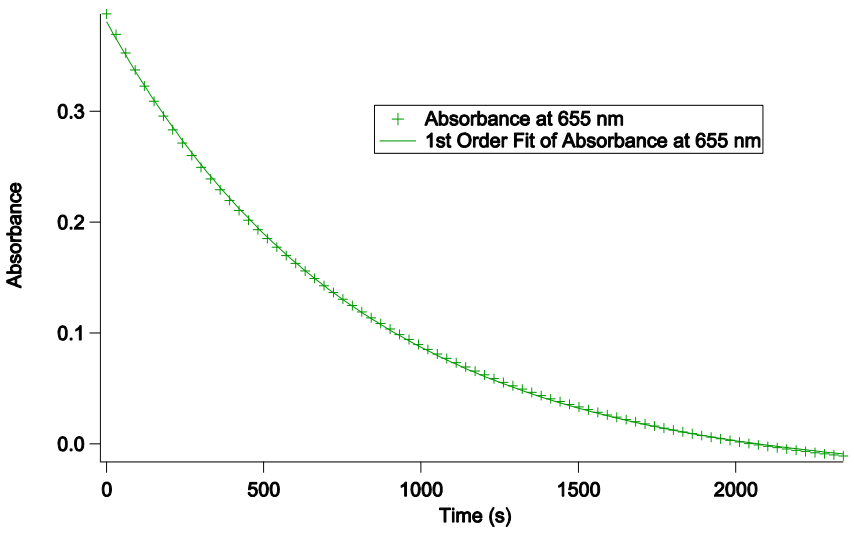

Figure 4.2. Absorbance change as a function of time during the decomposition reaction of $[Ph_3PCuH]_6^{+\bullet}$. Successive half-lives are the same demonstrating that this reaction obeys first order kinetics. The first order rate constant determined for the 655 nm trace is 1.25(1) x 10^{-3} s^{-1}.

By NMR, H_2 can be observed after $[Ph_3PCuH]_6$ is oxidized by $Cp^*_2Fe^+$ and two new hydride resonances can be observed in the ^{1}H NMR at δ = 4.13 (**A**) and 3.76 (**B**) in THF-d_8. The new peaks are both broad, indicating coupling to ^{63}Cu and ^{65}Cu nuclei. Coupling to phosphorous is not well resolved for **B**; however, ^{31}P decoupling the ^{1}H NMR spectrum results in sharpening of this peak (Figure 4.3). Other peaks in the spectrum are minimally affected or slightly broadened upon ^{31}P decoupling. The second new signal which appears at δ = 4.13 (**A**) is a well resolved septet which resembles the septets observed (discussed in chapter 1) at low temperature for the hydride ligand resonance in $[Ph_3PCuH]_6$ and $[(p\text{-anisyl})_3PCuH]_6$. However, due to a larger coupling constant between phosphorus and the hydride ligand protons in this species than in $[Ph_3PCuH]_6$ or $[(p\text{-anisyl})_3PCuH]_6$, the J = 7.5 Hz coupling is easily observed at room temperature. This distinctive septet which collapses to a singlet in a ^{31}P decoupled ^{1}H NMR

spectrum indicates that this species contains six phosphorous nuclei and that the hydride ligands undergo rapid intramolecular exchange (like in neutral $[Ph_3PCuH]_6$) since the six phosphorus atoms in the structure are equivalent. The presence of six phosphorus atoms which are equivalent on the NMR time scale suggests that there are most likely also 6 copper atoms in the structure. These data and the chemical shifts of these signals demonstrate that these species are copper hydrides.

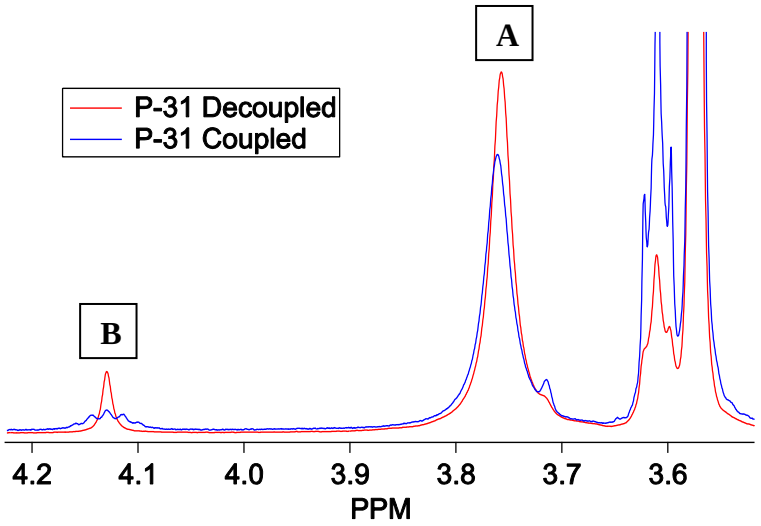

Figure 4.3. ^{1}H and $^{1}H\{^{31}P\}$spectra showing copper hydride resonances at 3.76 (**A**) and 4.13 (**B**) in THF-d_8. The peaks near 3.6 in the ^{1}H NMR are THF and the residual proton peak from THF-d_8. The small peak near 3.7 overlapping the 3.76 peak is a ^{13}C THF satellite.

Reactions between $[Ph_3PCuH]_6$ and trityl cations (Ar_3C^+) yield the same copper hydride products as oxidation by ferrocenium. The trityl cation essentially abstracts hydride from the copper hydride cluster, although this process goes by a stepwise mechanism as discussed in chapter 3 in the case of copper hydrides. Transfer of a hydride ligand from copper hydride should result in a species with the formula $(Ph_3P)_6Cu_6H_5^+$. While **B** clearly contains six phosphorus atoms and could plausibly be this species, the dominant copper hydride species in

solution has a ^{1}H resonance at $\delta = 3.76$ in THF-d_8 (**A**). The ratio of these two peaks does not remain constant as a function of time which demonstrates that the two peaks do not belong to the same species.

The ^{1}H NMR resonance of A corresponds to a peak of approximately $\delta = 4.1$ in toluene-d_8 or benzene-d_6. In toluene-d_8, this peak does not show resolvable coupling to ^{31}P even when cooled to 250 K in (figure 4.4) and the same behavior was observed in THF-d_8.

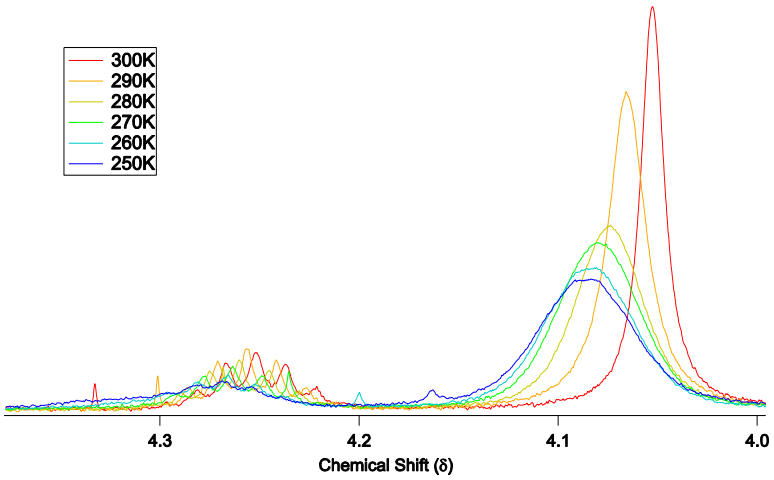

Figure 4.4. VT-NMR in Toluene-d_8.

In fact, this peak broadens as temperature is reduced contrasting with the behavior of $[Ph_3PCuH]_6$ discussed in chapter 1. The ^{1}H resonances of the hydride ligands in neutral copper hexamers $[Ph_3PCuH]_6$ and $[(p\text{-anisyl})_3PCuH]_6$ sharpen as temperature decreases because of the impact of solvent viscosity on quadrupolar relaxation. However, as also discussed in chapter 1, there are two competing phenomena as temperature changes. The fact that six equivalent phosphorus nuclei are coupled to the hydride ligands demonstrates that there is rapid intramolecular exchange. As was seen in chapter 1, at very low temperatures this exchange can be slowed resulting in a spectrum that is broad at high and low temperatures but sharp at

intermediate temperatures. In the case of this species, only broadening is observed with decreased temperature which suggests that intramolecular exchange occurs at an intermediate rate in this species and is the dominant cause of broadening in the ^{1}H NMR spectrum of the hydride ligand. To determine the structure of this copper hydride species, it was necessary to obtain crystals for x-ray diffraction.

4.3 Structural Characterization of An Unexpected Cationic Hepta-copper Hydride

By oxidation of $[Ph_3PCuH]_6$ with $Cp^*_2Fe^+$ followed by careful layering with pentane, small needle crystals suitable for x-ray structure determination were obtained. Surprisingly the cationic seven-copper cluster $(Ph_3P)_7Cu_7H_6^+$ was obtained as a $(C_6F_5)_4B^-$ salt. This species can also be produced using a trityl cation as the oxidant instead of $Cp^*_2Fe^+$. In the case where a trityl cation is used as the oxidant, the triarylmethane product is also observed by ^{1}H NMR although it is formation is not quantitative because some H_2 is also produced in the reaction at a rate competitive with hydrogen atom transfer to $(p\text{-}^t\text{Bu})_3\text{C}\bullet$. The mechanism by which H_2 is lost accounts for the same copper containing products when $Cp^*_2Fe^+$ is used as the oxidant.

$$[Ph_3PCuH]_6 + (p\text{-}^t\text{Bu})_3C^+ \longrightarrow [Ph_3PCuH]_6^{+\bullet} + (p\text{-}^t\text{Bu})_3C\bullet \quad (4.1)$$

$$[Ph_3PCuH]_6^{+\bullet} + (p\text{-}^t\text{Bu})_3C\bullet \longrightarrow (Ph_3P)_6Cu_6H_5^+ + (p\text{-}^t\text{Bu})_3C\text{-H} \quad (4.2)$$

$$(Ph_3P)_6Cu_6H_5^+ + [Ph_3PCuH]_6 \longrightarrow (Ph_3P)_7Cu_7H_6^+ + [Ph_3PCuH]_5 \quad (4.3)$$

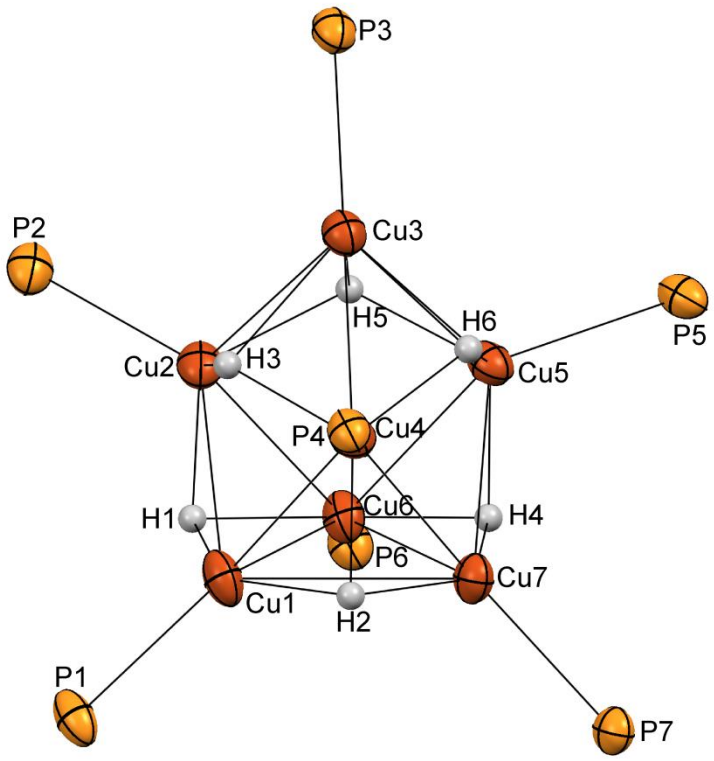

Figure 4.5. Core ellipsoid plot of $[(Ph_3P)_7Cu_7H_6]^+$

The cationic cluster $[(Ph_3P)_7Cu_7H_6]^+$ is effectively a copper hydride hexamer with one face capped by an additional CuP^+ unit. $[Ph_3PCuH]_6$ clusters are approximately a "squashed" octahedron with six smaller Cu_3 faces capped by hydride ligands and two larger Cu_3 faces which lack hydride ligands,[9] as discussed earlier in chapter 1. The CuP^+ unit occupies one of Cu_3 faces lacking hydride ligands; the CuP^+ unit consists of Cu3 and P3 in figure 4.5. The Cu-Cu distances on the CuP^+ capped face expand to average 3.11 Å (distances around the triangle formed by Cu2, Cu4, and Cu5), substantially longer than the longer set of Cu-Cu distances in $[Ph_3PCuH]_6$ (average 2.74 Å for the set of longer Cu-Cu bonds uncapped by a hydride ligand in $[Ph_3PCuH]_6$) [10] and longer than those in metallic copper (2.5562 Å)[11] which suggests that metal-

metal bonding is not significant between these atoms. The distances between the capping CuP^+ unit and the Cu atoms in the Cu_3 face average 2.48 Å (distance from Cu3 to Cu2, Cu4, and Cu5). These are the shortest Cu-Cu distances in the cluster, and are shorter than those in metallic copper (2.5562 Å) suggesting metal-metal interactions. This seven copper cluster has 96 valence electrons suggesting there could be *up to* 15 metal-metal bonds. In this seven-copper structure, there are 12 Cu-Cu distances shorter than 2.72 Å along with the additional three longer distances on the Cu_3 face capped by the CuP^+ unit.

4.4 Chemical Reactions of the $[(Ph_3P)_7Cu_7H_6]^+$

While we suspected that a copper hydride species should be acidic after losing a hydride ligand, the positive overall charge on $[(Ph_3P)_7Cu_7H_6]^+$ is the only factor that might suggesting acidity. Treatment of $[(Ph_3P)_7Cu_7H_6]^+$ with triethylamine gave no reaction. The possibility of converting $[(Ph_3P)_7Cu_7H_6]^+$ back to neutral $[Ph_3PCuH]_6$ using KO^tBu under a H_2 atmosphere was tested. Upon addition of KO^tBu, the red color of $[Ph_3PCuH]_6$ appeared and ^1H NMR confirmed that $[Ph_3PCuH]_6$ had been formed by the characteristic chemical shift of its hydride ligands at δ = 3.50 (figure 4.6).

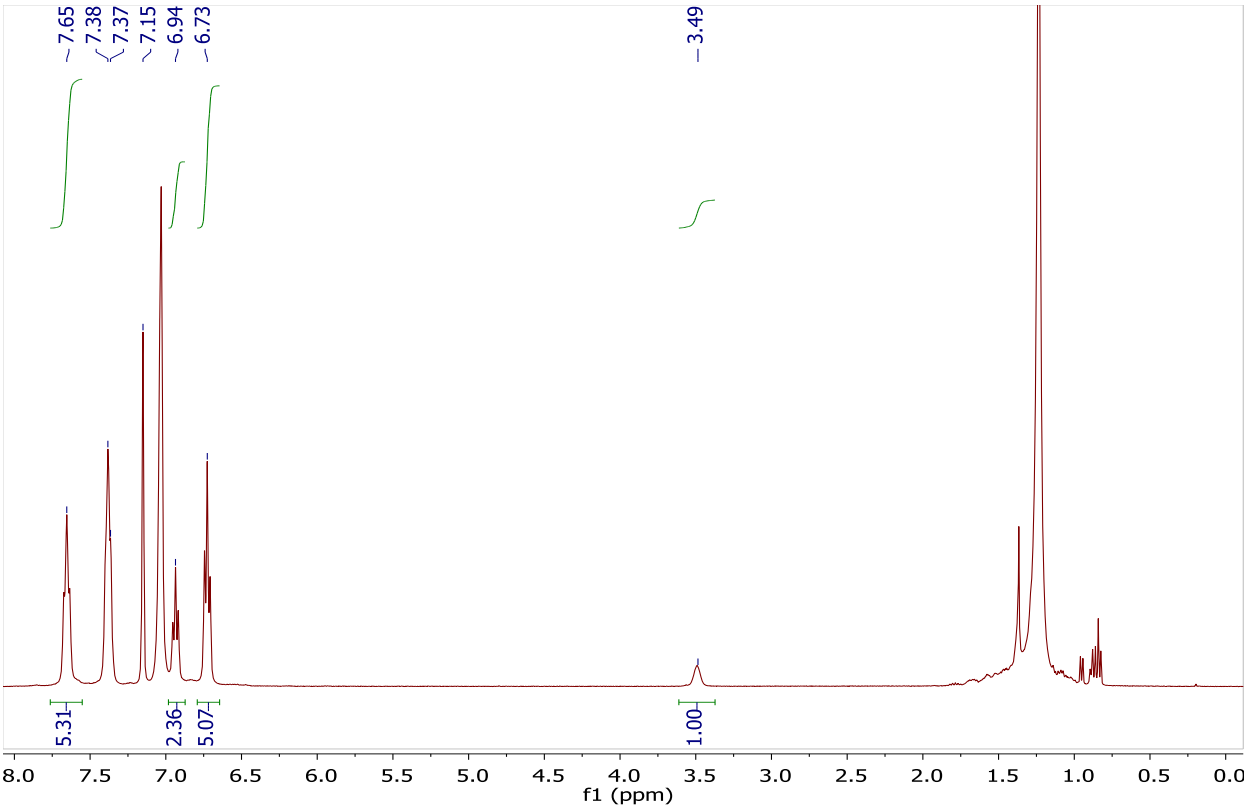

Figure 4.6. ^{1}H NMR of Stryker's reagent generated by addition of KO^{t}Bu to $[(Ph_3P)_7Cu_7H_6]^+[(C_6F_5)_4B]^-$.

Balancing the reaction between $[(Ph_3P)_7Cu_7H_6]^+[(C_6F_5)_4B]^-$ and KO^{t}Bu gives the following:

$$[(Ph_3P)_7Cu_7H_6][(C_6F_5)_4B] + KO^tBu \longrightarrow [Ph_3PCuH]_6 + Ph_3P + CuO^tBu + [K][(C_6F_5)_4B] \qquad (4.2)$$

Copper(I) t-butoxide is a known compound that occurs as a tetramer. There are crystallographically characterized adducts with carbonyl[12] or isonitrile ligands[13] coordinated to each of the four copper atoms in a copper-oxygen cubane structure, a copper(I) phenoxide triphenylphosphine adduct[14] also has a copper-oxygen cubane core. While the structure of a triphenylphosphine adduct of copper(I) t-butoxide has not been reported in the literature, it is reasonable to assume that this species is the other copper containing product of the reaction

between potassium t-butoxide and $[(Ph_3P)_7Cu_7H_6]^+[(C_6F_5)_4B]^-$. In addition, the Caulton[15] and Stryker methods[16] of preparing copper hydrides use copper(I) t-butoxide in the presence of phosphine, which means that once the reaction has been placed under hydrogen pressure, all of the necessary ingredients are present to regenerate $[Ph_3PCuH]_6$. The major problem with actually achieving regeneration of copper hydrides from hydrogen gas is the sensitivity of $[Ph_3PCuH]_6$ to excess t-butoxide. Copper hydrides eventually decompose, forming a copper mirror in the presence of excess *t*-butoxide. Although the synthesis of $[Ph_3PCuH]_6$ frequently uses KO^tBu or NaO^tBu, these are never used in excess and the synthesis will fail if a significant excess of $^-O^tBu$ is used. In the ^1H NMR spectrum, peaks are observed at $\delta = 7.38$ and 6.94, which are similar to those of free triphenylphosphine in C_6D_6. These peaks are not the same as the commonly encountered impurities with broad resonances at $\delta =$ "7.6 and 6.8" that Stryker et al have reported are often present in samples of $[Ph_3PCuH]_6$.

In equation 4.2, $^-O^tBu$ is acting as a nucleophile/Lewis base rather than as a Brønsted base as it might in a reaction with hydrogen gas. What other species can be used in place of KO^tBu to remove a PCu^+ unit from $[(Ph_3P)_7Cu_7H_6]^+[(C_6F_5)_4B]^-$? When $[(Ph_3P)_7Cu_7H_6]^+[(C_6F_5)_4B]^-$ is treated with LiCl or PPNCl (PPN = bis(triphenylphosphine)iminium), $[Ph_3PCuH]_6$ is formed just as in the reaction with KO^tBu. Copper(I) chloride forms an adduct with triphenylphosphine[17] that is structurally similar to the copper alkoxide complexes.[14] In the 1:1 adduct, there is a copper/chloride cubane structure and each copper atom has one phosphine ligand. A mononuclear species of the form $(Ph_3P)_3CuCl$ also exists and is a useful starting material for the synthesis of copper hydrides so this species should be dominant in the presence of excess triphenylphosphine.

Experimental

Preparation of $[(Ph_3P)_7Cu_7H_6]^+[(C_6F_5)_4B]^-$

Using a vial equipped with a stir bar in an argon glovebox, 228 mg $[Ph_3PCuH]_6$ (0.116 mMol) was dissolved in 3 mL benzene and 100.5 mg $[Cp^*_2Fe][(C_6F_5)_4B]$ (0.100 mMol) was slowly added while the solution was rapidly stirred. The solution was stirred for 30 minutes until the dark green color of $[Ph_3PCuH]_6^{+\bullet}$ disappeared giving a dark yellow/brown solution. The solution was carefully layered with pentane and allowed to stand overnight which resulted in a small crop of needle shaped crystals suitable for x-ray diffraction. A significant amount of the product remained as an oil and the product is difficult to crystallize. Yield of $[(Ph_3P)_7Cu_7H_6]^+[(C_6F_5)_4B]^-$ is approximately 67% in NMR scale reactions.

^{1}H NMR (500 MHz, C_6D_6) δ 7.25 (t, *J* = 8.5 Hz, 42 H), 6.88 (t, J = 6.9 Hz, 21 H), 6.67 (mult., 42 H), (br s, 4.03, 6 H)

^{31}P NMR (162 MHz, C_6D_6) δ −1.85

Preparation of $[Cp^*_2Fe]^+[(C_6F_5)_4B]^-$

Decamethylferrocenium tetrakispentafluorophenylborate was synthesized by a procedure similar to the literature method for synthesis of ferrocenium tetrakis[3,5-bis(trifluoromethylphenyl)]borate.[18] 789 mg decamethylferrocene (2.414 mmol) was stirred in 3.6 mL acetone to which 12 mL deionized water was added forming a pale orange slurry. To

this 676 mg $Fe_2(SO_4)_3 \cdot 6H_2O$ were added and the mixture was stirred for two hours forming a dark green solution. The solution was then filtered to remove any insoluble materials. 1.736 g $K(C_6F_5)_4B$ were then added to the solution which resulted in the formation of a green slurry which was collected on a frit and washed with water followed by hexane and then dried under vacuum. Yield 1.749 g (72%). Danger! Fluorine containing boron compounds are potentially explosive and are often sensitive to shock and electrostatic discharge, heating is also potentially hazardous.

Preparation of decamethylferrocene

A THF solution (60 mL) containing pentamethylcyclopentadiene (4.70 mL, 30 mmol) was cooled to -78 °C while stirring, to this 30 mmol nBuLi was added dropwise as a 2.2 mol/L solution in cyclohexane (13.6 mL). The reaction was allowed to warm to room temperature and was opened briefly while maintaining a stream of nitrogen to add anhydrous ferrous chloride (1.90 g, 15 mmol). The reaction was stirred overnight, filtered to remove any undissolved materials and the solvent removed by rotary evaporation. The product was dissolved in hot hexanes and cooled to -20 °C forming 2.243 g of large crystals overnight. The solvent was removed from the filtrate and this was redissolved in pentane and chilled to -20 °C to give a second crop of large crystals 1.417 g. Total yield is 3.660 g (75 %)

Cyclic Voltammetry

Cyclic voltammetry on $[Ph_3PCuH]_6$ in the presence of base was carried out in THF containing 0.1 mol/L tetrabutylammonium tetrakis(pentafluorophenyl)borate as a supporting electrolyte (synthesized by literature procedures[19]). The analyte solution was contained $[Ph_3PCuH]_6$ at a

concentration of 0.001 Mol/L and KO^tBu at a concentration of 0.036 Mol/L. The scan rate shown was 100 mV/s. The reference electrode was Ag/Ag^+ in CH_3CN (0.01 Mol/L $AgNO_3$), and was separated from the analyte solution by a vycor frit; the counter electrode was not isolated from the analyte solution. The potentials were converted to Fc/Fc^+ by considering the potential of ferrocene to be -245 V vs Ag/Ag^+, ferrocene could not be used as an internal standard because oxidation of $^-O^tBu$ prevented observation of its redox wave.

Chapter 4 References

1. Mahoney, W. S.; Stryker, J. M., Hydride-mediated homogeneous catalysis. Catalytic reduction of α,β-unsaturated ketones using $[(Ph_3P)CuH]_6$ and H_2. *Journal of the American Chemical Society* **1989,** *111* (24), 8818-8823.

2. Riant, O., *Copper(I) hydride reagents and catalysts*. Pt. 2 ed.; John Wiley & Sons Ltd.: 2009; p 731-773.

3. Plotzitzka, J.; Kleeberg, C., CuI-Catalyzed Conjugate Addition of Silyl Boronic Esters: Retracing Catalytic Cycles Using Isolated Copper and Boron Enolate Intermediates. *Organometallics* **2014,** *33* (23), 6915-6926.

4. Norton, J. R.; Spataru, T.; Camaioni, D. M.; Lee, S.-J.; Li, G.; Choi, J.; Franz, J. A., Kinetics and Mechanism of the Hydrogenation of the $CpCr(CO)_3$•/$[CpCr(CO)_3]_2$ Equilibrium to $CpCr(CO)_3H$. *Organometallics* **2014,** *33* (10), 2496-2502.

5. Tilset, M., 1.11 - Organometallic Electrochemistry: Thermodynamics of Metal–Ligand Bonding. In *Comprehensive Organometallic Chemistry III*, Editors-in-Chief: Robert, H. C.; Mingos, D. M. P., Eds. Elsevier: Oxford, 2007; pp 279-305.

6. Kaljurand, I.; Kütt, A.; Sooväli, L.; Rodima, T.; Mäemets, V.; Leito, I.; Koppel, I. A., Extension of the Self-Consistent Spectrophotometric Basicity Scale in Acetonitrile to a Full Span of 28 pKa Units: Unification of Different Basicity Scales. *The Journal of Organic Chemistry* **2005,** *70* (3), 1019-1028.

7. Jitariu, L. C.; Masters, A. J.; Hillier, I. H., The acidity of tert-butyl alcohol in near- and supercritical water: A polarizable continuum approach. *The Journal of Chemical Physics* **2004,** *121* (16), 7795-7802.

8. Bohme, D. K.; Lee-Ruff, E.; Young, L. B., Standard acidity scale. The pKa of alcohols in the gas phase. *Journal of the American Chemical Society* **1971,** *93* (18), 4608-4609.

9. Stevens, R. C.; McLean, M. R.; Bau, R.; Koetzle, T. F., Neutron diffraction structure analysis of a hexanuclear copper hydrido complex, $H_6Cu_6[P(p\text{-tolyl})_3]_6$: an unexpected finding. *Journal of the American Chemical Society* **1989,** *111* (9), 3472-3473.

10. Albert, C. F.; Healy, P. C.; Kildea, J. D.; Raston, C. L.; Skelton, B. W.; White, A. H., Lewis-base adducts of Group 11 metal(I) compounds. 49. Structural characterization of hexameric and pentameric (triphenylphosphine)copper(I) hydrides. *Inorganic Chemistry* **1989,** *28* (7), 1300-1306.

11. Lide, D. R., *Handbook of Chemistry and Physics, 75th Edition*. CRC: 1994; p 2, 608 pp.

12. Geerts, R. L.; Huffman, J. C.; Folting, K.; Lemmen, T. H.; Caulton, K. G., Concerning the structure and stability of a copper(I) alkoxy carbonyl. *Journal of the American Chemical Society* **1983,** *105* (11), 3503-3506.

13. Oguadinma, P. O.; Schaper, F., Bis(2-phenylethyl)-nacnac: A Chiral Diketiminate Ligand and Its Copper Complexes. *Organometallics* **2009,** *28* (14), 4089-4097.

14. Lopes, C.; Håkansson, M.; Jagner, S., Products of the reaction between copper(I) phenoxide and triphenylphosphine. *Inorganica Chimica Acta* **1997,** *254* (2), 361-366.

15. Lemmen, T. H.; Folting, K.; Huffman, J. C.; Caulton, K. G., Copper polyhydrides. *Journal of the American Chemical Society* **1985,** *107* (25), 7774-7775.

16. Brestensky, D. M.; Huseland, D. E.; McGettigan, C.; Stryker, J. M., Simplified, "one-pot" procedure for the synthesis of $[(Ph_3P)CuH]_6$, a stable copper hydride for conjugate reductions. *Tetrahedron Letters* **1988,** *29* (31), 3749-3752.

17. Churchill, M. R.; Kalra, K. L., Molecules with an M4X4 core. I. Crystal and molecular structure of tetrameric triphenylphosphinecopper(I) chloride, a cubane-like molecule, including the location and refinement of all hydrogen atoms. *Inorganic Chemistry* **1974,** *13* (5), 1065-1071.

18. Le Bras, J.; Jiao, H.; Meyer, W. E.; Hampel, F.; Gladysz, J. A., Synthesis, crystal structure, and reactions of the 17-valence-electron rhenium methyl complex $[(\eta^5\text{-}C_5Me_5)Re(NO)(P(4\text{-}C_6H_4CH_3)_3)(CH_3)]+ B(3,5\text{-}C_6H_3(CF_3)_2)_4^-$: experimental and computational bonding comparisons with 18-electron methyl and methylidene complexes. *Journal of Organometallic Chemistry* **2000,** *616* (1–2), 54-66.

19. LeSuer, R. J.; Buttolph, C.; Geiger, W. E., Comparison of the Conductivity Properties of the Tetrabutylammonium Salt of Tetrakis(pentafluorophenyl)borate Anion with Those of Traditional Supporting Electrolyte Anions in Nonaqueous Solvents. *Analytical Chemistry* **2004,** *76* (21), 6395-6401.

Appendix – X-ray Structures

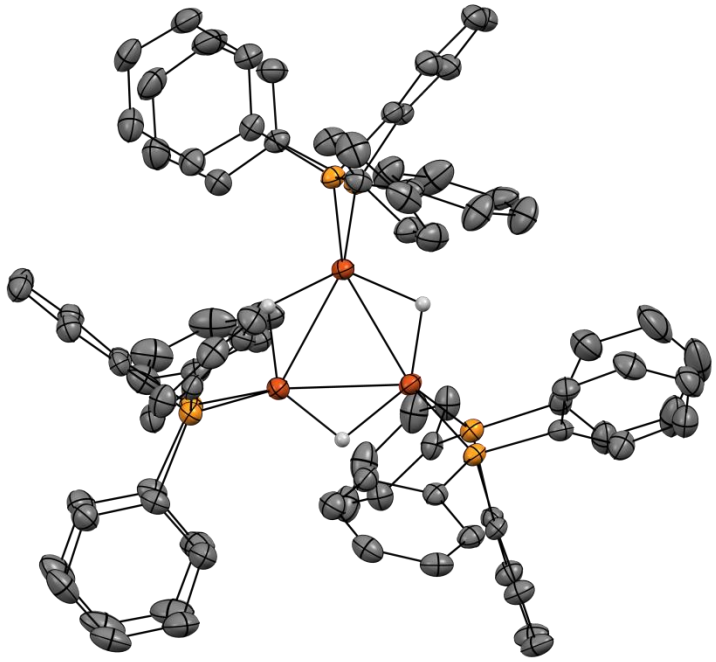

Figure A-1. Thermal ellipsoid (50% probability) plot for $[(dppbz)CuH]_3$.

Table A-1. Crystal data and structure refinement for $[(dppbz)CuH]_3$.

Identification code	mic2s10	
Empirical formula	C30 H25 Cu P2	
Formula weight	510.98	
Temperature	130(2) K	
Wavelength	0.71073 A	
Crystal system, space group	Monoclinic, $P2_1/n$	
Unit cell dimensions	a = 21.758(13) Å	α = 90°
	b = 15.190(9) Å	β = 112.054(9)°
	c = 26.251(16) Å	γ = 90°
Volume	8041(8) $Å^3$	
Z, Calculated density	12, 1.266 Mg/m^3	
Absorption coefficient	0.949 mm^{-1}	
F(000)	3168	
Crystal size	0.55 x 0.27 x 0.17 mm	

Theta range for data collection	1.53 to 30.82 deg.
Limiting indices	-31<=h<=31, -21<=k<=21, -37<=l<=37
Reflections collected / unique	128437 / 24937 [R(int) = 0.0784]
Completeness to theta = 30.82	98.8 %
Absorption correction	Empirical
Max. and min. transmission	0.8553 and 0.6233
Refinement method	Full-matrix least-squares on F^2
Data / restraints / parameters	24937 / 0 / 904
Goodness-of-fit on F^2	1.008
Final R indices [I>2sigma(I)]	R1 = 0.0509, wR2 = 0.1124
R indices (all data)	R1 = 0.0867, wR2 = 0.1230
Largest diff. peak and hole	0.831 and -0.377 e $Å^{-3}$

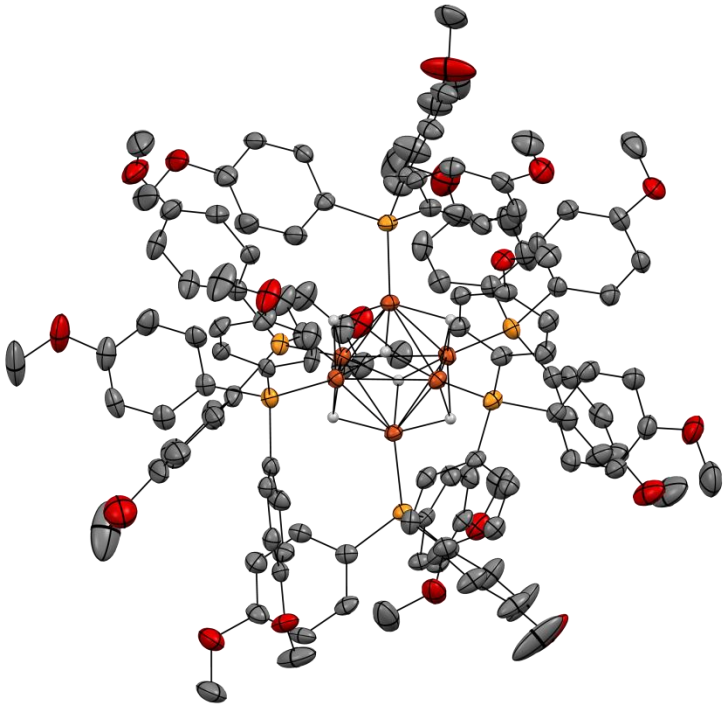

Figure A-2. Thermal ellipsoid (50% probability) plot for $[(p\text{-anisyl})_3PCuH]_6$.

Table A-2. Crystal data and structure refinement for $[(p\text{-anisyl})_3PCuH]_6$.

Identification code	mecus10	
Empirical formula	C126 H132 Cu6 O18 P6	
Formula weight	2501.38	
Temperature	130(2) K	
Wavelength	0.71073 A	
Crystal system, space group	Monoclinic, $P2_1/n$	
Unit cell dimensions	a = 21.5852(12) Å	α = 90°
	b = 20.8629(12) Å	β = 99.4840(10)°

	c = 26.8356(15) Å γ = 90°
Volume	11919.7(12) $Å^3$
Z, Calculated density	4, 1.394 Mg/m^3
Absorption coefficient	1.197 mm^{-1}
F(000)	5184
Crystal size	0.24 x 0.14 x 0.08 mm
Theta range for data collection	1.37° to 30.63°
Limiting indices	-30<=h<=30, -29<=k<=29, -38<=l<=38
Reflections collected / unique	192218 / 36660 [R(int) = 0.1991]
Completeness to theta = 30.63	99.7 %
Absorption correction	Empirical
Max. and min. transmission	0.9104 and 0.7622
Refinement method	Full-matrix least-squares on F^2
Data / restraints / parameters	36660 / 0 / 1458
Goodness-of-fit on F^2	1.007
Final R indices [I>2sigma(I)]	R1 = 0.0670, wR2 = 0.1169
R indices (all data)	R1 = 0.2123, wR2 = 0.1577
Largest diff. peak and hole	0.964 and -0.739 e $Å^{-3}$

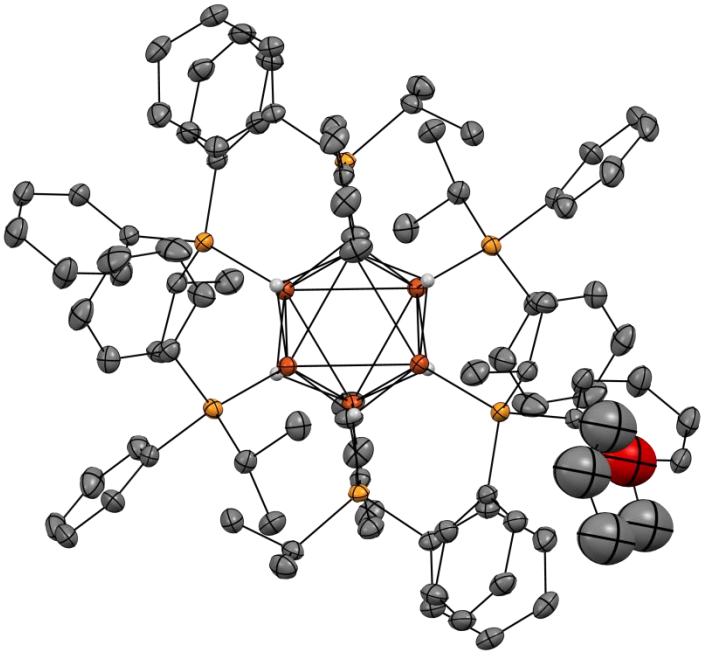

Figure A-3. Thermal ellipsoid (50% probability) plot for $[^{i}PrPh_2PCuH]_6$•THF.

Table A-3. Crystal data and structure refinement for $[^{i}PrPh_2PCuH]_6$•THF.

Identification code	mews10
Empirical formula	C98 H124 Cu6 O2 P6

Formula weight	1901.03
Temperature	150(2) K
Wavelength	0.71073 A
Crystal system, space group	Triclinic, $P\bar{1}$
Unit cell dimensions	a = 13.0054(10) Å α = 68.9350(10)°
	b = 13.8810(11) Å β = 74.6210(10)°
	c = 14.6853(12) Å δ = 72.0680(10)°
Volume	2317.8(3) $Å^3$
Z, Calculated density	1, 1.362 Mg/m^3
Absorption coefficient	1.502 mm^{-1}
F(000)	992
Crystal size	0.21 x 0.20 x 0.04 mm
Theta range for data collection	1.51° to 28.28°
Limiting indices	-17<=h<=17, -18<=k<=18, -19<=l<=19
Reflections collected / unique	32576 / 11504 [R(int) = 0.0350]
Completeness to theta = 28.28	99.9 %
Absorption correction	EMPIRICAL
Max. and min. transmission	0.9424 and 0.7433
Refinement method	Full-matrix least-squares on F^2
Data / restraints / parameters	11504 / 30 / 499
Goodness-of-fit on F^2	1.131
Final R indices [I>2sigma(I)]	R1 = 0.0368, wR2 = 0.0901
R indices (all data)	R1 = 0.0539, wR2 = 0.0978
Largest diff. peak and hole	1.118 and -0.666 e $Å^{-3}$

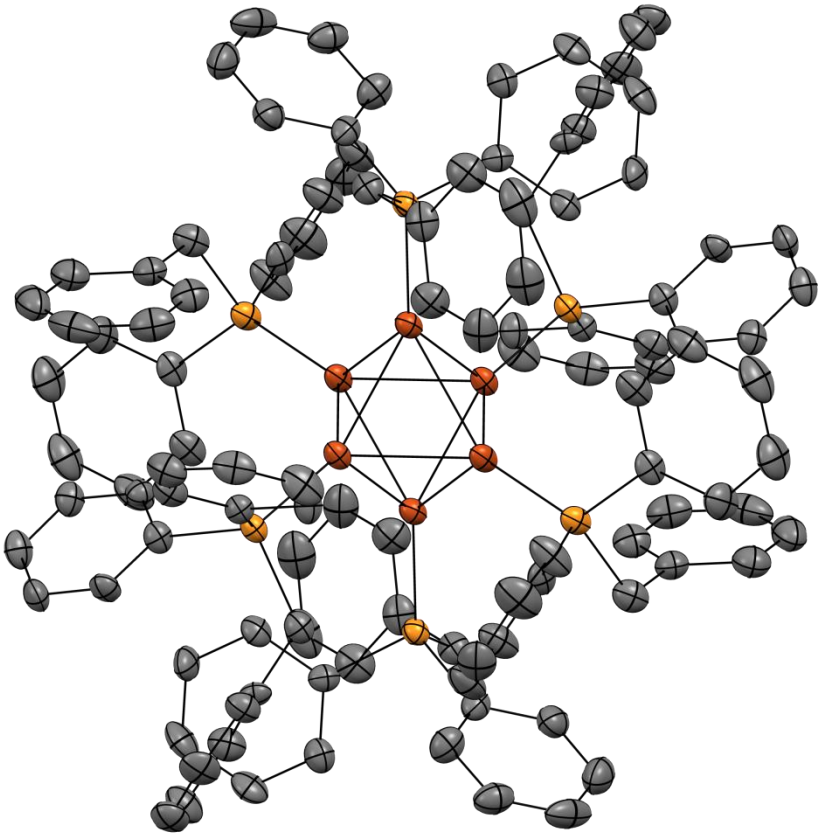

Figure A4. Thermal ellipsoid (50% probability) plot for $[BnPh_2PCuH]_6 \bullet C_6H_6$.
The unit cell contains two independent $[BnPh_2PCuH]_6$ hexamers and two benzene molecules, only one of each is shown for clarity. See the .cif file for complete structure.

Table A-4. Crystal data and structure refinement for $[BnPh_2PCuH]_6 \bullet C_6H_6$.

Identification code	meta5	
Empirical formula	C120 H108 Cu6 P6	
Formula weight	2117.12	
Temperature	150(2) K	
Wavelength	0.71073 Å	
Crystal system, space group	Monoclinic, $P2_1/c$	
Unit cell dimensions	a = 19.318(2) Å	α= 90°
	b = 25.327(3) Å	β = 91.781(2)°

	c = 20.917(2) Å δ = 90°
Volume	10229(2) $Å^3$
Z, Calculated density	4, 1.375 Mg/m^3
Absorption coefficient	1.368 mm^{-1}
F(000)	4368
Crystal size	0.20 x 0.18 x 0.08 mm
Theta range for data collection	1.61 to 33.26°
Limiting indices	-29<=h<=29, 0<=k<=36, 0<=l<=27
Reflections collected / unique	248713 / 31567 [R(int) = 0.2086]
Completeness to theta = 25.00	100.0 %
Absorption correction	Empirical
Max. and min. transmission	0.8984 and 0.7715
Refinement method	Full-matrix least-squares on F^2
Data / restraints / parameters	31567 / 0 / 1190
Goodness-of-fit on F^2	1.013
Final R indices [I>2sigma(I)]	R1 = 0.0810, wR2 = 0.1383
R indices (all data)	R1 = 0.2020, wR2 = 0.1802
Largest diff. peak and hole	1.132 and -1.070 e A^{-3}

Figure A-5. Thermal ellipsoid (50% probability) plot for $[(Ph_3P)_7Cu_7H_6][B(C_6F_5)_4]$.

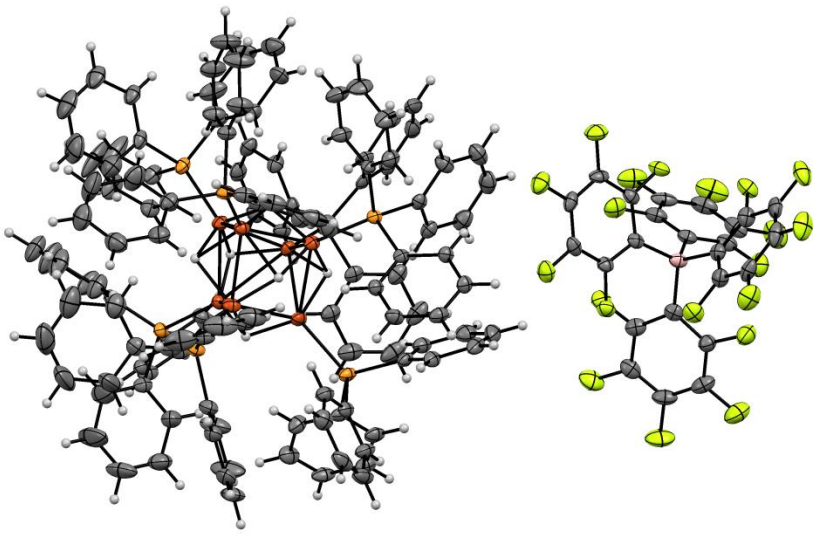

Table A-5. Crystal data and structure refinement for $[(Ph_3P)_7Cu_7H_6][B(C_6F_5)_4]$.

Identification code	cu7h6p-sr

Empirical formula	C166 H143 B Cu7 F20 O4 P7
Formula weight	3254.18
Temperature	130(2) K
Wavelength	0.71073 A
Crystal system, space group	Monoclinic, P2(1)/c
Unit cell dimensions	a = 18.193(4) A alpha = 90 deg. b = 16.401(3) A beta = 92.094(3) deg. c = 46.871(9) A gamma = 90 deg.
Volume	13976(5) $Å^3$
Z, Calculated density	4, 1.547 Mg/m^3
Absorption coefficient	1.211 mm^{-1}
F(000)	6656
Crystal size	1.150 x 0.070 x 0.020 mm
Theta range for data collection	1.315 to 30.635 deg.
Limiting indices	-26<=h<=26, -23<=k<=23, -67<=l<=66
Reflections collected / unique	228212 / 42947 [R(int) = 0.1384]
Completeness to theta = 25.000	100.0 %
Absorption correction	Empirical
Max. and min. transmission	0.7461 and 0.6456
Refinement method	Full-matrix least-squares on F^2
Data / restraints / parameters	42947 / 0 / 1690
Goodness-of-fit on F^2	1.002
Final R indices [I>2sigma(I)]	R1 = 0.0593, wR2 = 0.0997
R indices (all data)	R1 = 0.1349, wR2 = 0.1139
Extinction coefficient	n/a
Largest diff. peak and hole	0.551 and -0.585 e.A^-3

Table A-6. Atomic coordinates (x 10^4) and equivalent isotropic displacement parameters ($Å^2$ x 10^3) for $[(Ph_3P)_7Cu_7H_6][B(C_6F_5)_4]$. U(eq) is defined as one third of the trace of the orthogonalized Uij tensor.

	x	y	z	U(eq)
Cu(1)	3772(1)	2070(1)	6660(1)	26(1)
Cu(2)	2432(1)	1681(1)	6661(1)	26(1)
Cu(3)	1992(1)	2120(1)	6181(1)	23(1)
Cu(4)	3280(1)	2632(1)	6191(1)	23(1)
Cu(5)	2712(1)	863(1)	6086(1)	24(1)
Cu(6)	3293(1)	518(1)	6569(1)	23(1)
Cu(7)	4020(1)	1340(1)	6167(1)	24(1)
P(1)	4480(1)	2754(1)	6985(1)	28(1)
P(2)	1619(1)	1730(1)	7012(1)	28(1)
P(3)	920(1)	2643(1)	6022(1)	25(1)
P(4)	3495(1)	3885(1)	6009(1)	21(1)
P(5)	2459(1)	1(1)	5717(1)	25(1)
P(6)	3207(1)	-748(1)	6757(1)	23(1)
P(7)	5074(1)	1132(1)	5942(1)	24(1)
B(1)	8091(2)	7017(2)	5994(1)	26(1)
C(1)	5098(2)	2101(2)	7202(1)	30(1)
C(2)	4814(2)	1350(2)	7285(1)	34(1)
C(3)	5241(2)	821(2)	7455(1)	39(1)
C(4)	5953(2)	1032(2)	7537(1)	37(1)
C(5)	6239(2)	1769(2)	7456(1)	34(1)
C(6)	5817(2)	2307(2)	7289(1)	33(1)
C(7)	5093(2)	3531(2)	6846(1)	27(1)
C(8)	4923(2)	4364(2)	6861(1)	30(1)
C(9)	5388(2)	4939(2)	6744(1)	36(1)
C(10)	6023(2)	4694(2)	6614(1)	39(1)
C(11)	6188(2)	3869(2)	6595(1)	38(1)
C(12)	5716(2)	3290(2)	6705(1)	33(1)
C(13)	3987(2)	3314(2)	7257(1)	29(1)
C(14)	4337(2)	3576(2)	7510(1)	37(1)
C(15)	3946(3)	3990(2)	7712(1)	45(1)
C(16)	3211(3)	4152(2)	7664(1)	46(1)
C(17)	2857(2)	3896(2)	7412(1)	41(1)
C(18)	3251(2)	3469(2)	7210(1)	34(1)
C(19)	2010(2)	1858(2)	7376(1)	32(1)
C(20)	2659(2)	1447(3)	7446(1)	56(1)

C(21)	2994(3)	1569(3)	7716(1)	69(2)
C(22)	2680(2)	2077(3)	7911(1)	52(1)
C(23)	2045(2)	2481(2)	7842(1)	41(1)
C(24)	1701(2)	2365(2)	7577(1)	34(1)
C(25)	948(2)	2557(2)	6994(1)	30(1)
C(26)	1158(2)	3301(2)	6882(1)	34(1)
C(27)	685(3)	3952(2)	6883(1)	50(1)
C(28)	-1(3)	3880(3)	6987(1)	61(1)
C(29)	-223(2)	3152(3)	7096(1)	56(1)
C(30)	247(2)	2483(2)	7101(1)	43(1)
C(31)	1037(2)	828(2)	7032(1)	35(1)
C(32)	979(3)	351(3)	7273(1)	75(2)
C(33)	510(4)	-322(3)	7272(1)	97(2)
C(34)	107(3)	-527(3)	7036(1)	83(2)
C(35)	139(3)	-58(3)	6793(1)	71(2)
C(36)	611(2)	616(2)	6789(1)	50(1)
C(37)	111(2)	2080(2)	6138(1)	32(1)
C(38)	-246(2)	2300(2)	6386(1)	42(1)
C(39)	-847(2)	1855(3)	6478(1)	51(1)
C(40)	-1094(2)	1178(3)	6322(1)	55(1)
C(41)	-740(2)	961(3)	6090(1)	71(2)
C(42)	-145(2)	1409(3)	5993(1)	57(1)
C(43)	781(2)	2636(2)	5634(1)	28(1)
C(44)	404(2)	3244(2)	5483(1)	40(1)
C(45)	295(2)	3184(3)	5189(1)	53(1)
C(46)	567(2)	2528(2)	5042(1)	49(1)
C(47)	948(2)	1927(2)	5191(1)	42(1)
C(48)	1061(2)	1985(2)	5483(1)	35(1)
C(49)	725(2)	3702(2)	6117(1)	27(1)
C(50)	22(2)	4026(2)	6114(1)	33(1)
C(51)	-85(2)	4845(2)	6179(1)	42(1)
C(52)	511(3)	5345(2)	6243(1)	46(1)
C(53)	1208(2)	5033(2)	6244(1)	46(1)
C(54)	1317(2)	4213(2)	6180(1)	33(1)
C(55)	4381(2)	4075(2)	5846(1)	24(1)
C(56)	4448(2)	4505(2)	5592(1)	32(1)
C(57)	5133(2)	4634(2)	5480(1)	40(1)
C(58)	5757(2)	4345(2)	5620(1)	42(1)
C(59)	5699(2)	3915(2)	5872(1)	40(1)
C(60)	5016(2)	3779(2)	5985(1)	30(1)
C(61)	3469(2)	4696(2)	6277(1)	21(1)
C(62)	3056(2)	4575(2)	6518(1)	26(1)
C(63)	3004(2)	5185(2)	6722(1)	31(1)
C(64)	3370(2)	5916(2)	6690(1)	31(1)
C(65)	3792(2)	6041(2)	6455(1)	26(1)
C(66)	3834(2)	5440(2)	6248(1)	24(1)

C(67)	2853(2)	4206(2)	5723(1)	23(1)
C(68)	2660(2)	3632(2)	5518(1)	34(1)
C(69)	2215(2)	3839(2)	5284(1)	44(1)
C(70)	1951(2)	4628(2)	5256(1)	49(1)
C(71)	2128(2)	5197(2)	5461(1)	43(1)
C(72)	2576(2)	5001(2)	5694(1)	32(1)
C(73)	2812(2)	-1052(2)	5743(1)	33(1)
C(74)	3486(2)	-1192(2)	5880(1)	27(1)
C(75)	3779(2)	-1972(2)	5893(1)	33(1)
C(76)	3407(2)	-2615(2)	5769(1)	54(1)
C(77)	2743(3)	-2474(3)	5635(1)	94(2)
C(78)	2439(3)	-1709(2)	5623(1)	87(2)
C(79)	1503(2)	-195(2)	5609(1)	28(1)
C(80)	1263(2)	-301(2)	5326(1)	35(1)
C(81)	555(2)	-560(2)	5258(1)	49(1)
C(82)	85(2)	-719(3)	5472(1)	61(1)
C(83)	304(2)	-608(3)	5750(1)	68(1)
C(84)	1009(2)	-334(3)	5821(1)	51(1)
C(85)	2833(2)	384(2)	5386(1)	26(1)
C(86)	3096(2)	-112(3)	5171(1)	46(1)
C(87)	3312(2)	245(3)	4915(1)	60(1)
C(88)	3256(2)	1068(3)	4873(1)	53(1)
C(89)	3013(2)	1552(3)	5083(1)	42(1)
C(90)	2813(2)	1221(2)	5339(1)	31(1)
C(91)	4047(2)	-1364(2)	6745(1)	26(1)
C(92)	4594(2)	-1160(2)	6558(1)	31(1)
C(93)	5232(2)	-1616(2)	6553(1)	36(1)
C(94)	5334(2)	-2286(2)	6730(1)	35(1)
C(95)	4794(2)	-2497(2)	6915(1)	33(1)
C(96)	4153(2)	-2041(2)	6925(1)	27(1)
C(97)	3010(2)	-822(2)	7136(1)	27(1)
C(98)	3523(2)	-515(2)	7329(1)	47(1)
C(99)	3412(3)	-546(3)	7621(1)	50(1)
C(100)	2794(3)	-862(3)	7721(1)	59(1)
C(101)	2285(3)	-1167(4)	7534(1)	111(3)
C(102)	2393(3)	-1162(4)	7237(1)	81(2)
C(103)	2491(2)	-1381(2)	6586(1)	25(1)
C(104)	2628(2)	-2129(2)	6473(1)	48(1)
C(105)	2057(3)	-2586(3)	6345(1)	73(2)
C(106)	1352(2)	-2290(3)	6334(1)	56(1)
C(107)	1217(2)	-1534(3)	6443(1)	56(1)
C(108)	1783(2)	-1068(2)	6564(1)	48(1)
C(109)	5266(2)	1753(2)	5631(1)	25(1)
C(110)	4712(2)	2258(2)	5521(1)	29(1)
C(111)	4792(2)	2672(2)	5268(1)	40(1)
C(112)	5431(2)	2587(2)	5122(1)	41(1)

C(113)	5993(2)	2087(2)	5227(1)	38(1)
C(114)	5908(2)	1667(2)	5479(1)	30(1)
C(115)	5224(2)	115(2)	5789(1)	25(1)
C(116)	4846(2)	-64(2)	5532(1)	29(1)
C(117)	4900(2)	-831(2)	5411(1)	32(1)
C(118)	5322(2)	-1425(2)	5541(1)	32(1)
C(119)	5704(2)	-1252(2)	5795(1)	30(1)
C(120)	5659(2)	-485(2)	5918(1)	27(1)
C(121)	5822(2)	1273(2)	6208(1)	27(1)
C(122)	5717(2)	927(2)	6476(1)	32(1)
C(123)	6245(2)	1017(2)	6696(1)	42(1)
C(124)	6873(2)	1463(2)	6653(1)	48(1)
C(125)	6975(2)	1830(2)	6391(1)	43(1)
C(126)	6449(2)	1739(2)	6168(1)	35(1)
C(127)	8697(2)	6565(2)	5789(1)	27(1)
F(128)	7932(1)	5441(1)	5641(1)	40(1)
C(128)	8592(2)	5832(2)	5646(1)	32(1)
F(129)	8999(1)	4723(1)	5365(1)	52(1)
C(129)	9140(2)	5441(2)	5500(1)	36(1)
F(130)	10363(1)	5395(2)	5351(1)	60(1)
C(130)	9968(2)	6487(2)	5634(1)	40(1)
F(131)	10645(1)	6824(2)	5635(1)	58(1)
C(131)	9826(2)	5773(3)	5492(1)	40(1)
F(132)	9590(1)	7556(1)	5920(1)	42(1)
C(132)	9412(2)	6861(2)	5779(1)	32(1)
C(133)	8410(2)	6759(2)	6315(1)	27(1)
F(134)	9038(1)	8006(1)	6429(1)	44(1)
C(134)	8887(2)	7217(2)	6491(1)	31(1)
F(135)	9658(1)	7417(2)	6903(1)	57(1)
C(135)	9214(2)	6926(2)	6742(1)	40(1)
F(136)	9374(1)	5872(1)	7080(1)	57(1)
C(136)	9074(2)	6152(2)	6831(1)	39(1)
F(137)	8452(1)	4905(1)	6754(1)	50(1)
C(137)	8607(2)	5678(2)	6672(1)	35(1)
F(138)	7883(1)	5439(1)	6261(1)	37(1)
C(138)	8300(2)	5974(2)	6417(1)	32(1)
C(139)	7230(2)	6749(2)	5922(1)	24(1)
F(140)	6857(1)	6602(1)	6402(1)	32(1)
C(140)	6688(2)	6608(2)	6118(1)	25(1)
F(141)	5464(1)	6369(1)	6251(1)	39(1)
C(141)	5959(2)	6490(2)	6048(1)	28(1)
F(142)	4998(1)	6404(1)	5694(1)	42(1)
C(142)	5720(2)	6500(2)	5767(1)	30(1)
F(143)	6007(1)	6626(1)	5285(1)	44(1)
C(143)	6228(2)	6618(2)	5561(1)	30(1)
F(144)	7406(1)	6922(1)	5428(1)	38(1)

C(144)	6953(2)	6760(2)	5643(1)	28(1)
C(145)	8034(2)	8025(2)	5948(1)	25(1)
F(146)	8530(1)	8067(1)	5485(1)	37(1)
C(146)	8208(2)	8446(2)	5705(1)	31(1)
F(147)	8253(1)	9641(1)	5418(1)	48(1)
C(147)	8063(2)	9270(2)	5659(1)	35(1)
F(148)	7558(1)	10503(1)	5826(1)	52(1)
C(148)	7724(2)	9705(2)	5866(1)	39(1)
F(149)	7215(1)	9744(1)	6322(1)	49(1)
C(149)	7545(2)	9322(2)	6112(1)	34(1)
F(150)	7471(1)	8164(1)	6394(1)	40(1)
C(150)	7692(2)	8502(2)	6149(1)	31(1)